CHEMICAL ENGINEERING SCIENCE
GENIE CHIMIQUE

VOL. I DECEMBER 1951 NO. 2

Studies on fluidization. II—Heat transfer

C. VAN HEERDEN, P. NOBEL and D. W. VAN KREVELEN

Staatsmijnen in Limburg, Central Laboratory, Geleen, The Netherlands

(Received 1 May 1951)

This paper is the second part of an experimental study on the characteristics of the fluidized state. Part I [1] dealt with the critical mass velocity at which fluidization starts. Part II gives an extensive investigation of the rate of heat transfer.

Summary—In a small scale apparatus the heat transfer coefficient to the cylindrical wall of a fluidizing bed ("dense phase") was measured under strongly varying conditions of gas and solids. The solids used were closely sized samples as well as mixtures of different sizes of carborundum, ironoxide (Fe_3O_4), coke, lead, Devarda's alloy, and fly ash. The gases used were air, mixtures of nitrogen and hydrogen, carbon dioxide, argon, town's gas and methane.

For a correlation of the measuring results use is made of a system of dimensionless numbers that may be considered as a complete representation of all variables which may be expected to influence the value of the transfer coefficient. The gas rate is characterized by the reduced mass velocity G/G_0 where G_0 is the mass velocity at which fluidization starts. A correlation based on this variable proves to be successful for $Re < 5$ and can be written as:

$$\frac{Nu}{Pr^{0.5}} \frac{1}{\varphi'^{0.45}} \left(\frac{\varrho_{bm}}{\varrho}\right)^{0.18} \left(\frac{\varrho c_p}{\varrho_{bm} c_s}\right)^{0.36} = \psi(G/G_0),$$

when $\psi(G/G_0) = 0{,}028\ (G/G_0)^{0.45}$ for $2 < G/G_0 < 20$; a larger region ($1 < G/G_0 < 30$) can be covered by

$$\psi(G/G_0) = 0{,}035\ (G/G_0 - 1)^{0.36}.$$

With the aid of the generalized shape factor B introduced in Part I of this study, the above mentioned relationship can be transformed into a correlation restricted to the region $2 < G/G_0 < 20$. This can be written as

$$\frac{Nu}{Pr^{0.5}} \left(\frac{\varrho_{bm}}{\varrho}\right)^{0.18} \left(\frac{\varrho c_p}{\varrho_{bm} c_s}\right)^{0.36} = \chi(B\,Re),$$

where for $Re < 5$, $\chi\ (B\ Re) = 0{,}58\ (B\ Re)^{0.45}$.

Résumé—Dans un appareil de laboratoire, il a été mesuré le coefficient de transmission de la chaleur vers la paroi cylindrique d'un lit fluidifié (phase dense) à des conditions fort variantes quant au gaz et aux substances solides. Les substances solides employées étaient tant des échantillons de grosseur exacte que des mélanges de carborundum, d'oxyde de fer (Fe_3O_4), de coke, de plomb, d'alliage Devarda et de cendre volante étant différants en grosseur. Les gaz employés étaient l'air, les mélanges azote-hydrogène, le bioxyde de carbone, l'argon, le gaz de ville et le méthane.

Pour une corrélation des résultats de mesure, il a été utilisé un système de nombres sans dimensions qu'on peut considérer comme une représentation complète de tous les variables qui influencent la valeur du coefficient de transmission de la chaleur. La vitesse du gaz se caractérise par la vitesse de masse réduite G/G_0 dans laquelle G_0 est la vitesse de masse à laquelle la fluidification commence. Il paraît qu'une corrélation basée sur ce variable est exacte pour $Re < 5$ et s'écrit comme suit:

$$\frac{Nu}{Pr^{0.5}} \frac{1}{\varphi'^{0.45}} \left(\frac{\varrho_{bm}}{\varrho}\right)^{0.18} \left(\frac{\varrho c_p}{\varrho_{bm} c_s}\right)^{0.36} = \psi(G/G_0)$$

dans laquelle

$$\psi(G/G_0) = 0{,}028\ (G/G_0)^{0.45} \quad \text{pour} \quad 2 < G/G_0 < 20.$$

Une plus vaste région ($1 < G/G_0 < 30$) peut être dominée par

$$\psi(G/G_0) = 0{,}035\ (G/G_0 - 1)^{0.36}.$$

A l'aide du facteur de forme généralisé B, introduit dans la partie I de la présente étude, la relation susnommée peut être modifiée dans une corrélation limitée à la région $2 < G/G_0 < 20$. On peut écrite:

$$\frac{Nu}{Pr^{0.5}} \left(\frac{\varrho_{bm}}{\varrho}\right)^{0.18} \left(\frac{\varrho c_p}{\varrho_{bm} c_s}\right)^{0.36} = \chi(B\,Re)$$

dans laquelle, pour

$$Re < 5,\ \chi\ (B\ Re) = 0{,}58\ (B\ Re)^{0.45}.$$

INTRODUCTION

One of the great advantages of a fluidized bed for carrying out heterogeneous reactions between gases and solids and gas reactions in the presence of a solid catalyst is the property that even at a locally high rate of heat production the differences in temperature throughout the bed are very small.

This uniform temperature distribution may be traced to the rapid exchange of solid particles between the various places in the bed and this, combined with the great heat capacity of the fluidized solid mass, is responsible for a very "fast" exchange of heat.

Moreover the marked turbulence of the solid particles causes the coefficient of heat transfer to a cooling or heating surface present in the fluidized bed to be several times as large as in the case of a fixed bed or an empty tube, all other conditions being the same.

The present article describes an extensive investigation of the value of this heat transfer coefficient (as it occurs in apparatus on laboratory scale) under widely varying conditions of granular material and fluidizing gas.

PREVIOUS WORK

Experiments in this field have been published *inter alia* by LOGWINUK [6], LEVA, WEINTRAUB and GRUMMER [4] and MICKLEY and TRILLING [7]*. Like the present article the two former publications deal with heat transfer under the condition of "dense phase" fluidization *i.e.* at such a rate of gas flow that the expansion of the bed is only relatively small. MICKLEY and TRILLING, however, chiefly study the region where the density of the bed depends upon the gas rate and is up to 20 times as small as the density of the fixed bed (dilute phase fluidization).

LOGWINUK, who measures heat transfer to a water-cooled tube positioned axially in the bed, correlates the results of his experiments made with fluidized aluminium oxide, carborundum, silica gel and "SiO_2" of four different particle sizes and air, carbon dioxide and helium as fluidizing gas, in the equation:

$$h = \frac{8800 G^{0.32} k_g^{0.072} l^{2.4}}{d^{0.36} c_p^{1.6} \mu^{0.8}}. \qquad (1)^{**}$$

LEVA *et al.* study the heat transfer to the cylindrical wall of the bed and give for their measurements on various kinds of sand and an iron catalyst, using air, helium and carbon dioxide as fluidizing medium, the following greatly different relationship:

$$h = 0{\cdot}95\, c_p\, G^{1.15}. \qquad (2)$$

The most striking feature is the large difference in the exponent of the mass velocity of the two correlations. In addition, the formula given by LEVA *et al.* is improbably simple in view of the great number of physical constants of solid and gas which may be expected to influence the value of the heat transfer coefficient. MICKLEY and TRILLING used glass spheres of varying diameters with air as fluidizing medium.

Thus they could only study the influence of the gas velocity and particle size. They correlate their results in two formulas, one for heat transfer to the cylindrical wall:

$$h = 0{\cdot}072 \left(\frac{\varrho_f G}{d^3}\right)^{0.263} \qquad (3)$$

and the other for heat transfer to a tube positioned axially in the bed:

$$h = 0{\cdot}028 \left(\frac{\varrho_f^2}{d^3}\right)^{0.238}. \qquad (4)$$

A comparison of the exponent of mass velocity with (1) and (2) cannot readily be made, since the formulas of MICKLEY and TRILLING include the factor ϱ_f for the density of the fluidized bed, which quantity greatly decreases with increasing gas rate in the region studied by them. The real exponent of G in eq. (3) therefore is in any case smaller than 0·26 and in eq. (4) this value is even negative.

It seems, therefore, in no way superfluous to extend experimental facts while varying the properties of both solids and gases as widely as possible.

The present article deals with heat transfer measurements in a fluidized bed of carborundum, coke, iron oxide (Fe_3O_4), Devarda's alloy and lead† with air, hydrogen, various mixtures of hydrogen and nitrogen, argon, carbon dioxide, town gas and raw methane as fluidizing gases.

Of the two first-mentioned solids a great many homogeneous sieve fractions varying in size from 75 to 800 μ and a few mixtures of various particle sizes were investigated.

All our experiments were confined to dense phase fluidization, the variation in the density of the bed being sufficiently small as to consider this quantity constant for a given powder.

* The above mentioned authors give enough details to compare their results with our final correlation. Other papers on heat transfer in fluidized beds are by L. J. JOLLEY, Fuel 1949 **28** 114–115; O. LEVENSPIEL and J. S. WALTON, Chem. Eng. News 1949 **27** 1999; O. P. AGARWAL and J. A. STORROW, Chem. and Ind. 1951 278, 321; J. R. CAMPBELL and F. RUMFORD, J.S.C.I., 1950 **69** 373.

** See nomenclature at the end of the paper.

† Experiments with sand failed to give reproducible results, which was probably caused by electrostatic effects.

VOL. 1 1952

EXPERIMENTAL

Apparatus

The very simple measuring apparatus (Fig. 1) consists of a brass cooler measuring 8·5 cm in inner diameter and 10 cm in length and fixed between two glass cylinders of the same inner diameter and respectively 10 and 40 cm long. The lower side is closed with a removable conical brass inlet in which a filter of sintered glass has been provided.

The apparatus is filled, to just above the cooler, with powder to be examined and the fluidizing gas is supplied through an orifice, by which the flow rate is measured.

An extended brass section at the top side of the upper cylinder and having a diameter of 17 cm, served as dust collector.

Just above the filter in the bed an electrical heating coil is provided which develops an amount of energy q_e which was determined by current and voltage measurement. The bed will now adopt such a temperature that this energy can be eliminated through the cooler. At a cooling water temperature of 13 to 15° C it was always possible to regulate the heat production in the coil so that the bed adopted appr. room temperature, so that heat losses to the surroundings were practically negligible. As an additional precaution the remainder of the apparatus was insulated by means of a coating of wadding approx. 1 cm thick.

Another important advantage of the fact that the bed was kept at room temperature during the measurement is that the amount of heat q_g added by the passing gas, whose inlet temperature t_g was measured in the conical inlet, is only a fraction of q_e and can be calculated as a small correction from:

$$q_g = w\, c_p\, (t_g - t_b). \qquad (5)$$

Thus no special care need be taken to measure this inlet temperature.

The bed temperature t_b was measured with a copper constantan thermocouple (wire 0·5 mm thick) the junction of which was situated in the middle of the bed half way up the cooler. The temperature was determined by direct reading from a galvanometer, the other junction and a calibrated thermometer being placed in a Dewar vessel at room temperature.

When previously examining the temperature distribution in the bed by means of a movable thermocouple it was found that in the bed zone surrounded by the cooler the temperature differed nowhere more than 0·1–0·2° C from that of the middle of the bed. At a temperature difference of about 10° C between bed and cooling surface a measurement of the bed temperature at one place in the middle is therefore quite sufficient.

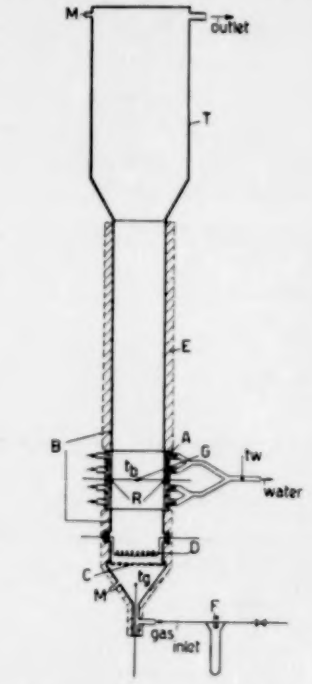

A Cooler
B Glass cylinder
C Glass filter
D Heating element
E Insulation
F Orifice
G Thermocouple
M Manometer connections
T Dust trap
R Rubber stops

Fig. 1. Apparatus for measuring the coefficient of heat transfer.

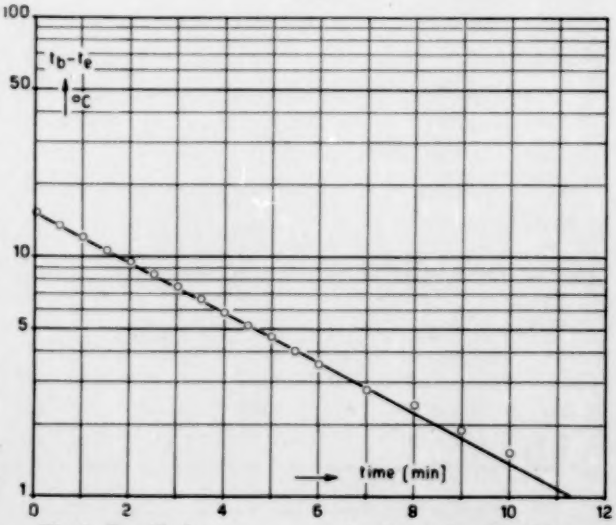

Fig. 2. Specific heat measurement carborundum 75–110 μ.

In order to ensure a uniform flow of water inside the cooler, it was provided with four parallel feed and discharge pipes and filled with glass beads with a view to good heat transfer. When varying the water velocity from 1 to 12 l/min, the "overall" heat transfer coefficient proved to be constant under given conditions (see Table 1), so that, as the velocity of 12 l/min applied for all experiments, the resistance on the side of the cooling water could be neglected and the temperature of the cooling surface identified with the water temperature measured.

In this way the value of the heat transfer coefficient was calculated from:

$$h = \frac{q_e - q_g}{A(t_b - t_w)} \qquad (6)$$

where $A = 0{\cdot}0264$ m² represents the cooling surface area.

Table 1. Control of the influence of water velocity.

Water velocity litres min	*Water temperature °C*		*"overall" h J/m² °C sec*
	inlet	*outlet*	
1·1	14·9	15·45	239
4·2	12·9	12·9	238
6·3	13·4	13·45	237
11·0	12·75	12·75	240

The reliability of the measuring procedure is demonstrated by the results obtained with a few control measurements, where the heat transfer coefficient calculated from (6) did not vary with abnormal deviations in the bed temperature with respect to the temperature of the surroundings nor did such variations occur when the heating coil was shifted from a position just over the filter to just under the cooler (Table 2).

Table 2. Control of the influence of the bed temperature and the position of the heating coil

$t_{surr.}$	t_w	t_g	t_b	G	q_g	q_e	h	*coil*
23·7	14·7	24·3	31·75	0·411	−17·4	212·8	434	just over filter
24·0	14·4	23·5	17·5	0·418	14·3	21·5	437	just over filter
20·2	14·2	20·6	19·4	0·420	3·6	57·4	445	just under cooler

Data of materials used (solids-gases)

In view of the great number of data to be known of the solids and gases used, later on a survey will be given of the physical constants to be applied in this paper and of the way in which these constants were obtained. All gases and the greater part of the solids are identical to those mentioned in our previous paper "Studies on fluidization I."

Solids

All solids used as well as the required data are given in Table 3.

Since the *diameter of the particles* has only a relatively slight influence on the heat transfer, as will be discussed later, we have, for the sake of simplicity, not used the effective diameter, introduced in Part I of these studies, and have based the diameter on screen analysis.

As diameter d of the homogeneous sieve fractions we chose the average of the sieve limits. For mixtures of different particle sizes we invariably performed a sieve analysis, the diameter being calculated from:

$$d = \frac{1}{\sum x_i/d_i} \qquad (7)$$

where x_i is the percentage by weight of the fraction with diameter d_i (see Part I).

The *density* ϱ_s was determined with a pyknometer except for fly ash and coke. Of *fly ash*, which through the microscope appears as beautiful transparent spheres (see Figure 1 A), the helium and the mercury density were determined separately which two values proved to be equal with an accuracy within 1%. From this it is obvious that the fly ash particles are perfectly gas tight hollow spheres. This means that for our purposes fly ash may be considered to consist of "non porous" material of a very small density (600 kg/m³).

Coke powder consists of particles whose surfaces show relatively large cavities and holes. Nevertheless both the helium and the mercury density proved to be practically independent of particle size (see Part I). In Table 3 the mercury density is given, the helium density being 10% higher.

The way in which the *density of the bed*, at maximum porosity ϱ_{bm} was determined has been fully described in Part I.

The *specific heat* c_s of the solid was determined for every species of material by means of the heat transfer apparatus described above. To this end the powder was fluidized with air and a normal measurement of the heat transfer coefficient was performed in the

VOL. 1 1952

Table 3

No.	*Solid*	*Sieve limits (μ)*	*d (μ)*	ϱ_s	ϱ_{bm}	c_s	k_s	G_0 *(air)*	*B*
a	carborundum	75–90	82	3180	1680	641	18	0·0134	0·66
b	,,	90–100	95	3180	1680	641	18	0·0178	0·67
c	,,	110–125	117	3180	1600	641	18	0·026	0·66
d	,,	150–175	162	3180	1630	641	18	0·054	0·62
e	,,	175–210	192	3180	1665	641	18	0·069	0·69
f	,,	210–240	225	3180	1670	641	18	0·084	0·78
g	,,	75–110	94	3180	1680	641	18	0·0175	0·66
h	iron oxide	75–110	92	5180	2620	632	—	0·0288	0·60
i	coke	75–110	93	1800	790	741	0·5	0·0146	0·37
k	,,	125–175	149	1800	745	741	0·5	0·0295	0·43
l	,,	150–210	181	1800	763	741	0·5	0·041	0·47
m	,,	210–240	225	1800	740	741	0·5	0·067	0·43
n	,,	240–300	275	1800	720	741	0·5	0·100	0·42
o	,,	300–420	360	1800	677	741	0·5	0·161	0·42
p	,,	420–500	465	1800	664	741	0·5	0·225	0·50
q	,,	500–800	650	1800	621	741	0·5	0·350	0·58
r	Dev. alloy	60–110	83	4320	2050	578	—	0·02	0·605
s	lead	50–210	78·5	11120	5360	142	35	0·097	0·265
t	fly ash + graphite	90–125	107	600	340	713	—	0·0046	—
u	carborundum	50–210	90	3180	1700	641	18	0·0193	—
v	,,	75–210	110	3180	1663	641	18	0·025	0·62
w	,,	75–90–50% 210–240–50%	120	3180	1825	641	18	0·0194	1·04
x	iron oxide	50–300	122	5180	2870	632	—	0·033	—
z	coke	50–210	111	1800	720	741	0·5	0·0195	—

way already described. Then the heating coil was suddenly switched off while the rate of gas flow was kept constant. From this moment the bed temperature will fall according to an exponential curve and adjust itself at a temperature t_e just above that of the cooling water. This temperature follows from the equation:

$$w\,c_p(t_g - t_e) = h\,A\,(t_e - t_w). \qquad (8)$$

When the heat capacity of the bed amounts to W_b and that of the glass wall with glass filter to W_w it can be easily derived that the fall of temperature of the bed as a function of time τ takes place according to:

$$t_b - t_e = C \exp\left\{-\frac{h\,A + W c_p}{W_b + W_w}\,\tau\right\}. \qquad (9)$$

By plotting $t_b - t_e$ logarithmically versus time a linear curve is obtained, from the slope of which W_b can be calculated. W_w was determined by weighing the glass cylinder (under the cooler) together with the glass filter, a correction being made for that section of the other cylinder (above the cooler) that was under the level of the bed. The value of W_w was maximum 15% of W_b. In Fig. 2 a measurement of the specific heat has been exemplified.

As a guidance Table 3 gives such values of the *heat conductivity* k_s of the various solids as are available. From our experimental results to be discussed later it will be seen that the influence of this quantity on the rate of heat transfer may be neglected.

Finally the critical mass velocity G_0 of air and the generallized shape factor B derived herefrom (see Part I) is mentioned.

Fig. 1A gives the microphotographs of fly ash and lead. For photographs of other materials see Part I.

Gases

In Table 4 all gases used are given together with the various constants.

The *viscosity* μ of the various gases was determined relatively with respect to air (Part I).

The *heat conductivity* k was taken from PERRY [8]; the values for N_2–H_2 mixtures are based on measurements by IBBS and HIRST [2]. The value of towns

gas and crude methane were calculated, according to LINDSAY and BROMLEY [5], from the gas analysis (Table 5).

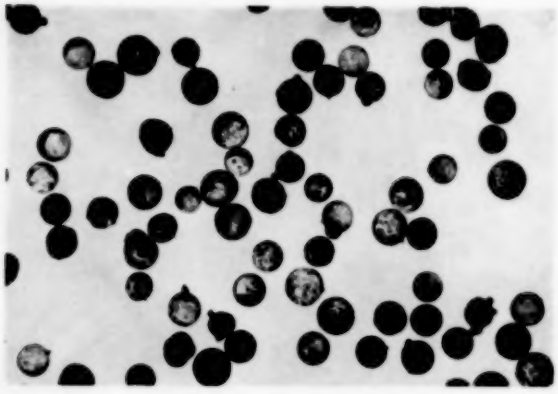

a

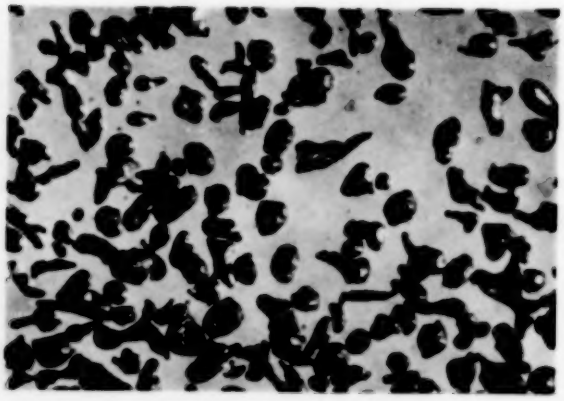

b

Fig. 1A. Microphotographs of a) flyash 90–125 μ, b) lead 50–210 μ. For other materials see part I.

Table 4

Gas (25°)	$\mu \times 10^5$	k	ϱ	$c_p \times 10^{-2}$	Pr
98% H_2 + 2% N_2	0·93	0·1765	0·104	11·292	0·594
80% H_2 + 20% N_2	1·31	0·1195	0·297	3·976	0·436
65% H_2 + 35% N_2	1·495	0·090	0·458	2·577	0·427
45% H_2 + 55% N_2	1·64	0·064	0·671	1·764	0·451
25% H_2 + 75% N_2	1·71	0·044	0·886	1·353	0·526
Air	1·85	0·026	1·185	1·01	0·712
Argon	2·23	0·0175	1·65	0·528	0·667
Coal dioxide	1·50	0·016	1·82	0·834	0,785
Town gas	1·22	0·1055	0·349	0·603	0·416
Methane (raw)	1·24	0·039	0·700	2·002	0·62

The volume ratios of the N_2–H_2 mixtures tabulated are rounded off. The real ratio naturally varied more or less from the value tabulated and was therefore

Table 5

Gas	CO_2	C_2H_2	O_2	CO	H_2	CH_4	C_2H_6	N_2
Towns gas	0·1	1·3	0·5	5·1	64·5	23·5	1·0	4·0
Methane (crude)	0·0	0·2	0·7	9·1	10·4	70·0	3·0	6·6

determined by analysing the contents of every fresh bomb. The values of μ and k for these mixtures were determined by interpolation for every composition: c_p and ϱ were calculated as weight means.

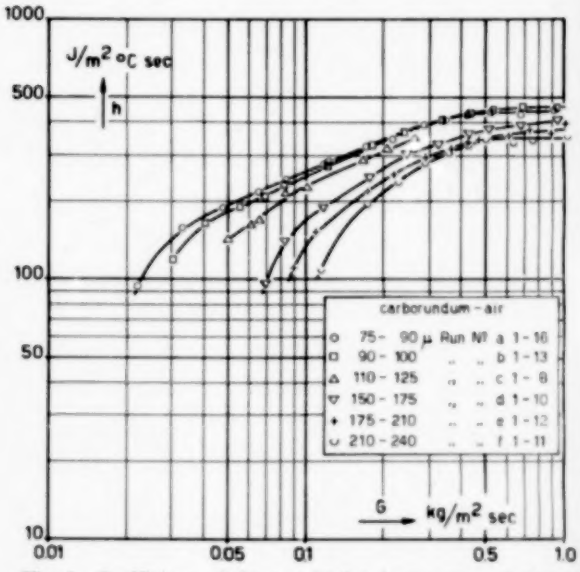

Fig. 3. Coefficient of heat transfer h *vs* mass velocity for various carborundum fractions with air.

For the various N_2–H_2 mixtures the *Pr number* deviates fairly considerably from the value of air, which enabled us to study also the influence of *Pr* on the rate of heat transfer.

Experimental results

In view of the large number of measurements Table 6 only gives the heat transfer coefficients and the corresponding experimental conditions for carborundum-air.

A complete table giving all the experimental results may be obtained from the authors.

Discussion of Results

In the following development of a correlation of our results all measurements for which $Re > 5$ have been omitted since these values proved to deviate systematically from the correlation holding for the region of viscous flow. This point will be discussed later.

Fig. 3 gives h as a function of the mass velocity G for the various sieve fractions of carborundum with air as fluidizing medium. The equivalent course of these curves from the starting point of fluidization, the value of h ranging from 100 to 400 J/m² °C sec, is demonstrated in Fig. 4, where the same measurements have been plotted as a function of G/G_0.

Hence it is obvious when trying to develop a correlation to take into account the gas rate in the ratio G/G_0, the reduced mass velocity.

This reduced mass velocity may be considered to be a measure of the agitation of the bed, which from $G/G_0 = 1$ (fixed bed) gradually increases.

For a given value of G/G_0 the value of h may also depend on the following numbers:

constants of the solid: ϱ_{bm}, k_s, c_s and d
constants of the gas: ϱ, k, c_p and μ
and finally the acceleration of gravity g.

The 9 constants may, in combination with h, be reduced to a max. of 6 dimensionless numbers, which were chosen as:

$$Nu = \frac{h \cdot d}{k}, \quad \varphi' = \frac{\varrho\,\varrho_{bm}\,g d^3}{\mu^2}, \quad Pr = \frac{c_p \mu}{k}, \quad \frac{\varrho_{bm}}{\varrho}, \quad \frac{c_s \varrho_{bm}}{c_p \varrho} \text{ and } \frac{k_s}{k}. \qquad (10)$$

In a complete dimensional analysis of all *independent* variables the Re-number Gd/μ would also have appeared. However, from dimensional considerations it is permitted to substitute this Re-number, *via the dependent variable* G_0, by G/G_0.

The numbers mentioned in (10) together with the reduced mass velocity may be considered as a *complete* set of dimensionless combinations of *all* independent variables which may reasonably be expected to influence the value of the heat transfer coefficient.

From this set of numbers k_s/k is directly omitted since the experimental results do not indicate any systematic influence of the thermal conductivity of the solid, notwithstanding the fact that its value differs greatly for the various solids. This omission proves later to be justified when no systematic devations, of equal trend with k_s, occur from our ultimate correlation.

So the experimental results will have to be correlated in the functional relationship:

$$Nu = \text{function}\left(\frac{G}{G_0},\ Pr,\ \varphi',\ \frac{\varrho}{\varrho_{bm}},\ \frac{\varrho\, c_p}{\varrho_{bm}\, c_s}\right) \qquad (11)$$

for which we chose the equation:

$$\frac{Nu}{Pr^x}\,\varphi'^{\,y}\left(\frac{\varrho_{bm}}{\varrho}\right)^z\left(\frac{\varrho\, c_p}{\varrho_{bm}\, c_s}\right)^t = \text{function}\,(G/G_0). \qquad (12)$$

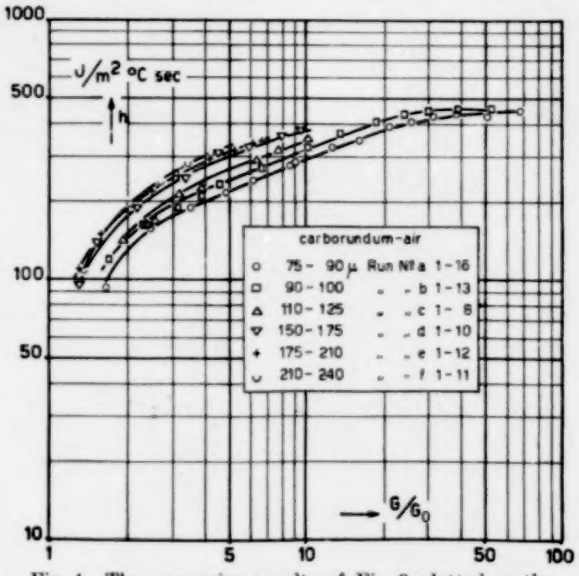

Fig. 4. The measuring results of Fig. 3 plotted *vs* the reduced mass velocity G/G_0.

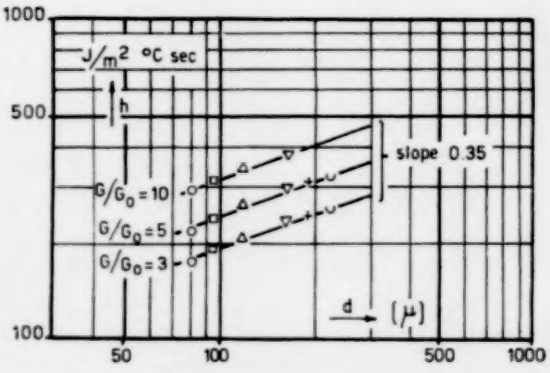

carborundum-air			
○	75 - 90 μ	Run № a	1-16
□	90 - 100	„ „ b	1-13
△	110 - 125	„ „ c	1- 8
▽	150 - 175	„ „ d	1-10
+	175 - 210	„ „ e	1-12
∪	210 - 240	„ „ f	1-11

Fig. 5. Dependency on the diameter for various values of G/G_0 derived by interpolation from Fig. 4.

Particle diameter

For the measurements on the various carborundum fractions with air as the fluidizing gas all numbers on the left-hand side of eq. (12) are constant with the exception of Nu and φ', which vary with the diameter. In Fig. 5 where these measurements are represented,

* See note page 60.

Table 6. Experimental results for the system carborundum-air *

Run No.	Solid	Gas	$w \times 10^{-3}$	G	G/G_0	t_g	t_b	t_w	q_c	q_g	h	Nu	$\frac{Nu}{Pr^{0.5}} \times \frac{1}{\varphi'^{0.45}} \times \left(\frac{\varrho_{bm}}{\varrho}\right)^{0.18} \times \left(\frac{\varrho c_p}{\varrho_{bm} c_s}\right)^{0.36}$	Re	BRe	$\frac{Nu}{Pr^{0.5}} \times \left(\frac{\varrho_{bm}}{\varrho}\right)^{0.18} \times \left(\frac{\varrho c_p}{\varrho_{bm} c_s}\right)^{0.36}$
a 1	carborundum	air	0·966	0·1698	12·68	21·9	22·15	13·3	75·2	−0·2	321	1·001	0·0800	0·752	0·495	0·379
a 2	75–90 μ		0·692	0·1215	9·07	21·1	21·45	13·25	61·2	−0·2	282	0·880	0·0704	0·539	0·354	0·333
a 3	$d = 82$ μ		2·39	0·420	31·4	21·0	22·95	13·9	107·1	−4·7	429	1·339	0·1069	1·868	1·229	0·506
a 4	$G_0 = 0{\cdot}0134$		1·98	0·347	25·9	21·1	21·70	13·5	89·5	−1·2	408	1·273	0·1018	1·540	1·012	0·481
a 5	$\varphi' = 31{\cdot}6$		1·612	0·283	21·1	21·1	20·85	13·4	76·3	+0·4	390	1·218	0·0974	1·255	0·826	0·461
a 6	$B = 0{\cdot}66$		1·222	0·215	16·05	21·3	20·9	13·1	70·0	+0·5	343	1·070	0·0855	0·954	0·627	0·405
a 7			0·966	0·1696	12·65	21·7	20·8	13·05	64·9	+0·9	321	1·001	0·0800	0·752	0·495	0·379
a 8			0·66	0·1160	8·65	21·8	21·6	13·35	59·3	+0·15	274	0·855	0·0683	0·514	0·338	0·323
a 9			0·473	0·0831	6·20	20·7	21·6	13·15	53·8	−0·45	240	0·748	0·0598	0·368	0·242	0·283
a 10			0·372	0·0652	4·86	20·7	21·6	13·0	49·0	−0·35	215	0·671	0·0535	0·289	0·190	0·253
a 11			0·269	0·0472	3·52	20·0	21·6	12·85	43·7	−0·40	187	0·583	0·0465	0·209	0·138	0·220
a 12			0·188	0·0330	2·46	20·0	22·0	12·75	38·4	−0·40	156	0·486	0·0388	0·1462	0·0963	0·184
a 13			0·126	0·0221	1·65	20·5	25·4	12·85	31·5	−0·60	93	0·290	0·0232	0·0980	0·0646	0·110
a 14			2·95	0·518	38·6	18·9	21·8	13·1	109·3	−8·55	439	1·370	0·1095	2·30	1·512	0·519
a 15			3·84	0·675	50·3	19·2	21·75	12·95	109·3	−9·8	429	1·338	0·1069	2·99	1·968	0·506
a 16			5·20	0·913	68·1	20·0	21·5	12·9	109·3	−7·8	446	1·391	0·1111	4·05	2·66	0·526
b 1	carborundum	air	2·42	0·425	23·9	23·1	21·25	12·95	90·25	+4·5	432	1·561	0·1021	2·185	1·459	0·591
b 2	90–100 μ		1·885	0·331	18·6	22·7	22·5	12·95	102·6	+0·35	407	1·472	0·0965	1·700	1·133	0·558
b 3	$d = 95$ μ		1·358	0·238	13·4	22·2	23·05	12·8	100·0	−1·15	365	1·320	0·0865	1·225	0·816	0·500
b 4	$G_0 = 0{\cdot}0178$		1·02	0·179	10·05	22·8	24·4	12·85	100·0	−1·65	322	1·163	0·0762	0·918	0·612	0·440
b 5	$\varphi' = 49{\cdot}0$		0·672	0·118	6·63	23·0	24·35	12·95	81·95	−0·9	270	0·975	0·0639	0·606	0·404	0·369
b 6	$B = 0{\cdot}67$		0·464	0·0813	4·57	21·1	20·9	12·8	49·3	+0·1	231	0·835	0·0547	0·418	0·278	0·316
b 7			0·393	0·0690	3·88	21·3	23·1	12·6	58·55	−0·7	208	0·751	0·0492	0·354	0·236	0·284
b 8			0·317	0·0556	3·13	21·1	22·0	12·8	45·9	−0·3	188	0·679	0·0445	0·286	0·191	0·257
b 9			0·231	0·0405	2·28	21·0	23·2	12·85	45·1	−0·5	163	0·589	0·0386	0·208	0·139	0·223
b 10			0·172	0·0303	1·70	21·0	24·25	13·0	35·75	−0·55	119	0·430	0·0282	0·1555	0·1037	0·163
b 11			3·02	0·531	29·8	22·8	22·15	13·05	106·0	+1·95	449	1·622	0·1064	2·73	1·82	0·615
b 12			3·91	0·686	38·6	22·1	23·85	13·05	136·6	−6·85	454	1·640	0·1074	3·53	2·35	0·621
b 13			5·29	0·929	52·1	22·0	24·85	13·15	154·2	−15·1	451	1·631	0·1070	4·77	3·18	0·619
c 1	carborundum	air	0·283	0·0497	1·91	20·0	25·0	13·05	46·05	−1·4	142	0·636	0·0318	0·315	0·209	0·243
c 2	110–125 μ		0·376	0·0659	2·54	21·4	22·65	13·1	43·05	−0·45	169	0·758	0·0380	0·419	0·277	0·290
c 3	$d = 117{\cdot}5$ μ		0·472	0·0828	3·18	22·4	20·9	13·1	43·05	+0·7	213	0·951	0·0476	0·525	0·348	0·364
c 4	$G_0 = 0{\cdot}0260$ $\varphi' = 88{\cdot}1$ $B = 0{\cdot}66$		0·570	0·100	3·8	21·7	20·45	13·0	43·05	+0·7	223	0·996	0·0495	0·635	0·420	0·382
c 5			0·940	0·165	6·34	22·2	21·45	13·05	63·25	+0·7	288	1·287	0·0638	1·046	0·692	0·492

c 6			1·15	0·202	7·77	22·0	21·6	13·1	70·85	+0·45	318	1·420	0·0705	1·282	0·849	0·544
c 7			1·485	0·260	10·0	21·4	21·3	13·1	74·75	+0·15	346	1·545	0·0767	1·65	1·092	0·592
c 8			0·348	0·061	2·35	19·8	23·0	13·4	42·2	−1·1	162	0·726	0·0364	0·388	0·257	0·278
d 1	carborundum	air	2·89	0·507	9·4	21·5	21·3	13·0	81·1	+0·6	373	2·300	0·0747	4·44	2·76	0·873
d 2	150–175 μ		3·86	0·677	12·5	21·3	21·6	12·95	89·7	−1·15	388	2·390	0·0778	5·92	3·68	0·909
d 3	$d = 162{,}5$ μ		5·32	0·935	17·3	21·5	21·4	12·9	89·7	+0·5	402	2·480	0·0806	8·17	5·07	0·941
d 4	$G_0 = 0{\cdot}054$		2·445	0·429	7·95	25·6	22·15	12·95	78·45	+8·45	358	2·205	0·0717	3·75	2·33	0·838
d 5	$\varphi' = 236$		1·83	0·321	5·95	24·4	22·4	12·85	78·25	+3·6	324	1·995	0·0649	2·81	1·75	0·757
d 6	$B = 0{\cdot}62$		1·375	0·241	4·46	24·2	22·9	12·85	77·8	+2·4	302	1·860	0·0605	2·11	1·31	0·706
d 7			1·00	0·175	3·24	24·0	24·55	12·7	77·0	−0·55	244	1·503	0·0489	1·53	0·95	0·571
d 8			0·665	0·117	2·17	23·5	25·95	12·9	65·6	−1·65	186	1·147	0·0373	1·025	0·636	0·435
d 9			0·469	0·0822	1·52	23·7	27·15	12·8	54·0	−1·60	138	0·850	0·0276	0·718	0·445	0·323
d 10			0·395	0·0693	1·28	21·7	25·65	13·9	31·05	−1·55	95	0·585	0·0190	0·605	0·376	0·222
e 1	carborundum	air	2·42	0·424	6·15	21·1	24·8	13·65	74·05	−1·7	336	2·453	0·0626	4·40	3·06	0·929
e 2	175–210 μ		2·065	0·362	5·25	21·1	21·1	13·6	62·4	0·0	315	2·30	0·0587	3·76	2·61	0·871
e 3	$d = 192{\cdot}5$ μ		1·650	0·290	4·20	21·1	21·4	13·55	60·95	−0·5	292	2·13	0·0544	3·01	2·09	0·806
e 4	$G_0 = 0{\cdot}069$		1·250	0·219	3·17	21·3	21·85	13·6	55·6	−0·7	252	1·84	0·0469	2·27	1·58	0·696
e 5	$\varphi' = 402$		0·983	0·1725	2·50	21·2	22·55	13·55	53·35	−1·35	219	1·598	0·0408	1·79	1·24	0·605
e 6	$B = 0{\cdot}69$		0·625	0·1095	1·59	21·2	23·8	13·45	41·9	−0·85	150	1·093	0·0279	1·14	0·791	0·414
e 7			0·511	0·0895	1·30	21·2	25·5	13·3	37·8	−2·2	110	0·803	0·0205	0·931	0·646	0·304
e 8			5·10	0·896	13·0	20·4	23·5	12·7	119·1	−15·8	363	2·648	0·0675	9·31	6·46	1·003
e 9			4·20	0·737	10·7	19·6	22·55	12·85	107·5	−12·4	372	2·715	0·0692	7·66	5·31	1·028
e 10			3·43	0·602	8·73	19·8	21·4	12·5	89·15	−5·5	357	2·605	0·0665	6·25	4·34	0·988
e 11			2·64	0·463	6·70	19·9	20·5	12·6	73·45	−1·6	344	2·51	0·0640	4·80	3·33	0·95
e 12			5·80	1·020	14·6	19·7	22·5	12·7	118·8	−16·25	396	2·89	0·0738	10.58	7·34	1·095
f 1	carborundum	air	2·025	0·356	4·23	20·8	21·45	13·35	66·3	−1·3	304	2·60	0·0534	4·33	3·38	0·985
f 2	210–240 μ		2·41	0·422	5·03	20·8	21·95	13·25	77·7	−2·75	327	2·80	0·0575	5·15	4·02	1·06
f 3	$d = 225$ μ		1·65	0·289	3·45	20·8	21·8	13·1	65·9	−1·65	280	2·395	0·0492	3·53	2·76	0·908
f 4	$G_0 = 0{\cdot}084$		1·295	0·227	2·70	20·9	22·4	13·1	60·3	−1·95	238	2·035	0·0418	2·76	2·16	0·771
f 5	$\varphi' = 647$		0·978	0·172	2·05	20·2	23·65	13·05	57·9	−3·35	195	1·668	0·0342	2·10	1·64	0·632
f 6	$B = 0{\cdot}78$		0·649	0·114	1·36	20·8	24·8	13·0	36·0	−2·6	108	0·924	0·0190	1·392	1·09	0·350
f 7			2·815	0·494	5·88	21·0	22·85	13·1	93·1	−5·2	342	2·925	0·0602	6·02	4·70	1·11
f 8			3·60	0·631	7·52	21·2	23·25	13·1	97·5	−7·4	337	2·88	0·591	7·70	6·01	1·09
f 9			4·29	0·752	8·95	21·3	23·1	13·1	97·25	−7·7	340	2·905	0·597	9·15	7·15	1·10
f 10			5·85	1·027	12·22	21·4	22·65	13·1	96·0	−7·3	352	3·010	0·0619	12·52	9·80	1·14
f 11			4·82	0·846	10·07	21·5	22·65	13·05	95·5	−5·55	355	3·040	0·0624	10·30	8·04	1·15
b 14	carborundum	air	0·354	0·0621	7·6	20·8	21·65	14·0	44·8	−0·15	221	0·797	0·0644	0·319	—	—
		$\varrho = 0{\cdot}555$														
b 15	90–100 μ	$\varrho = 0{\cdot}507$	0·260	0·0456	6·3	20·7	22·35	13·95	44·8	−0·2	202	0·730	0·0601	0·234	—	—
b 16	$d = 95$ μ	$\varrho = 0{\cdot}645$	0·441	0·0773	8·3	20·7	20·75	13·95	45·1	−0·0	251	0·906	0·0700	0·397	—	—

* A complete table of all experimental results is obtainable from the authors upon request.

h has been plotted as a function of d for three different values of G/G_0 (3, 5 and 10). The points which were

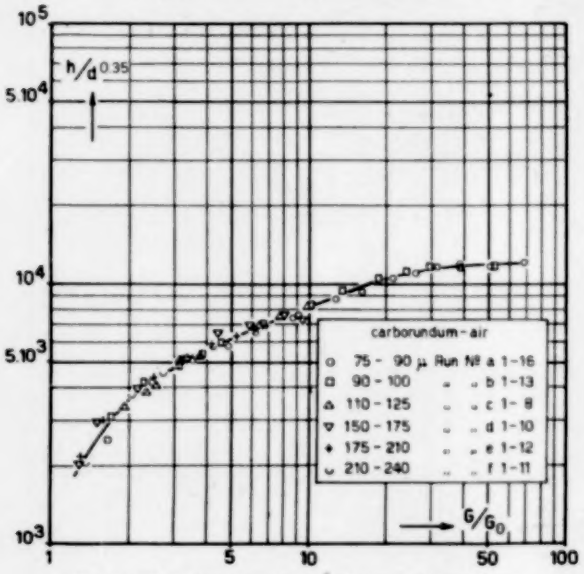

Fig. 6. Diameter correlation of the carborundum measurements.

interpolated from Fig. 4 are very satisfactorily correlated by parallel lines with a slope of 0·35

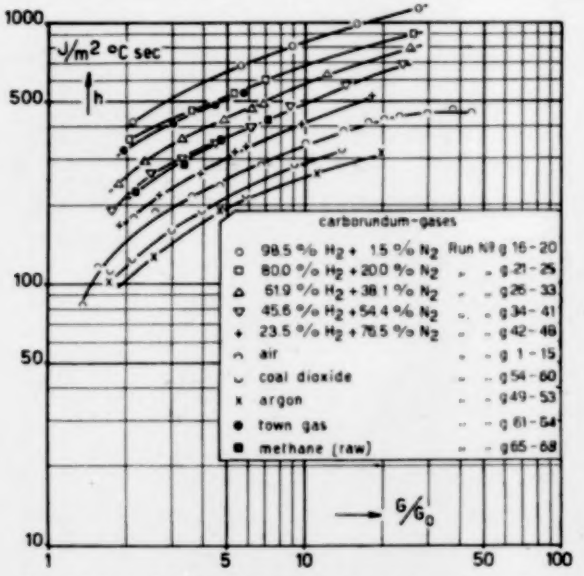

Fig. 7. h *vs* G/G_0 for different gases with carborundum 75–110 μ.

so that for the exponent of φ' in eq. (12) is found $y = -0{\cdot}45$.

In Fig. 6 the correlation of the diameter relationship is demonstrated by plotting $h/d^{0{\cdot}35}$ (instead of $Nu/\varphi'^{0{\cdot}45}$) versus G/G_0.

Prandtl exponent

Fig. 7 gives, again as a function of G/G_0, the transfer coefficients measured for the 75–110 μ carborundum fraction with various gases.

For determining the exponents x and z in eq. (12) we took advantage of the fact that the product ϱc_p is practically equal for all diatomic gases so that for the gases air, hydrogen and the hydrogen-nitrogen mixtures in combination with carborundum the number $\varrho c_p/\varrho_{bm} c_s$ is constant*.

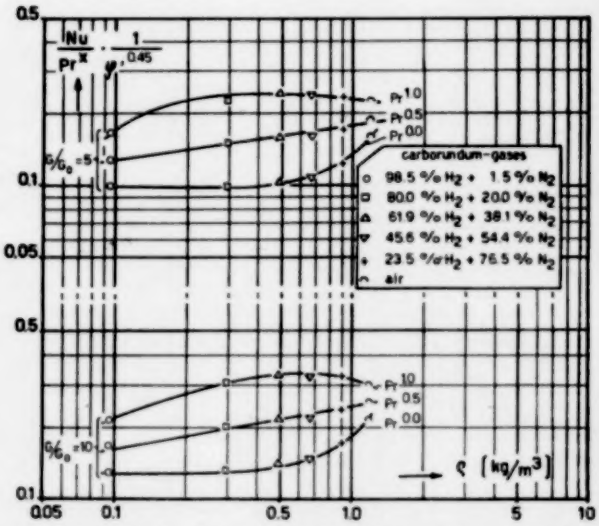

Fig. 8. Plot for determining the Pr-exponent x derived by interpolation from Fig. 7.

For the measurements of Fig. 7 with the above-mentioned diatomic gases Fig. 8 gives the number $Nu/Pr^x\varphi'^{0{\cdot}45}$ as a function of ϱ for a given value of G/G_0 and for $x =$ respectively 1, 0·5 and 0. From this Fig. the points of which have again been interpolated from Fig. 7, it appears that *only for* $x = 0{\cdot}5$ *a linear relationship occurs*. The variation in the value of Pr is too small to permit a more exact *definition* of this exponent. The value $x = 0{\cdot}4$ is rather satisfactory too.

Exponent of the ratios $\frac{\varrho_{bm}}{\varrho}$ *and* $\frac{\varrho\, c_p}{\varrho_{bm}\, c_s}$

For an exact determination of the exponent z of ϱ_{bm}/ϱ for the 75–110 μ fraction of coke, carborundum and iron oxide in combination with the diatomic gases the number $Nu/Pr^{0{\cdot}5}\varphi'^{0{\cdot}45}$ has been plotted in Fig. 9 versus ϱ for $G/G_0 = 5$ and 10. The points are again very satisfactorily correlated by a system of

* This is the reason why in (10) the number $\varrho c_p/\varrho_{bm} c_s$ was chosen instead of the quotient c_p/c_s which is perhaps more obvious.

parallel straight lines; from the slope of these lines it follows that $z = 0{\cdot}18$.

The fact that for $x = 0{\cdot}5$, $y = -0{\cdot}45$ and $z = 0{\cdot}18$ the results for the gases with equal values of ϱc_p are well correlated is proved by Fig. 10 where for all measuring results with these gases

$$\frac{Nu}{Pr^{0{\cdot}5}\,\varphi'^{0{\cdot}45}}\left(\frac{\varrho_{bm}}{\varrho}\right)^{0{\cdot}18}$$

has been plotted as a function of G/G_0.

Finally we still have to determine the exponent t. To this end Fig. 11 represents

$$\frac{Nu}{Pr^{0{\cdot}5}\,\varphi'^{0{\cdot}45}}\left(\frac{\varrho_{bm}}{\varrho}\right)^{0{\cdot}18}$$

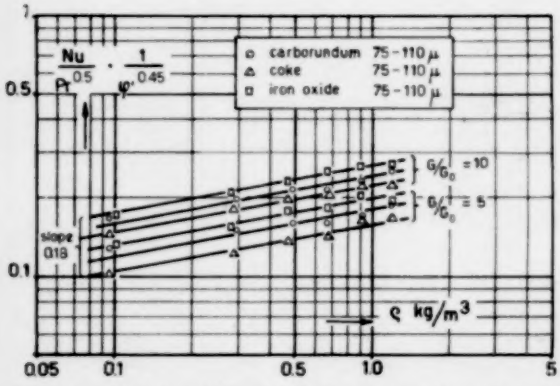

Fig. 9. Plot for determining the exponent z of ϱ_{bm}/ϱ from the results with diatomic gases (ϱc_p = constant).

for the various solid-gas system as plotted versus $\frac{\varrho c_p}{\varrho_{bm} c_s}$ for $G/G_0 = 5$ or 10 respectively. Because of the extreme values of the physical constants of Devarda's alloy and more particularly of lead, the results of these solids, which were only available as mixtures of different sizes, are also included here. It will later be shown more fully that the results on mixtures correlate very well with those on samples of closely cut sizes. These lines have a slope $t = 0{\cdot}36$, so that the ultimate correlation reads:

$$\frac{Nu}{Pr^{0{\cdot}5}\,\varphi'^{0{\cdot}45}}\left(\frac{\varrho_{bm}}{\varrho}\right)^{0{\cdot}18}\left(\frac{\varrho c_p}{\varrho_{bm} c_s}\right)^{0{\cdot}36} = f(G/G_0). \qquad (13)$$

All data points for which $Re < 5$ have been plotted in Fig. 12 in this way. In view of the extensive experimental data the spread proves to be satisfactorily small*.

From the course of the individual curves in Fig. 3 and from the correlation curve in Fig. 12 we may distinguish between three regions:

(1) $1 < G/G_0 < 2$, the transition region from the fixed bed ($G/G_0 = 1$) to complete fluidization. The

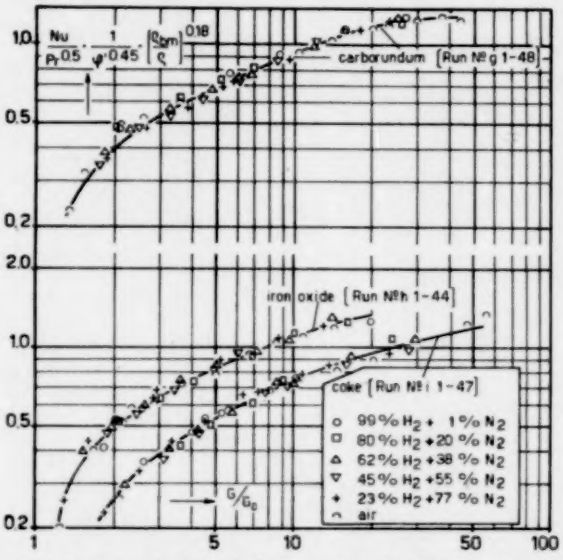

Fig. 10. Correlation of the gas properties for two atomic gases (ϱc_p = constant).

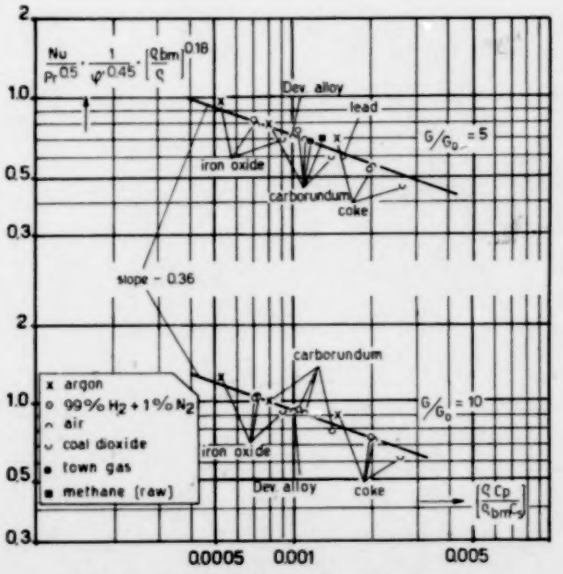

Fig. 11. Plot for determining the exponent t of $\varrho c_p/\varrho_{bm} c_s$.

* The values obtained with Ar, as plotted in Fig. 11 and 12, are systematically too high, those obtained with CO_2 too low, whereas the other systems of gases and solids give a good correlation with the aid of the number $\frac{\varrho c_p}{\varrho_{bm} c_s}$. This suggests the possibility that also the quotient $\varkappa$ of the specific heat values at constant pressure and constant volume should be included in the correlation. ($\varkappa_{Ar} = 1{,}67$, $\varkappa_{CO_2} = 1{,}30$, $\varkappa_{diatomic} = 1{,}40$.) The spread in the ultimate correlation is too large to permit a definite conclusion to be drawn on this point.

spread in this region is fairly large in consequence of the fact that one powder needs a greater value of G/G_0 than another to adopt a complete mobility.

For $G/G_0=2$ this was the case with all solids examined.

(2) $2<G/G_0<20$, the region with constant slope.

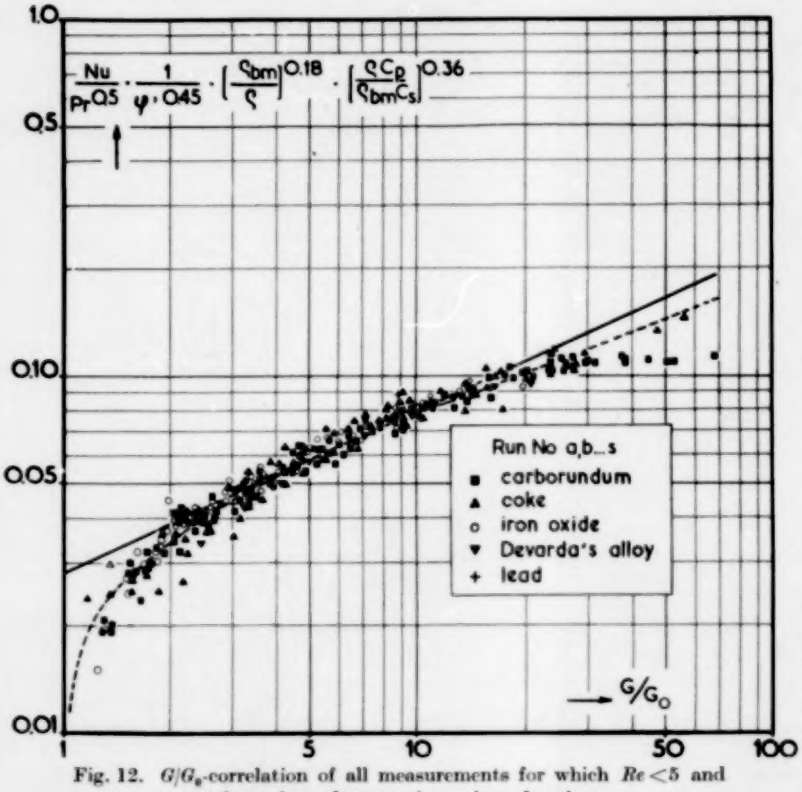

Fig. 12. G/G_0-correlation of all measurements for which $Re<5$ and performed on homogenious sieve fractions.

(3) $G/G_0>20$, in this region the slope decreases to become probably negative for larger values of G/G_0 than those applied by us (MICKLEY and TRILLING [3].

The transition at $G/G_0\sim20$ is undoubtedly related with the transition from dense phase to dilute phase fluidization.

A simple calculation shows that this transition must actually occur at such a value of G/G_0. It must be expected that the bed density will decrease greatly as soon as the gas rate becomes comparable with the velocity of free fall of the particles.

For smooth spheres the starting point of fluidization is defined by (see Part I, eq. 6):

$$Re_0=\frac{\varphi}{1350}. \tag{14}$$

For the velocity of free fall STOKES' law is valid:

$$Re_v=\frac{\varphi}{18}, \tag{15}$$

so that for $G/G_0=\frac{1350}{18}\sim75$ the velocity of free fall is reached. It is clear that an appreciable decrease of the bed density must occur much earlier since the gas rate between the particles in the bed at the original bed density already for $G/G_0=75\times$ porosity ~30 reaches the velocity of free fall.

The region $2<G/G_0<20$ can be described by the equation:

$$\left.\begin{aligned}\frac{Nu}{Pr^{0.5}}\frac{1}{\varphi'^{0.45}}\left(\frac{\varrho_{bm}}{\varrho}\right)^{0.18}\left(\frac{\varrho c_p}{\varrho_{bm}c_s}\right)^{0.36}\\ =0.028(G/G_0)^{0.45}.\end{aligned}\right\} \tag{16}$$

This equation is represented by the straight line in Fig. 12.

By substituting G/G_0-1 for G/G_0 a larger region of the correlation may be represented by a single equation, reading:

$$\left.\begin{aligned}\frac{Nu}{Pr^{0.5}}\frac{1}{\varphi'^{0.45}}\left(\frac{\varrho_{bm}}{\varrho}\right)^{0.18}\left(\frac{\varrho c_p}{\varrho_{bm}c_s}\right)^{0.36}\\ =0.035(G/G_0-1)^{0.36}.\end{aligned}\right\} \tag{17}$$

In Fig. 12 eq. (17) is represented by the dotted curve.

The equality of the exponent 0·45 of φ' and G/G_0 in (16) suggest that φ' should be transferred to the right-hand side of the equation resulting in a new variable $\varphi'.G/G_0$, which by means of the generalized shape factor $B=\frac{0.00123\,\varphi'}{Re_0}$, introduced in Part I, can be directly reduced to BRe.

In Fig. 13 all measuring results have been correlated on this basis, with the exception of those data points for which $G/G_0>20$ resp. <2.

As for the various particle sizes the transition for $G/G_0\sim20$ from dense phase to dilute phase fluidization occurs at different values of the Re-number, it is obvious that a correlation based on a kind of modified Re-number viz. BRe can never include the points $G/G_0>20$.

This also holds for the transition at $G/G_0=2$ so that the equation:

$$\frac{Nu}{Pr^{0.5}}\left(\frac{\varrho_{bm}}{\varrho}\right)^{0.18}\left(\frac{\varrho c_p}{\varrho_{bm}c_s}\right)^{0.36}=0.58(BRe)^{0.45} \tag{18}$$

derived from Fig. 13 is only valid for $2<G/G_0<20$ and $BRe<5$.

The nature of the variation of the data points with $Re>5$ is illustrated in Fig. 14, where h has

VOL. 1 1952

been plotted versus Re for those measuring series, which include experiments with $Re > 5$.

By way of comparison the "normal" curve for carborundum 75–90 μ has also been included. The Figure clearly shows that the transition to the region of decreasing slope, which in the case of the normal curve occurs for $G/G_0 \sim 20$, is more and more shifted to the left side according as the curve is shifted to higher Re-numbers. The transition to decreasing slope now occurs for $Re \sim 5$ so that for those curves for which $G/G_0 = 2$ already corresponds with $Re > 5$, the linear upward slope for $G/G_0 > 2$ even does not occur at all. From some measurements with glass beads ($\varnothing \sim 1$ mm) h shows a marked decline already for $G/G_0 = 2$.

A possible explanation of the nature of these deviations for $Re > 5$ in the G/G_0 correlation is the following. In the region of complete turbulence ($Re > 100$) LEVA [3] finds for the pressure drop in a bed of spheres:

$$\Delta p \sim \frac{2G^2}{d\varrho_g} \frac{1-\delta}{\delta^3}, \qquad (19)$$

from which for the starting point of fluidization (see Part I) is found:

$$Re_0 = 0{\cdot}2 \sqrt{\varphi}. \qquad (20)$$

For the velocity of free fall Newton's law is valid:

$$Re_v = 1{\cdot}7 \sqrt{\varphi}. \qquad (21)$$

From this it follows that in the region of turbulence the velocity of free fall is reached already for $G/G_0 \sim 8{\cdot}5$, whereas in the viscous region $G/G_0 \sim 70$ was found. The transition from dense phase to dilute phase fluidization which for $Re < 5$ occurs for $G/G_0 \sim 20$ may therefore be expected already at $G/G_0 \sim 2{\cdot}5$. This is in accordance with Fig. 14 where for increasing particle sizes this transition occurs at ever decreasing G/G_0-values.

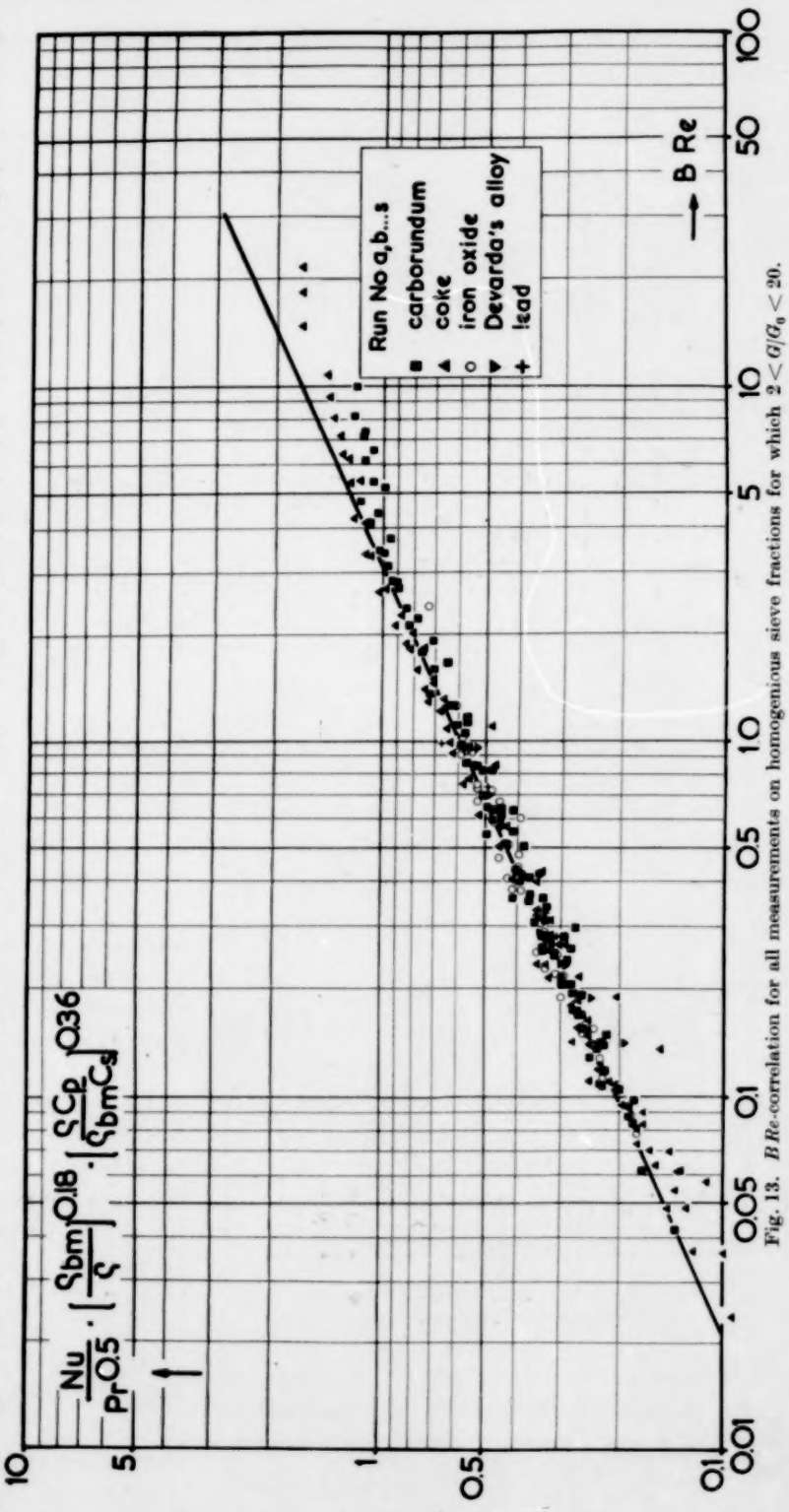

Fig. 13. BRe-correlation for all measurements on homogenious sieve fractions for which $2 < G/G_0 < 20$.

The points for which $Re > 5$ have been included in the BRe correlation of Fig. 13. From this it proves that these data points are now actually

correlated although the transition is revealed by a decreasing slope.

Summarizing we may say that the G/G_0 correlation of Fig. 12 is confined to the region of viscous flow

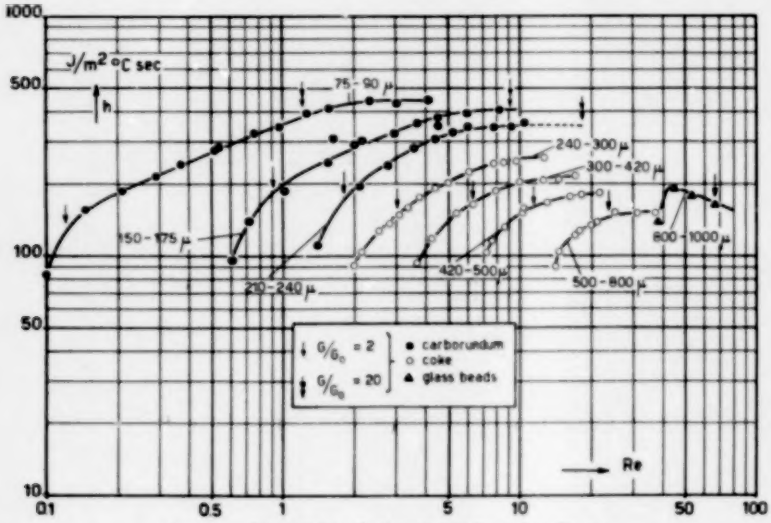

Fig. 14. Character of the deviations for $Re > 5$.

($Re < 5$), whereas BRe correlation of Fig. 13 is subject to the restriction $2 < G/G_0 < 20$.

It would not seem excluded, however, that the BRe correlation may also be extended for $G/G_0 > 20$ if the

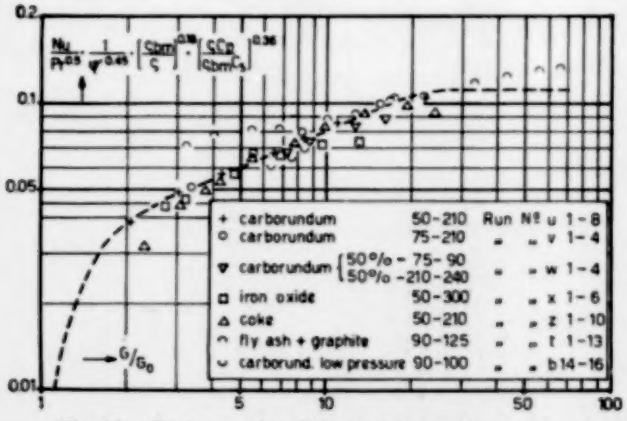

Fig. 15. Check on the G/G_0 correlation by means of some special measurements.

actual density of the fluidizing bed is introduced as a variable instead of the density of the fixed bed. A further extension of the experimental data is therefore required.

CONTROL OF THE CORRELATION FOUND

The correlation of Fig. 12 is based on more or less homogeneous sieve fractions. Since as a rule narrow sieve fractions are less suitable for fluidization than mixtures of various particle sizes, heat transfer measurements were carried out with some *mixtures* of iron oxide, carborundum and coke. The results of these measurements have been compared in Fig. 15 with the correlation curve of Fig. 12: the correspondence proves to be quite satisfactory. The influence of the diameter ($d^{0.35}$) is too small for a reliable conclusion to be given on the question whether, as in the case of the correlation of the starting point of fluidization (see Part I) also here the definition according to eq. (7) of the average diameter of a mixture is the most correct.

With a view to the largest possible variation in the properties of the solid it seemed worth while to make a few measurements with the light fly ash. It proved, however, that during fluidization of this fly ash, serious electrostatic effects occurred, so that the reproducibility of the values measured for the heat transfer coefficient was very small*. By mixing fly ash with approx. 10% graphite (conductor!) these charging phenomena can be avoided.

A new trouble now experienced was the increasing segregation of the fly ash and the graphite at a decreasing gas rate. This phenomenon is probably responsible for the slight deviations of these results from our correlation (Fig. 15).

Since k, μ and c_p are substantially independent of the gas pressure it was possible to control the influence of the gas density ϱ, as it occurs in the correlation, by pressure variation and independent of the other properties of the gas. The apparatus was not suitable for pressures higher than one atmosphere so that our measurements were restricted to lower pressures. The resulting data points are also included in Fig. 15 and satisfy the correlation reasonably.

Finally Fig. 16 gives the results of other investigators as compared with the correlation found by ourselves. Only in LEVA's paper the values of the starting point of fluidization under the experimental conditions of the heat transfer measurements are mentioned. In LOGWINUK's experiments, G_0 was determined at room temperature, so that for every

* See foot note on page 52.

measurement this value had to be recalculated for the temperature at which the heat transfer was determined viz. 100–300° C. MICKLEY and TRILLING do not mention a G_0 value at all. Since these investigators only used spheres for their experiments it was possible to calculate G_0 from (14).

There is no correspondence between the correlation found by us and the results obtained by LEVA *et al*, as could be expected already in view of the correlating eq. (2) used by them. This great deviation may exclusively be due to the different experimental procedures.

A better correspondence exists with LOGWINUK's results though even here the differences are still considerable. This may be due to the fact that LOGWINUK measures heat transfer to a tube placed axially in the centre of the bed, whereas our measurements refer to heat transfer to the wall. MICKLEY and TRILLING found a marked difference for these two cases. In addition the accuracy of LOGWINUK's measurements is substantially limited as a result of the fact that the correction for the resistance to heat flow at the side of the cooling water is considerable.

Of MICKLEY's and TRILLING's measurements of transfer to the wall only a very limited number could be compared with our correlation since the greater part of their experiments were made at $G/G_0 > 100$ or $Re > 5$. Although their results are approx. 25% lower than ours their data points are located more or less parallel to our correlation curve.

When this paper was ready for printing we came across an article by BAERG, KLASSEN and GISHLER [9], who measured heat transfer of a fluidized bed in dense phase to a copper tube placed along the axis of the bed. The solids used were iron, sand, silicon, Scotchlite beads, a cracking catalyst and alumina, the fluidizing gas was air. The relation used by the authors to correlate their results is rather artificial and far from dimensionless. Their results are included in Figure 16. Taking account of the uncertainty in the specific heat of the solids, which quantity was not mentioned by them and of the fact that their particle diameters were determined microscopically, which method usually leads to higher values than a screening analysis, the agreement with our correlation is reasonably good.

Finally it was interesting to check the validity of our correlation formulas for the calculation of heat transfer coefficients in fluidized beds on a technical scale. The authors had the opportunity to carry out a single measurement in a fluidizer on a semi-technical scale. The solid used was calcium sulfite powder (50–500 μ), the fluidizing gas was nitrogen and the temperature of the bed 320° C.

The height of bed was 2·30 m and the diameter was 30 cm. The heat transfer coefficient to a water cooled tube of 1 m length and 3·5 cm diameter was determined by measuring the in- and outlet temperatures of the cooling water. The result for G/G_3—25

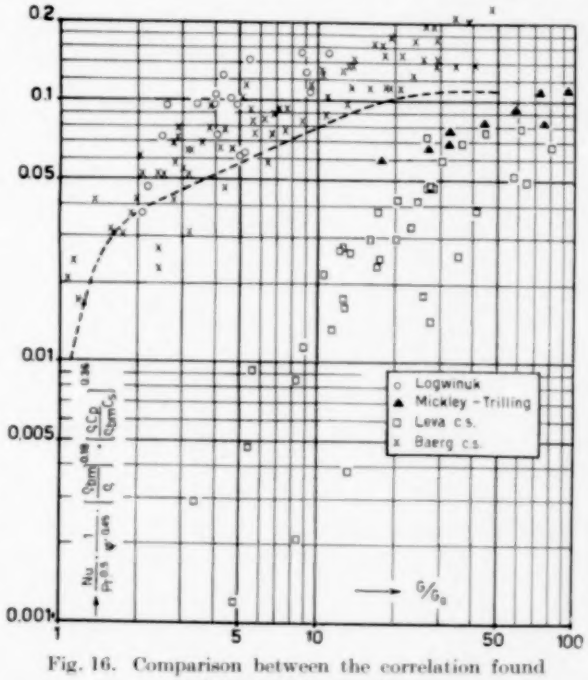

Fig. 16. Comparison between the correlation found and the results of others.

was 315 J/m² °C sec which was only 10% lower than the value calculated from our correlation. Though the agreement of a single measurement is quite insufficient to establish the accuracy of our correlation for the design of large scale equipment, it will certainly satisfy the need of a rather accurate estimation.

NOTATION

A = surface area of cooler, m² (= 10·76 ft²)
B = generalized shape factor (dimensionless)
G = mass velocity based on empty tube, kg/m² sec (= 738 lb/ft² hr)
G_0 = critical mass velocity
G/G_0 = reduced mass velocity (dimensionless)
$Nu = \frac{h \cdot d}{k}$ Nusselt number (dimensionless)
$Pr = \frac{c_p \mu}{k}$ Prandtl number (dimensionless)
$Re, Re_0 = \frac{G d}{\mu}$ resp. $\frac{G_0 d}{\mu}$ Reynolds number (dimensionless)

c_p, c_s = specific heat of gas (at constant pressure) of solid J/kg °C (0·00024 BTU/lb °F)
d = particle diameter based on screen analysis m (= 3·28 ft)
g = acceleration of gravity 9·8 m/sec² (= 4·13 × 10^8 ft/hr²)
h = heat transfer coefficient J/m² °C sec (= 0·176 BTU/hr ft² °F)
k, k_s = heat conductivity of gas or solid J/m °C sec (= 0·578 BTU/ft °F h)
q_e, q_g = quantity of heat per unity of time delivered by electric coil resp. by flowing gas J/sec (= 3·415 BTU/h)
t_g, t_b, t_w = temperature of gas, resp. of bed, or of wall °C
w = mass flow rate kg/sec (= 7920 lb/h)
$\varphi = \frac{\varrho \varrho_s g d^3}{\mu^2}$, $\varphi' = \frac{\varrho \varrho_{bm} g d^3}{\mu^2}$ (dimensionless)
δ = porosity of the bed (dimensionless)
Δp = pressure drop through bed N/m² (= 8·7 × 10^6 lb force/ft²)
μ = dyn. viscosity of gas kg/m sec (= 2420 lb/hr ft)
ϱ, ϱ_s = density of gas or of solid kg/m³ (= 0·0624 lb/ft³)
ϱ_{bm} = density of bed at maximal porosity
ϱ_f = density of fluidizing bed

References

[1] van Heerden, Nobel and v. Krevelen; Chem. Eng. Sci. 1951 **1** No. 1. [2] Ibbs and Hirst; Proc. Roy. Soc. (London) 1929 **123** A 134. [3] Leva, M.; Chem. Eng. Prog. 1947 **43** 549. [4] Leva, M., Weintraub, M. and Grummer, M.; Chem. Eng. Prog. 1949 **45** 563. [5] Lindsay, A. L. and Le Roy A. Bromley,; Ind. Eng. Chem. 1950 **12** 1508. [6] Logwinuk, K.; *Thesis* Case Inst. Techn. Aug. 1948. [7] Mickley, H. S. and Trilling, C. A.; Ind. Eng. Chem. 1949 **41** 1135. [8] Perry, J. H.; Chem. Eng. Handbook 2nd ed. 1941 [9] Baerg, A., Klassen, J. and Gishler, P. E.; Can. J. Res., Sect. F 1950 **28** 287.

VOL. 1 1952

Estimation of the free enthalpy (Gibbs free energy) of formation of organic compounds from group contributions

D. W. van Krevelen and H. A. G. Chermin

Staatsmijnen in Limburg, Central Laboratory, Geleen, The Netherlands

(Received 6 May 1951)

Summary—A method is proposed whereby the free enthalpy of formation of organic compounds in the ideal gaseous state is resolved into contributions attributable to atomic groups.

Free enthalpies of formation of complex molecules are readily estimated by summation of the contributions of their component groups. The average deviation of the free enthalpy of formation of organic compounds calculated by this method is ± 0·6 kcal/mol.

I. Introduction

Now and again every chemist and chemical engineer will face the problem whether the preparation of a particular product according to a new reaction-principle is possible.

Chemical thermodynamics, enabling chemical equilibria to be calculated, can give the solution to this problem, provided sufficient data be known about reactants and reaction products.

In fact, the thermodynamic potentials constitute the driving forces causing every natural process to proceed in the direction of its eventual state of equilibrium.

Whether or not a reaction will proceed depends on kinetic factors. A certain amount of *activation energy* is necessary to keep up practically any reaction. However, in many of the cases in which a reaction was thermodynamically possible it also proved possible to find a catalyst that was sufficiently active and selective to realize this reaction.

The combined knowledge of the thermodynamic driving forces and of the corresponding rate factors presents the stock from which the chemical engineer may take the data enabling him to calculate converters. Thermodynamics determine the *possibility*, kinetics the *rate* of the process.

Unfortunately the application of thermodynamics is in many cases handicapped by a lack of sufficient data. In these cases it is important to have at hand a simple and quick method for calculating these data, if only by approximation. This will provide an insight into the ranges of temperature and pressure in which to look for a catalyst.

II. Thermodynamic Stability and Equilibrium

Given the reaction of formation of a compound C from its composing elements E_1 and E_2

$$n E_1 + m E_2 \rightleftharpoons C. \qquad \text{(II-1)}$$

The equilibrium of reaction (II–1) at a given temperature, is given by the equilibrium-constant

$$K_f = \frac{(C)}{(E_1)^n \cdot (E_2)^m} \cdot \qquad \text{(II–2)}$$

Thermodynamics gives the relation between the equilibrium-constant and the free enthalpy of formation

$$\Delta G_f = -R \cdot T \cdot \ln K_f. \qquad \text{(II–3)}$$

From (II–2) we see that the equilibrium in (II–1) is shifted to the right if $K_f > 1$ and to the left if $K_f < 1$, from which it follows that—bearing in mind (II–3)—the equilibrium lies to the right in (II–1) if ΔG_f is negative and to the left if ΔG_f is positive. In other words: at a given temperature a compound is stable if at that temperature $\Delta G_f < 0$.

The value of ΔG_f is a measure of the stability of a compound with respect to the elements. If it be asked to define the position of the equilibrium of the reaction

$$C + D \rightleftharpoons F + G \qquad \text{(II–4)}$$

this equilibrium is determined by the constant

$$K_{eq} = \frac{(F) \cdot (G)}{(C) \cdot (D)} \cdot \qquad \text{(II–5)}$$

Which again bears relation to the change in free enthalpy in consequence of the reaction

$$\Delta G_{\text{reaction}} = -R \cdot T \cdot \ln K_{eq} \qquad \text{(II–6)}$$

in which

$$\Delta G_{\text{reaction}} = \Delta G_{f_F} + \Delta G_{f_G} - \{\Delta G_{f_C} + \Delta G_{f_D}\}. \qquad \text{(II–7)}$$

If the free enthalpy of formation of the compounds participating in the equilibrium is known, it is possible to calculate the position of this equilibrium.

From the preceding it follows that it is of great importance to know the numerical value of the free enthalpy of formation.

III. Molecular Structure and Thermodynamic Properties of Organic Compounds

Only a very small part of the overwhelming number of known organic compounds have been examined for their thermodynamic behaviour; besides it is highly improbable that the thermodynamic data of all these compounds will ever be measured exactly. Hence it is obvious that methods have been and are being sought to calculate these data.

Theoretically it is possible to calculate these data according to a statistical-mechanical method. However, this method is very laborious and moreover the spectroscopic data required to this end are usually lacking. Of late years Rossini and co-workers [39] have performed excellent work on the subject in the National Bureau of Standards (A.P.I. Research project 44).

For years a method has been sought to calculate the numerical values of thermodynamic properties in a simple manner and with the help of as few data as possible. More or less rough correlations between structure and thermodynamic properties have been known for a long time, as may be seen *e.g.* from the work of Karasch [30] and Parks and Huffman [34]. Only of late years did it prove possible to state a more or less accurate relation between structure and thermodynamic properties of an organic compound. Some methods will be mentioned here:

1. *The method of Anderson, Beyer and Watson* [1]

These investigators consider every compound to be built up of a base group in which other molecular groups were substituted for the atoms in the base group. They make corrections for contributions from double bonds, cis- and trans-isomerization, conjugation effects and ortho-meta and para-substitution. In this way they consider *e.g.* all the paraffins as derived from the base group methane by substituting the hydrogen atoms by CH_3 groups. In a similar manner they obtain values for the secondary amines by starting from the base group $HN(CH_3)_2$.

The disadvantage of this method is that it only gives values for the heats of formation and the entropies at 25° C, so that the free enthalpies of formation, the heats of formation and the entropies at other temperatures have to be calculated with the help of a correlation of specific heat given by them. Moreover the result of their method depends upon the way selected in building up the equation for the specific heat.

2. *The method of Souders, Matthews and Hurd* [46]

Souders, Matthews and Hurd consider specific heat, heat content, heat of formation and entropy of a hydrocarbon as built up of vibration-, rotation- and translation-contributions of the composing molecular groups. In this way a thermodynamic magnitude of 2-methyl-pentane is *e.g.* built up of:

(a) Vibration contributions from:
3 —CH_3 groups, 2 —CH_2 groups and 1 —CH group
(b) Internal rotation contributions from:
3 groups rotating about the —CH group, 1 —CH_2—CH_2— rotation and 1 CH_3—CH_2— rotation.
(c) Translation contribution amounting to $4R$.
(d) In calculating the entropy a symmetry correction amounting to $R \ln \sigma$ (see note page 69).

This method gives very accurate results (see the original publication); however, it has the disadvantage of requiring a rather extensive knowledge of the molecular structure.

3. *The method of Bremner and Thomas* [9]

Bremner and Thomas developed a method for calculating the free enthalpy of formation of organic products based on the assumption that the molecule is built up of characteristic groups each of which giving a certain contribution to the free enthalpy of formation. Corrections for conjugation and mutual influence of various groups are not given by these investigators. However, they do give corrections for the formation of cyclohexane, cyclohexene, the furane ring and the tetrahydro-furane ring. The comparison between the free enthalpy of formation calculated according to their method and the known enthalpy is very concise, so that it is impossible to judge the value of this method from their publication. However, a comparison of this method with the other methods of calculation mentioned here renders the accuracy of the Bremner and Thomas correlation doubtful.

Temperature °K	$\frac{1}{T}(G^\circ - H_0^\circ)$ *cal. mol.*$^{-1}$. °K^{-1}					
	$i\,C_3H_7OH$		$CH_3—\overset{H}{\underset{|}{C}}=O$		CH_3COCH_3	
	calc.	*lit.* [44]	*calc.*	*lit.* [37]	*calc.*	*lit.* [21]
298·16			−51·50	−52·85	−58·69	−57·53
400	−64·82	−64·68	−55·03	−56·03	−62·64	−61·67
500	−68·64	−68·81	−58·04	−58·67		
600			−60·62	−61·05	−69·22	−68·55
800			−65 14	−65·28	−74·99	−74·40
1000			−69·12	−69·03	−80·19	−79·72
1200					−85·44	−84·61
1400					−89·95	−88·93
1500					−92·17	−91·10

4. *Rossini's rule*

A rather accurate correlation for calculating thermodynamic magnitudes is applied by Rossini and co-workers in compiling the A.P.I.–N.B.S. tables for the thermodynamic magnitudes of gaseous hydrocarbons (see references given in [39]). These investigators consider the thermodynamic magnitude as built up of the corresponding magnitudes of compounds with analogous structure, *e.g.*

$$\left.\begin{aligned}\Phi_{CH_3—\overset{CH_3}{\underset{CH_3}{\overset{|}{\underset{|}{C}}}}—CH=CH_2} &= \Phi_{CH_3—CH=CH_2} + \\ &+ \Phi_{CH_3—\overset{CH_3}{\underset{CH_3}{\overset{|}{\underset{|}{C}}}}—CH_3} - \Phi_{CH_3—CH_3}\end{aligned}\right\} \quad \text{(III–1)}$$

in which Φ is equal to $S^\circ - R\,.\ln\sigma$; $\dfrac{G^\circ - H_0^\circ}{T} - R\,.\ln\sigma$; $H^\circ - H_0^\circ$; C_p°; ΔH_f° or $\Delta G_f^\circ - R\,.\,T\,.\ln\sigma$.
Rossini and co-workers found that this rule gave excellent results with hydrocarbons.

It is of importance to know whether this rule is also applicable to non-hydrocarbons. Pitzer [6] states that it is possible to calculate the thermodynamic magnitudes of the higher normal mercaptans in this way, starting from ethyl mercaptan. In this manner the thermodynamic magnitudes of three compounds were calculated, by which it was found that the magnitudes obtained in this way tally very well with the corresponding magnitudes calculated from spectroscopic data *.

* Calculated were the free enthalpy functions of isopropyl alcohol, acetic aldehyde and acetone:

Free enthalpy functions were chosen in order to prevent the heat of formation from being introduced into the calculations, for as a rule the heat of formation is known only with insufficient accuracy. Due to a lack of necessary data it proved impossible to carry out more extensive control calculations. The calculations made, however, are sufficient proof of the validity of Rossini's rule for the carbon-carbon bond.

From this it may be concluded that this method, in as far as carbon-carbon bonds are concerned, gives rather accurate results. Pitzer [6] proposes a calculation of the thermodynamic data of dimethyl sulphoxide and dimethyl sulphone according to:

$$\left.\begin{aligned}\Phi_{(CH_3)_2SO} &= \Phi_{CH_3—S—CH_3} + \Phi_{SO_2} - \Phi_{SO_2} \\ \Phi_{(CH_3)_2SO_2} &= \Phi_{(CH_3)_2SO} + \Phi_{SO_2} - \Phi_{SO_2}.\end{aligned}\right\} \quad \text{(III–2)}$$

Owing to a lack of data it is impossible to check the validity of Rossinis rule for bonds other than carbon-carbon.

5. *Franklin's method* [15]

Franklin considers the molecule to be built up of molecular groups, each of which giving a particular contribution to the thermodynamic property. He gives group contributions to the heat of formation, heat content, free enthalpy function and free enthalpy of formation. In calculating the free enthalpy function and the free enthalpy of formation he applies a correction for symmetry (see note page 69).

For hydrocarbons Franklins method gives results within 2 kcal/mol. The value of the few group contributions he gives

$$\Phi_{CH_3—\overset{H}{\underset{CH_3}{\overset{|}{\underset{|}{C}}}}—OH} = \Phi_{CH_3—\overset{CH_3}{\underset{CH_3}{\overset{|}{\underset{|}{C}}}}—H} + \Phi_{C_2H_5OH} - \Phi_{C_2H_6}$$

$$\Phi_{CH_3—\overset{H}{\underset{|}{C}}=O} = \Phi_{CH_2O} + \Phi_{n\,C_4H_{10}} - \Phi_{C_3H_8}$$

$$\Phi_{CH_3—\overset{O}{\underset{||}{C}}—CH_3} = 2\,\Phi_{CH_3—\overset{H}{\underset{|}{C}}=O} - \Phi_{CH_2O}.$$

VOL. 1 1952

for non-hydrocarbons is doubtful. A more extensive discussion of Franklin's method, which is a very simple one, will be found hereafter.

IV. Modified Franklin Correlation for the free Enthalpy of Formation of Organic Compounds in the Ideal Gaseous State

Starting from a statistical-mechanical calculation by Pitzer [35] Franklin proved that a thermodynamic function of an arbitrary paraffin hydrocarbon may be built up as the sum of contributions from characteristic groups, of which that hydrocarbon may be conceived to be built up, and, if required, with the addition of a correction for the symmetry of the molecule. As this method gave excellent results for the paraffins Franklin assumed that it also held good for the other hydrocarbons, which afterwards appeared to be true. So for the free enthalpy of formation of a hydrocarbon we may put:

$$\Delta G_{f_{\text{h.c.}}} = \sum \begin{matrix}\text{contributions of}\\ \text{composing groups}\end{matrix} + R \,.\, T \,.\, \ln\sigma \quad \text{(IV–1)}$$

in which $R \,.\, T \,.\, \ln\sigma$ represents the correction for the symmetry*. The equation (IV–1) did not give accurate results over the entire range; for certain forms of molecules constant deviations were found. In order to make up for this Franklin introduced corrections for these forms of molecules, so that consequently (IV–1) changes into:

$$\left.\Delta G_{f_{\text{h.c.}}} = \sum \begin{matrix}\text{contributions of}\\ \text{composing groups}\end{matrix} + \sum \begin{matrix}\text{corrections}\\ \text{if necessary}\end{matrix} + \right\} \text{(IV–2)}$$
$$+ R \,.\, T \,.\, \ln\sigma \,.$$

Franklin denotes contributions to the enthalpy of formation at 0; 298·1; 400; 500; 600; 800; 1000; 1200 and 1500° K, which he calculates from the first terms of the homologous series.

Franklin's method gives information only for the temperatures at which contributions are given. In the present paper this is obviated by considering the group contributions as a linear function of the temperature.

$$\Delta G_{f_{\text{group}}} = A + \frac{B}{100} \,.\, T. \quad \text{(IV–3)}$$

This was based on an argumentation by Scheffer [43]. The equation (IV–3) shows a strong similarity to the general equation

$$\Delta G = \Delta H - T \,.\, \Delta S. \quad \text{(IV–4)}$$

If (IV–3) and (IV–4) are compared it follows that A has the dimension of a heat of formation and $B/100$ has the dimension of an entropy of formation. According to Ulich [54] A is by approximation equal to the heat of formation at 298·1° K and $B/100$ approximately the entropy of formation at 298·1° K.

It proved impossible to describe the variation of the contribution to the free enthalpy of formation in the entire temperature interval (300 ÷ 1500° K) by one linear temperature function. However, it was possible to represent the temperature dependence for all the contributions by two straight lines in the ranges 300 ÷ 600° K and 600 ÷ 1500° K.

V. Method of Calculation

The values for the free enthalpy of formation are as a rule stated for the ideal gaseous state at a fugacity of 1 atm. This also holds for the group contributions given in this paper.

As a basis for the calculation of the free enthalpy of formation contributions for hydrocarbon groups the free enthalpies of formation as given in the publications of the A.P.I. research project 44 [39], [40], [41] and [42] were chosen, with the addition of data concerning the free enthalpies of formation of cyclopropane [2] and naphthalene [6a].

Group contributions for non-hydrocarbon groups were calculated from data found in various publications. For the non-hydrocarbons only the free enthalpy function and the heat content are given in most cases, from which the free enthalpy of formation is calculated in the following manner:

$$\Delta G_f = T \,.\, \Delta\left(\frac{G^0 - H_0^0}{T}\right)_f + \Delta H_f^0 - \Delta(H^0 - H_0^0)_f \quad \text{(V–1)}$$

in which

$$\left.\begin{aligned}&\Delta\left(\frac{G^0 - H_0^0}{T}\right)_f\\ &= \left(\frac{G^0 - H_0^0}{T}\right)_{\text{compound}} - \sum \left(\frac{G^0 - H_0^0}{T}\right)_{\substack{\text{composing}\\ \text{elements}}}\end{aligned}\right\} \text{(V–2)}$$

and

$$\left.\begin{aligned}&\Delta(H^0 - H_0^0)_f\\ &= (H^0 - H_0^0)_{\text{compound}} - \sum (H^0 - H_0^0)_{\substack{\text{composing}\\ \text{elements}}}.\end{aligned}\right\}$$

The functions $\left(\frac{G^0 - H_0^0}{T}\right)$ and $(H^0 = H_0^0)$ are as a rule calculated from spectroscopic data and are fairly

* The symmetry number.

This is: "The number of indistinguishable positions in space the molecule may be made to take up by a simple rigid rotation."

The symmetry number of a molecule may be found by considering a space model of the molecule concerned. A great number of symmetry numbers is given in Herzberg's publication [25].

accurate. The magnitude ΔH_f^0 is calculated from the heat of combustion. In calculating the group contributions no values for ΔH_f^0 or for the heat of combustion of the compound were found in some cases. Then the heat of formation was calculated by means of the correlation given by ANDERSON, BEYER and WATSON [1], which for this magnitude corresponds rather well with the real values. Furthermore for the non-hydrocarbons, data were not always available up to the 1500° K limit. It was assumed that in these cases the temperature dependency up to 1500° K is approximated with sufficient accuracy by the formula given. In these cases the highest limit at which data from the literature were still available is denoted.

Table 1. Alkane-groups

Group	Group contribution $A + \frac{B}{100} \cdot T$ kcal/mol			
	300 ÷ 600° K		600 ÷ 1500° K	
	A	B	A	B
CH_4	−18·948	2·225	−21·250	2·596
$-CH_3$	−10·943	2·215	−12·310	2·436
$-CH_2-$	− 5·193	2·430	− 5·830	2·544
$-\overset{\vert}{C}H$	− 0·705	2·910	− 0·705	2·910
$-\overset{\vert}{C}-$	+ 1·958	3·735	+ 4·385	3·350

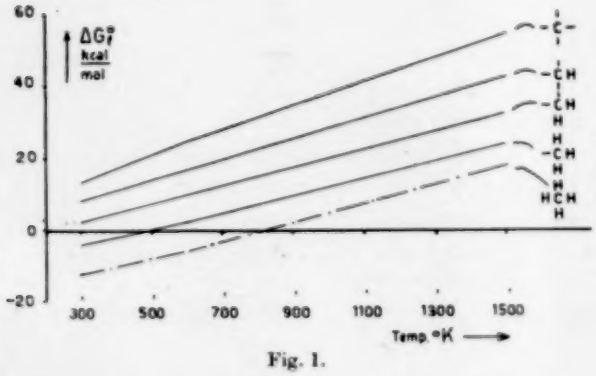

Fig. 1.

VI. THE GROUP CONTRIBUTIONS

1. Hydrocarbon groups

Contributions to the free enthalpy of formation were calculated for the various groups. In as far as possible average values were chosen for the contributions. The separate classes of group contributions will be discussed hereafter.

(a) Alkanes

As starting point for calculating the group contributions we chose the value for the $-CH_2-$ contribution, as given in [39]. Starting from this we calculated, by means of the formula (IV–2), contributions for the $-CH_3$, $-\overset{\vert}{C}H$ and $-\overset{\vert}{C}-$ groups. The results of these calculations are represented in Table 1.

Table 2. Alkene-groups

Group	Group contribution $A + \frac{B}{100} \cdot T$ kcal/mol			
	300 ÷ 600° K		600 ÷ 1500° K	
	A	B	A	B
$H_2C=CH_2$	+11·552	1·545	9·450	1·888
$H_2C=C\diagup^{H}$	13·737	1·655	12·465	1·762
$H_2C=C\diagup$	16·467	1·915	16·255	1·966
$H\diagup C=C\diagup^{H}$	17·663	1·965	16·180	2·116
$H\diagup C=C\diagup_{H}$	17·187	1·915	15·815	2·062
$H\diagup C=C\diagup$	20·217	2·295	19·584	2·354
$\diagup C=C\diagup$	25·135	2·573	25·135	2·573
$H_2C=C=CH_2$	45·250	1·027	43·634	1·311
$H_2C=C=C\diagup^{H}$	49·377	1·035	48·170	1·208
$H_2C=C=C\diagup$	51·084	1·474	51·084	1·474
$H\diagup C=C=C\diagup^{H}$	52·460	1·483	52·460	1·483

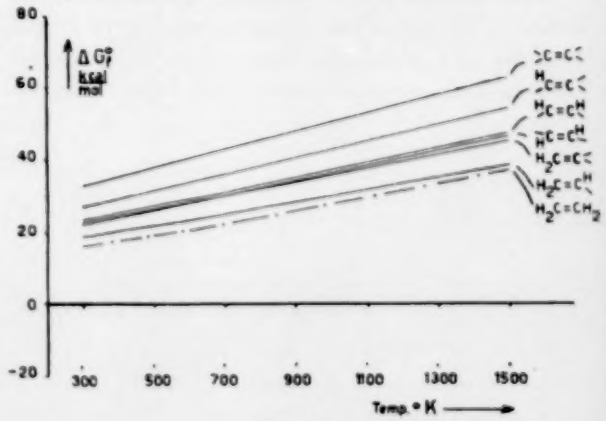

Fig. 2.

(b) Alkenes

Starting from the group contributions represented in Table 1 we calculated group contributions for alkene groups. It proved not possible to calculate contributions of sufficient constancy for the $H_2C=$ group. However, it was possible to calculate contributions for

VOL. 1 1952

the groups $H_2C{=}C\overset{H}{<}$; $H_2C{=}C<$; $H\overset{}{C}{=}C\overset{H}{<}$; $>C{=}C\overset{H}{<}$; $H_2C{=}C{=}C\overset{H}{<}$; $H_2C{=}C{=}C<$ and $H\overset{}{C}{=}C{=}C\overset{H}{<}$.

(c) Conjugated alkenes

In order to avoid correlations for conjugation effects, which correlations are neither constant, contributions were calculated for characteristic resonance groups that will be denoted by a double-headed arrow. Contributions were calculated for the $H_2C{\leftrightarrow}$; $H\overset{}{C}{\leftrightarrow}$ and $>C{\leftrightarrow}$ groups.

Table 3. Conjugated alkene-groups

Group	Group contribution $A + \frac{B}{100} \cdot T$ kcal/mol			
	300 ÷ 600° K		600 ÷ 1500° K	
	A	B	A	B
$H_2C{\leftrightarrow}$	5·437	0·675	4·500	0·832
$H\overset{}{C}{\leftrightarrow}$	7·407	1·035	6·980	1·088
$>C{\leftrightarrow}$	9·152	1·505	10·370	1·308

(d) Alkynes

As starting point for the contributions for the alkyne groups we chose the half of the value of the free enthalpy of formation of acetylene after subtraction of the correction for the symmetry. With the help of the contribution for the $HC{\equiv}$ group obtained in this way we calculated the contribution to the free enthalpy of formation for the $-C{\equiv}$ group.

Table 4. Alkyne-groups

Group	Group contribution $A + \frac{B}{100} \cdot T$ kcal/mol			
	300 ÷ 600° K		600 ÷ 1500° K	
	A	B	A	B
$HC{\equiv}$	27·048	−0·765	26·700	−0·704
$-C{\equiv}$	26·938	−0·525	26·555	−0·550

(e) Aromatics

As was the case with the conjugated alkenes, we also calculated contributions for the resonance groups for the aromatics. $HC\rightleftarrows$ was calculated from benzene and with the help of this group the $-C\rightleftarrows$ group was calculated. For the condensed aromatics we calculated the $\leftrightarrow C\rightleftarrows$ group from a free enthalpy function of naphthaline [6a] and the heat of combustion of naphthalene [28].

Table 5. Aromatic-groups

Group	Group contribution $A + \frac{B}{100} \cdot T$ kcal/mol			
	300 ÷ 600° K		600 ÷ 1500° K	
	A	B	A	B
$HC\rightleftarrows$	3·047	0·615	2·505	0·706
$-C\rightleftarrows$	4·675	1·150	5·010	0·988
$\leftrightarrow C\rightleftarrows$	6·608	0·514	6·260	0·583

(f) Ring formation

In order to create the possibility of calculating the free enthalpy of formation of the cyclo-alkanes and cyclo-alkenes it was necessary to calculate corrections for the formation of the various rings. Table 6 gives the corrections for the formation of the cyclo-alkane rings. The value for the formation of the 4-ring has been calculated under the assumption that the contribution for the formation of the cyclo-alkanes is a linear function of the angle of deviation (difference between the valence angle in the ring and the valence angle in the tetrahedron). Table 7 gives corrections for the formation of pentene and hexene rings.

Table 6. Ring formation I

Group	Correction $A + \frac{B}{100} \cdot T$ kcal/mol			
	300 ÷ 600° K		600 ÷ 1500° K	
	A	B	A	B
3 ring	23·458	−3·045	22·915	−2·966
4 ring	10·73	−2·65	10·60	−2·50
5 ring	4·275	−2·350	2·665	−2·182
6 ring	−1·128	−1·635	−1·930	−1·504

Table 7. Ring formation II

Group	Correction $A + \frac{B}{100} \cdot T$ kcal/mol			
	300 ÷ 600° K		600 ÷ 1500° K	
	A	B	A	B
Pentene ring	−3·657	−2·395	−3·915	−2·250
Hexene ring	−9·102	−2·045	−8·810	−2·071

(g) Branching

In order to obtain sufficiently accurate results, it proved to be necessary to calculate corrections taking into account the branching influence. In this way corrections were calculated for the influence of branching in paraffin chains (Table 8), for the influence of branching of cyclo-paraffins (Table 9) and in aromatics (Table 10).

Table 8. Branching in paraffin chains

Correction $A + \frac{B}{100} \cdot T$ kcal/mol

Groups	300 ÷ 600° K		600 ÷ 1500° K	
	A	B	A	B
Side chain with 2 or more C-atoms	1·31	0	1·31	0
3 Adjacent —CH— groups	2·12	0	2·12	0
Adjacent —CH and —C— groups	1·80	0	1·80	0
2 Adjacent —C— groups	2·58	0	2·58	0

Table 9. Branching in cyclo-paraffins

Correction $A + \frac{B}{100} \cdot T$ kcal/mol

Group	300 ÷ 600° K		600 ÷ 1500° K	
	A	B	A	B
Branching in 5 ring				
Single branching	−1·04	0	−1·69	0
Double branching				
1,1 position	−1·85	0	−1·190	−0·160
cis 1,2 position	−0·38	0	−0·38	0
trans 1,2 position	−2·55	0	−0·945	−0·266
cis 1,3 position	−1·20	0	−0·370	−0·166
trans 1,3 position	−2·35	0	−0·800	−0·264
Branching in 6 ring				
Single branching	−0·93	0	0·230	−0·192
Double branching				
1,1 position	0·835	−0·367	1·745	−0·556
cis 1,2 position	−0·19	0	1·470	−0·276
trans 1,2 position	−2·41	0	0·045	−0·398
cis 1,3 position	−2·70	0	−1·647	−0·185
trans 1,3 position	−1·60	0	0·260	−0·290
cis 1,4 position	−1·11	0	−1·11	0
trans 1,4 position	−2·80	0	−0·995	−0·245

Table 10. Branching in aromatics

Correction $A + \frac{B}{100} \cdot T$ kcal/mol

Group	300 ÷ 600° K		600 ÷ 1500° K	
	A	B	A	B
Double branching				
1,2 position	1·02	0	1·02	0
1,3 position	−0·31	0	−0·31	0
1,4 position	0·93	0	0·93	0
Triple branching				
1,2,3 position	1·91	0	2·10	0
1,2,4 position	1·10	0	1·10	0
1,3,5 position	0	0	0	0

2. Non-hydrocarbon groups

Contributions were calculated for the —OH; —C(=O)H; —C(=O)—; —C=C=O; >C=C=O; —C(=O)—OH; —C(=O)—O—; —O—; —C≡N; —N=C; —NH_2; >NH; —N<; N<; —NO_2; —SH; —S—; >SO; >SO_2; S<; —F; Cl; —B_2 and the —I groups. Furthermore a correction was calculated for the formation of the —C(—O—)—C— and >C(—O—)—C< rings. The free enthalpies of formation were considered as being built up of the contribution for hydrocarbon groups with the addition of a contribution for the non-hydrocarbon group and, if necessary with a contribution as a result of symmetry.

(a) Oxygen compounds

—OH In contradistinction to the ideas of FRANKLIN [15] and PARKS and HUFFMAN [34] only one contribution for the —OH is given. Neither are there corrections given for secondary, tertiary and aromatic —OH groups. This view is upheld by the validity of ROSSINI's rule (in the correlation proposed here the place effect is calculated in the hydrocarbon group). For it is possible to calculate the thermodynamic magnitude of isopropyl alcohol according to

$$\Phi_{CH_3-CH(OH)-CH_3} = \Phi_{C_2H_5OH} + \Phi_{CH_3-CH(CH_3)-H} - \Phi_{C_3H_8} \quad \text{(VI-1)}$$

Additional contributions in consequence of place effects as given by FRANKLIN and PARKS and HUFFMAN are to be attributed to errors in the determination

VOL. 1 1952

of the heat of combustion. The contribution for the —OH group was calculated from ethanol [44], [61]. Methanol shows a deviation, as appears from the following series of free enthalpies of formation at 25° C, calculated from data by Walker [58].

CH_3OH	$\Delta G_f^\circ = -38{\cdot}7$ kcal./mol.
C_2H_4OH	$\Delta G_f^\circ = -40{\cdot}3$ kcal /mol.
nC_3H_7OH	$\Delta G_f^\circ = -39{\cdot}9$ kcal./mol.
nC_4H_9OH	$\Delta G_f^\circ = -37{\cdot}5$ kcal./mol.
$nC_5H_{11}OH$	$\Delta G_f^\circ = -35{\cdot}5$ kcal./mol.
$nC_6H_{13}OH$	$\Delta G_f^\circ = -33{\cdot}7$ kcal./mol.

$\underline{\overset{H}{\underset{}{—C=O}}}$ This contribution was calculated from the free enthalpy of formation of acetaldehyde [36].

$\underline{>C=O}$ Calculated from the free enthalpy of formation of acetone given by Schuman and Aston [44], and Godnev, Payukhina and Sverdlin [21].

$\underline{H_2C=C=O \text{ and } >C=C=O}$ By applying Rossini's rule on the free enthalpy function of $H_2C=C=O$ [13] the corresponding functions for

$\begin{matrix}CH_3\\H\end{matrix}\!>\!C=C=O$ and $(CH_3)_2=C=C=O$ were calculated.

$$\left.\begin{aligned}\Phi_{\begin{matrix}CH_3\\H\end{matrix}>C=C=O} &= \Phi_{H_2C=C=O} + \Phi_{CH_3-\overset{H}{\underset{}{C}}=CH_2} - \Phi_{CH_3=CH_2}\\ \Phi_{\begin{matrix}CH_3\\CH_3\end{matrix}>C=C=O} &= \Phi_{H_2C=C=O} + \Phi_{\begin{matrix}CH_3\\CH_3\end{matrix}>C=CH_2} - \Phi_{CH_2=CH_2}\end{aligned}\right\} \text{(VI–2)}$$

$\underline{\overset{O}{\underset{}{\overset{\|}{C}—OH}}}$ This contribution was calculated from the free enthalpy function of acetic acid, which was again calculated from the corresponding function of formic acid by means of Rossini's rule [62].

$$\Phi_{CH_3—COOH} = \Phi_{HCOOH} + \Phi_{CH_3—CHO} - \Phi_{H_2CO} \quad \text{(VI–3)}$$

$\underline{\overset{O}{\underset{}{\overset{\|}{C}—O—}}}$ Vvedensky, Yvannikov and Nekrasova [56] measured the position of the equilibrium of the reaction

$$2\,C_2H_5OH_{(g)} \rightleftharpoons CH_3COOC_2H_{5(g)} + 2\,H_2. \quad \text{(VI–4)}$$

The contribution from this group was calculated from data by these investigators.

Table 11. Oxygen containing groups

Group	Group contribution $A + \frac{B}{100} \cdot T$ kcal/mol				Highest temperature of lit. value
	300 ÷ 600° K		600 ÷ 1500° K		
	A	B	A	B	°K
H_2O	−58·076	1·154	−59·138	1·316	1500
—OH	−41·56	1·28	−41·56	1·28	1500
—O—	−15·79	−0·85	—	—	600
$O\overset{\rightarrow}{\leftarrow}$	−18·37	0·80	−16·07	0·40	
H_2CO	−29·118	0·653	−30·327	0·854	1500
$\overset{H}{—C=O}$	−29·28	0·77	−30·15	0·83	1000
$>C=O$	−28·08	0·91	−28·08	0·91	1500
$HC(=O)-OH$	−87·660	2·473	−90·569	2·958	1500
$—C(=O)—OH$	−98·39	2·86	−98·83	2·93	1500
$—C(=O)—O—$	−92·62	2·61	−92·62	2·61	800
$H_2C=C=O$	−14·515	0·295	−14·515	0·295	900
$HC=C=O$	−12·86	0·46	−12·86	0·46	900
$\leq C=C=O$	− 9·62	0·72	− 9·38	0·73	900

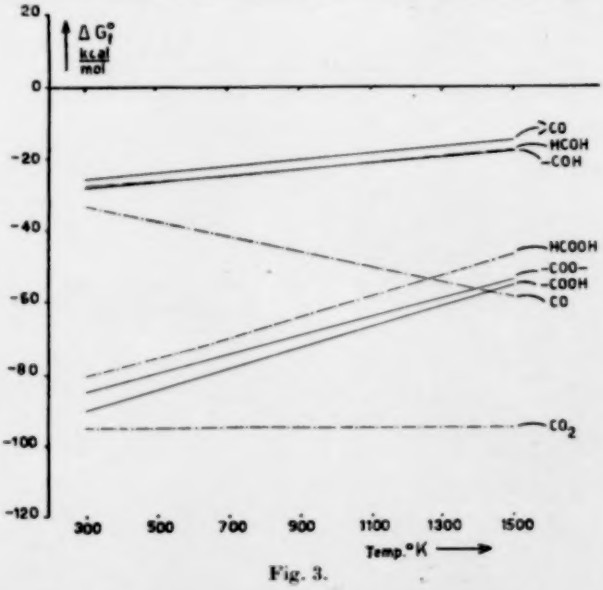

Fig. 3.

$\underline{—O—}$ Valentin [55] determined the positon of the equilibrium

$$2\,C_2H_5OH_{(g)} \rightleftharpoons C_2H_5OC_2H_{5(g)} + H_2O_{(g)} \quad \text{(VI–5)}$$

and from this calculated the change in free enthalpy of this reaction. From this magnitude the contribution for the —O— group was calculated.

Table 12. Nitrogen containing groups

Group	Group contribution $A + \frac{B}{100} \cdot T$ kcal/mol				Highest temperature of lit. value
	300 ÷ 600° K		600 ÷ 1500° K		
	A	B	A	B	°K
HCN	31·179	−0·826	30·874	−0·775	1500
—C≡N	30·75	−0·72	30·75	−0·72	1200
—N≡C	46·32	−0·89	46·32	−0·89	700
NH_3	−11·606	2·556	−12·972	2·784	1500
$—NH_2$	2·82	2·71	− 6·78	3·98	
>NH	12·93	3·16	12·93	3·16	
>N—	19·46	3·82	19·46	3·82	
⇄N	11·32	1·11	12·26	0·96	1000
$—NO_2$	− 9·0	3·70	−14·19	4·38	

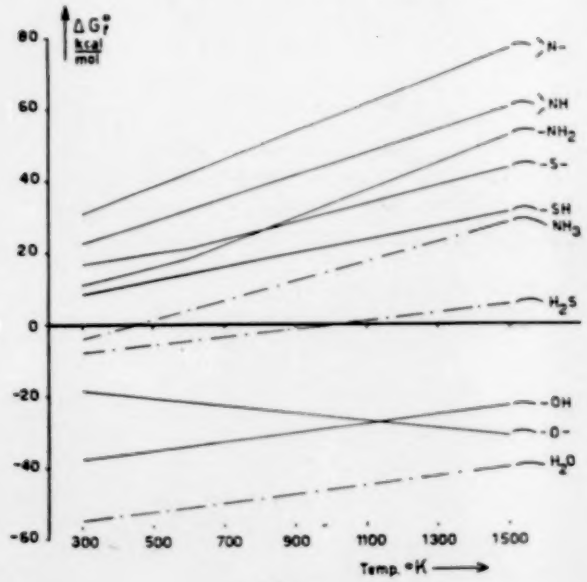

Fig. 4.

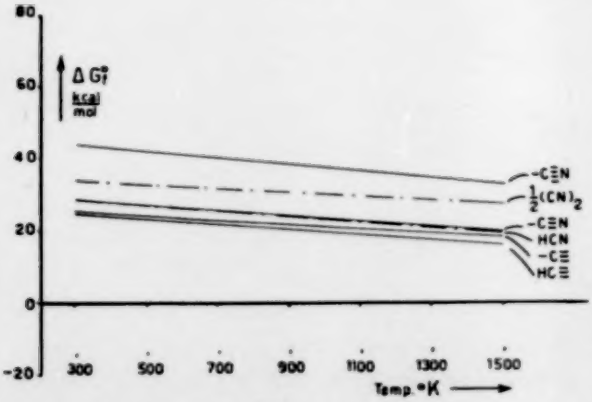

Fig. 5.

O⇄ BREMNER and THOMAS [9] give the heat of formation and the free enthalpy of formation of furane. Assuming ULICH's rule [54] to be valid in this case, the contribution from the O⇄ group was calculated with the help of these data.

(b) Nitrogen compounds

—C≡N and —N≡C These groups were calculated respectively from the free enthalpy functions of methyl cyanide [14], [35] and acrylonitril [27] and from the free enthalpy function of methyl isocyanide [14].

$—NH_2$; >NH and >N— Contributions for these groups were calculated from the heat of formation given by BICHOWSKY and ROSSINI [7] and entropies given by ASTON and co-workers [3], [4], [5], after which the free enthalpies of formation obtained in this manner were extended to higher temperatures by means of a specific heat correlation given by DOBRATZ [12]*.

$—NO_2$ Calculated from the heat of formation given by BICHOWSKY and ROSSINI [7] and the entropy given by PITZER and GWINN [36]. Contributions for higher temperatures were calculated with DOBRATZ's specific heat correlation. (The C_p^0 equation obtained in this way was adapted to some C_p^0 values measured by PITZER and GWINN [36].)

N⇄ The contribution for this group was calculated from the free enthalpy function of pyridine [31].

(c) Sulphur compounds

—SH and —S— Contributions calculated respectively from the free enthalpy functions of methyl mercaptan [6], [8] and ethyl mercaptan and from the free enthalpy function of dimethyl sulphide.

⇄S The contribution to the free enthalpy of formation of the resonance group ⇄S was calculated from the free enthalpy function of thiophene [57].

* DOBRATZ's correlation for the specific heat is based on the, approximately right, assumption that a given bond between two atoms shows two characteristic frequencies of vibration, which are independent of the nature of the molecule in which that bond occurs. In his publication DOBRATZ gives values for these frequencies for the various bonds and contributions of these frequencies to specific heat. By the further assumption that every degree of internal rotation contributes the full value of $R/2$ to the specific heat this investigator arrives at a specific heat correlation for gaseous compounds that corresponds rather well with the reality in the case of not too complex molecules. An extensive explanation of this correlation may be found in [12] and [26].

VOL. 1 1952

>SO and >SO_2 Contributions for these groups were calculated from the free enthalpy functions of dimethyl sulphoxide and dimethyl sulphone, which in their turn were calculated according to (III–2), following a suggestion by Barrow and Pitzer [6].

(d) Halogen compounds

—F Thompson and Temple [53] give the function of the free enthalpy of 1,1,1 trifluorethane, from which the contribution for this group was calculated.

—Cl The contribution for the —Cl group was calculated as the mean value of the increments from the free enthalpy functions of methyl chloride, methyl dichloride, methyl trichloride, carbon tetrachloride [49], dichlorethane [24], vinyl chloride, cis-dichlorethylene, trans-dichlorethylene [17] and methyl chlorethylene [63].

—Br The contribution for this group was found as the mean value of the increment calculated from methyl bromide, methyl dibromide, methyl tribromide, carbon tetrabromide [49] methyl bromo-acetylene [63].

Table 13. Sulphur containing groups

Group	Group contribution $A + \frac{B}{100} \cdot T$ kcal/mol				Highest temperature of lit. value
	300 ÷ 600° K		600 ÷ 1500° K		
	A	B	A	B	°K
H_2S	−10·942	1·026	−11·756	1·167	1500
—SH	5·12	1·07	5·12	1·07	1500
—S—	12·58	1·42	12·29	1·44	1500
⁄⁄S	14·83	0·51	15·15	0·44	1500
>SO	−14·39	3·39	−14·39	3·39	1200
>SO_2	5·22	5·58	7·11	5·26	1200

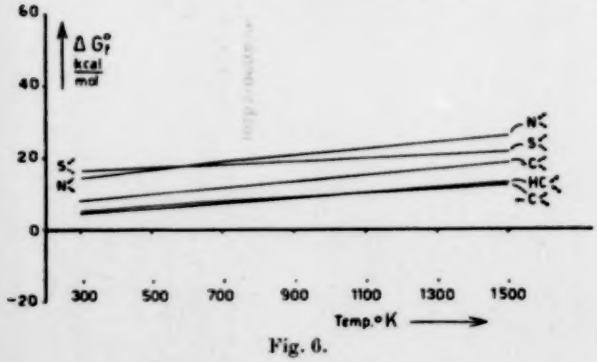

Fig. 6.

Table 14. Halogen containing groups

Group	Group contribution $A + \frac{B}{100} \cdot T$ kcal/mol				Highest temperature of lit. value
	300 ÷ 600° K		600 ÷ 1500 °K		
	A	B	A	B	°K
HF	−64·476	−0·145	−64·884	−0·081	1500
—F	−45·10	−0·20			600
HCl	−22·100	−0·215	−22·460	−0·156	1500
—Cl	− 8·25	0	− 8·25	0	1500
HBr	− 8·723	−0·234	− 9·180	−0·158	1500
—Br	2·21	−0·26	2·21	−0·26	1200
HI	0·690	−0·225	0·397	−0·176	1500
—I	15·26	0	15·26	0	1000

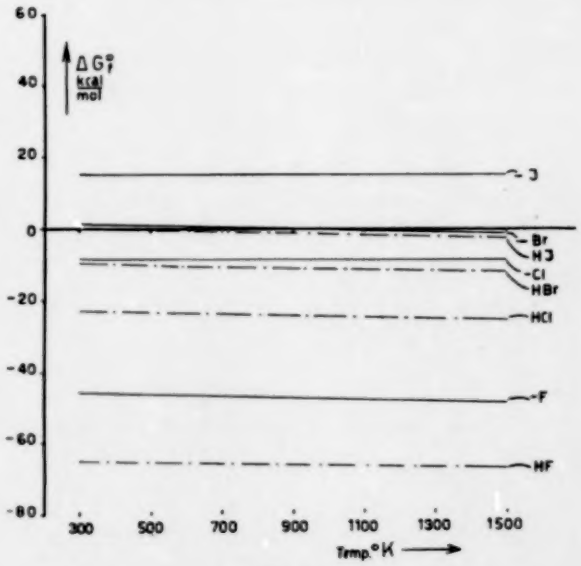

Fig. 7.

—I Contributions for this group were calculated from values of the free enthalpy functions of acetylene diiodide and methyl iodo-acetylene [63].

(e) Ring formation

Only few data about the free enthalpy of formation of heterogeneous ring molecules are given in the literature. The only possibilities proved to be calculations of corrections for the formation of the 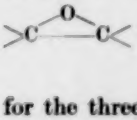 and 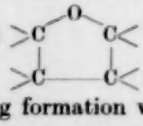 rings. The correction for the three-ring formation was calculated from the free enthalpy function of ethylene oxide [20].

Table 16. Comparison between calculated free enthalpies of formation and data from the literature

Compound	300° K		600° K		900° K		1200° K		1500° K		Literature
	Calculated kcal/mol	Found kcal/mol	Calculated kcal/mol	Found kcal/mol	Calculated kcal/mol	Found kcal/mol	Calculated kcal/mol	Found kcal/mol	Calculated kcal/mol	Found kcal/mol	
2,2 dimethylbutane	−1·83	−2·07	43·29	42·84	90·06	89·93	136·96	137·56	183·77	185·01	39
3,3 dimethylpentane	0·58	0·93	53·37	52·84	108·37	107·34					39
2,2 dimethylpropane	−2·55	−3·42	36·20	35·08	77·33	75·49	118·08	116·27	158·84	157·00	39
2 methylpropane	−3·45	−4·13	24·90	25·18	56·29	56·29	87·59	87·86	118·90	119·44	39
3 methylhexane	1·42	1·27	51·96	52·01	105·53	105·33					39
3 methylheptane	3·52	3·69	61·78	61·27	123·39	121·68					39
2,4 dimethylpentane	1·67	1·02	53·36	53·19	107·75	107·99					39
3,4 dimethylhexane	3·70	5·31	62·90	64·57	125·53	126·49					39
3,3 dimethylhexane	2·26	2·91	61·97	62·71	124·47	125·21					39
1 hexene	20·66	20·99	53·9	54·1	89·1	89·1	124·6	124·6	160·1	160·1	39
cis 2 hexene	19·57	19·86	53·5	53·7	89·8	89·9					39
trans 2 butene	14·75	15·42	33·91	34·83	54·84	55·80	76·06	77·25	97·28	98·77	39
cis 2 pentene	75·06	75·32	43·18	43·48	71·52	71·58	100·11	100·22	128·70	128·88	39
3 methyl 1 butene	18·13	18·03	44·76	44·63	73·06	72·82	101·69	101·46	131·32	130·00	39
3 methyl 1 pentene	20·23	20·47	54·17	54·00	90·1	89·2					39
2 methyl 2 pentene	16·30	16·54	50·2	50·5	86·7	86·6					39
cis 4 methyl 2 pentene	18·69	18·60	53·3	52·7	89·6	88·8					39
trans 4 methyl 2 pentene	18·36	17·96	52·4	52·2	88·6	88·4					39
2 ethyl 1 butene	18·22	18·71	52·3	52·5	88·6	88·4					39
2,3 dimethyl 1 butene	17·34	17·63	51·7	52·0	88·3	88·2					39
2,3 dimethyl 2 butene	16·49	16·72	51·54	51·80	89·2	89·2					39
1,2 butadiene	48·18	48·26	58·10	58·03	69·30	68·85	80·45	80·01	91·60	91·25	40
1,3 butadiene	36·36	36·49	46·93	47·20	58·76	58·82	70·70	70·72	82·63	82·66	40
1 butyne	47·91	48·57	57·72	58·45	68·65	69·36	79·83	80·62	91·01	91·99	39
2 butyne	43·20	44·78	53·89	55·34	65·82	67·10	78·27	79·29	90·71	91·60	39
2 methyl 1 butyne	49·55	49·23	66·90	67·17	85·68	86·40	105·27	106·04	124·85	125·68	39
1,2,3 trimethylbenzene	28·48	29·51	63·75	63·91	100·47	100·63	138·05	138·00	175·63	175·51	39
1,3 dimethylbenzene	28·49	28·55	55·20	55·10	83·40	83·63	112·83	112·72	142·26	141·85	39
1 methyl 4 ethylbenzene	30·21	30·47	64·44	64·16	100·46	100·10	137·11	136·60	173·7	173·2	39
n butylbenzene	34·57	34·86	75·51	75·70	119·01	118·90	162·8	162·7	206·5	206·5	39
methylcyclopentane	7·24	6·79	54·03	53·55	103·01	102·59	152·12	151·83	201·23	200·65	39
n hexylcyclopentane	18·72	19·20	92·7	92·9	170·8	170·2	249·0	248·2	327·2	326·2	39
trans 1,2 dimethylcyclohexane	7·81	8·55	63·5	63·4	121·0	120·6	178·1	178·1	235·2	234·9	39
cis 1,4 dimethylcyclohexane	8·69	9·38	64·1	64·3	122·7	121·8					39
styrene	51·29	51·20	68·30	68·67	86·52	87·53	105·36	106·77	124·20	126·03	40
trans 1 propenylbenzene	51·22	51·23	75·76	76·27	102·17	103·08	129·22	130·26	156·27	157·57	40

1 methyl 3 ethenylbenzene	49·87	50·17	74·80	74·61	100·81	100·85	127·79	127·58	154·77	154·35	40
1,1,1 trifluoro ethane	−127·6	−127·3	−110·8	−110·6							53
methylchloride	−11·9	−13·0	−4·7	−5·4	+3·3	+3·0	+11·2	+11·5			49
methylchloroacetylene	38·4	38·8	42·2	41·0	46·5	45·4					63
methyltrichloride	−16·1	−15·1	−6·7	−6·8							49
cis dichlorocthylene	7·5	8·6			20·1	20·7			32·7	33·3	17
vinylchloride	10·5	9·4	15·1	14·0	20·1	19·0	25·3	24·3	30·6	29·6	17
chlorobenzene	24·7*	23·8*									1, 59, 60
methylbromide	2·2	2·6	4·3	3·8	11·4	10·8	18·6	18·0			49
methyltetrabromide	20·3	22·2	29·9	31·9							49
methylbromoacetylene	48·5	48·1	51·3	51·8	54·7	54·6					63
vinylbromide	20·2	19·3	24·0	23·7	28·2	28·6	32·7	33·7	37·2	38·9	38
acetylenediiodide	−81·7	−81·5	−78·9	−79·6	−75·0	−75·0					63
vinyliodide	34·0	34·1	38·4	38·6	43·6	43·2	48·9	48·2	54·2	53·3	38
fluorobenzene	−11·7*	−12·7*									1, 59, 60
chlorotrifluoromethane	−134·5	−131·5	−124·6	−121·5							53
dichlorodifluoromethane	−95·2	−94·3	−85·7	−83·9							53
trichlorodifluoromethane	−57·0	−57·6	−46·3	−46·4							53
ethylmercaptan	6·1	6·3	23·3	23.3	41·4	41·4					6
dimethylsulphide	8·8	8·7	26·6	26·5	45·6	45·6			84·4	84·4	6
thiophene	36·3	36·4	45·6	45.8	55·8	55·9	66·0	66·0	76·2	76·2	57
dimethylsulphoxide	−12·8	−12·8	10·6	10·9	35·3	35·5	60·1	60·1			6
dimethylsulphone	13·9	13·8	44·1	44·2	74.9	75·2	105·7	105·7			6
acrylonitrile	47·3	47·3	49·8	50·3	53·6	53·7					27
methylisocyanide	40·0	40·0	44·6	44·6							14
trimethylamine	18·7	18·7	50·5	51·0	84·7	84·4	118·7	118·7	152·8	152·8	7, 5
pyridine	39·5	39·6	52·6	52·6	66·4	66·3					31
aniline	43·8*	44·9*									1
nitrobenzene	35·0*	37·2*									1
ethyl alcohol	−39·9	−40·3	−22·1	−22·1	−3·4	−3·5	15·4	15·3			44, 61
n butylalcohol	−37·0*	−37·5*									58
n hexylalcohol	−32·8*	−33·7*									58
benzylalcohol	−3·0*	−4·4*									28, 59, 60
phenol	−4·6*	−4·4*									1
pyrocatechol	−38·0*	−42·5*									15
acetone	−33·5	−33·4	−16·9	−16·6	+1·3	+1·4	+19·3	+19·5	+37·3	+37·9	44, 21
acetic acid	−94·1	−93·7	−78·9	−78·9	−62·8	−63·0	−46·7	−46·8	−30·6	−30·5	62
ethylacetate	−91·3	−91·3	−62·9	−62·7							56
diethylether	−22·1	−22·1	−3·2	−3·0							55
ethyleneoxide	−2·5	−2·7	8·2	7·7	19·5	19·1					20

* Temperature 298·1° K

Table 15. Ring formation

Group	Correction $A + \frac{B}{100} . T$ kcal/mol			
	300 ÷ 600° K		600 ÷ 1500° K	
	A	B	A	B
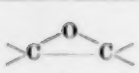	12·86	−0·63	12·86	−0·63
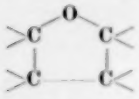	−5·82	0·25	−3·53	−0·16

BREMNER and THOMAS [9] give the heat of formation and the entropy of tetrahydrofurane at 300° K. From this the correction for the formation of the 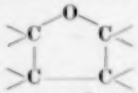 ring was calculated, assuming that ULICH's rule [54] is applicable.

The various tables for the group contributions show, besides these group contributions, formulae for the three enthalpies of formation of compounds differing only in one hydrogen atom from the group contributions.

These formulae were calculated from data about CH_4 [39]; C_2H_6 [39]; $H_2C{=}C{=}CH_2$ [40]; H_2O [39]; H_2CO [51]; HCOOH [62]; $H_2C{=}C{=}O$ [13]; HCN [22]; NH_3 [48]; H_2S [10]; HF [33]; HCl [18]; HB_2 [23]; HJ [32].

VII. EXAMPLES ON THE CALCULATION OF THE FREE ENTHALPY OF FORMATION

(1) 2,2 Dimethyl propane

$C(CH_3)_4$ $\qquad \sigma = 12$

300 ÷ 600° K

$$\begin{aligned} 4{-}CH_3 &= -43{\cdot}772 + 8{\cdot}860 \,.\, 10^{-2} \,.\, T \\ 1{-}C{-} &= 1{\cdot}958 + 3{\cdot}735 \,.\, 10^{-2} \,.\, T \\ RT \ln\sigma &= \qquad\qquad 0{\cdot}494 \,.\, 10^{-2} \,.\, T \\ \hline \Delta G_f^\circ &= -41{\cdot}814 + 13{\cdot}089 \,.\, 10^{-2} \,.\, T \end{aligned} +$$

(2) 1,3 Butadiene

$H_2C{=}C{-}C{=}CH_2$ (H H) $\qquad \sigma = 2$

600 ÷ 1500° K

$$2\,\frac{H}{H}C{\leftrightarrow} = 9{\cdot}000 + 1{\cdot}664 \,.\, 10^{-2} \,.\, T$$

$$\begin{aligned} 2\,\frac{H}{H}C{\leftrightarrow} &= 13{\cdot}960 + 2{\cdot}176 \,.\, 10^{-2} \,.\, T \\ RT \ln\sigma &= \qquad 0{\cdot}138 \,.\, 10^{-2} \,.\, T \\ \hline \Delta G_f^\circ &= 22{\cdot}960 + 3{\cdot}978 \,.\, 10^{-2} \,.\, T \end{aligned} +$$

(3) 1 Pentyne

$HC{\equiv}C{-}(CH_2)_2{-}CH_3$ $\qquad \sigma = 1$

600 ÷ 1500° K

$$\begin{aligned} 1{-}CH_3 &= -12{\cdot}310 + 2{\cdot}436 \,.\, 10^{-2} \,.\, T \\ 2{-}CH_2{-} &= -11{\cdot}660 + 5{\cdot}088 \,.\, 10^{-2} \,.\, T \\ 1{-}C{\equiv} &= 26{\cdot}555 - 0{\cdot}550 \,.\, 10^{-2} \,.\, T \\ 1\,HC{\equiv} &= 26{\cdot}700 - 0{\cdot}704 \,.\, 10^{-2} \,.\, T \\ \hline \Delta G_f^\circ &= 29{\cdot}285 + 6{\cdot}270 \,.\, 10^{-2} \,.\, T \end{aligned} +$$

(4) Anthracene

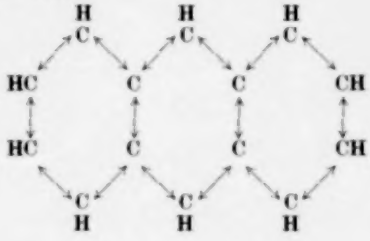

$\sigma = 4$

600 ÷ 1500° K

$$\begin{aligned} 10\,HC{\rightleftarrows} &= 25{\cdot}05 + 7{\cdot}06 \,.\, 10^{-2} \,.\, T \\ 4{\leftrightarrow}C{\rightleftarrows} &= 26{\cdot}432 + 2{\cdot}056 \,.\, 10^{-2} \,.\, T \\ RT \ln\sigma &= \qquad 0{\cdot}276 \,.\, 10^{-2} \,.\, T \\ \hline \Delta G_f^\circ &= 51{\cdot}48 + 9{\cdot}39 \,.\, 10^{-2} \,.\, T \end{aligned} +$$

(5) Trans 1,4 dimethyl cyclohexane

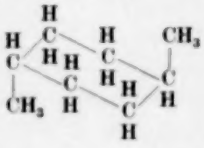

$\sigma = 2$

300 ÷ 600° K

$$\begin{aligned} 4{-}CH_2{-} &= -20{\cdot}780 + 9{\cdot}720 \,.\, 10^{-2} \,.\, T \\ 2{-}CH &= -1{\cdot}410 + 5{\cdot}820 \,.\, 10^{-2} \,.\, T \\ 2{-}CH_3 &= -21{\cdot}886 + 4{\cdot}430 \,.\, 10^{-2} \,.\, T \\ \text{6 ring formation} &= -2{\cdot}80 \\ \text{trans 1,4 branching} &= -1{\cdot}128 - 1{\cdot}635 \,.\, 10^{-2} \,.\, T \\ RT \ln\sigma &= \qquad\qquad 1{\cdot}138 \,.\, 10^{-2} \,.\, T \\ \hline \Delta G_f^\circ &= -48{\cdot}00 + 18{\cdot}47 \,.\, 10^{-2} \,.\, T \end{aligned} +$$

(6) Tertiary butyl alcohol

$(CH_3)_3C{-}OH$ $\qquad \sigma = 1$

600 ÷ 1500° K

$$\begin{aligned} 3{-}CH_3 &= -36{\cdot}930 + 7{\cdot}308 \,.\, 10^{-2} \,.\, T \\ 1{-}C{-} &= 4{\cdot}385 + 3{\cdot}350 \,.\, 10^{-2} \,.\, T \\ 1{-}OH &= -41{\cdot}56 + 1{\cdot}28 \,.\, 10^{-2} \,.\, T \\ \hline \Delta G_f^\circ &= -74{\cdot}10 + 11{\cdot}94 \,.\, 10^{-2} \,.\, T \end{aligned} +$$

(7) Quinoline

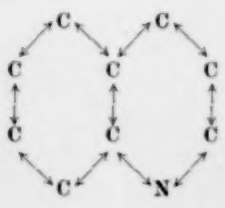

$\sigma = 1$

VOL. 1 1952

300 ÷ 600° K

$$\begin{array}{rl} 7\ HC\rightleftarrows & = 21{\cdot}329 + 4{\cdot}305\,.\,10^{-2}\,.\,T \\ 2 \leftrightarrow C\rightleftarrows & = 6{\cdot}608 + 0{\cdot}514\,.\,10^{-2}\,.\,T \\ 1\ \ N\rightleftarrows & = 11{\cdot}32 + 1{\cdot}11\ .10^{-2}\,.\,T \\ \hline \Delta G_f & = 39{\cdot}26 + 5{\cdot}93\ .10^{-2}\,.\,T \end{array} +$$

VIII. Discussion

Accuracy of the correlation—With the help of the correlation obtained in this manner free enthalpies of formation of gaseous compounds were calculated and the results compared with the free enthalpies of formation found in the literature (Table 16). It appeared that the values calculated in this way approach reality with a mean deviation of about 0·6 $\frac{kcal}{mol}$.

In the Figures 1 to 7 inclusive various group contributions have been plotted as a function of the temperature. Moreover—as was done in the preceding tables for the group contributions—those compounds were included in the diagrams which differ only in one hydrogen atom from the group contributions. For distinguishing from the real group contributions these latter materials are represented by special lines (–·–·–·–·–).

From Figure 1 it follows that a group contribution for the alkanes is, by approximation, found as half the sum of the preceding and the following group, in other words; the influence of the various hydrogen atoms is in these contributions approximately constant.

Figure 2 shows that a similar rule also holds for the contributions for the alkene groups, provided the average contributions for the $H_2C{=}C\!<$, $\overset{H}{>}C{=}C\!<$ and $\overset{H}{>}C{=}C\overset{H}{<}$ groups are considered.

In Figure 3 the contributions for carbon-oxygen groups have been plotted. From this diagram the ready decarboxylation of the acids and esters at higher temperatures is apparent.

Figure 4 shows that the stability of the nitrogen, sulphur and oxygen groups increases in the order as mentioned here. This diagram also shows the rather exceptional behaviour of the —O— group.

Contributions for carbon-nitrogen groups and alkyne groups were represented in Figure 5. From this graph it appears that the entropy terms of these group contributions are approximately equal.

The "aromatic" resonance groups $HC\rightleftarrows$; $-C\rightleftarrows$; $\leftrightarrow C\rightleftarrows$; $N\rightleftarrows$ and $S\rightleftarrows$ are represented in Figure 6.

Figure 7 gives a confirmation of what might be expected of the —F; —Cl; —Br and —J groups on account of their place in the periodical system.

Table 17 gives a representation of the free enthalpies of formation of a number of materials that cannot be calculated by means of this correlation and those of some inorganic gases. This opened the possibility of predicting in a first approximation the variation of the equilibrium with the temperature of the most important organic gas reactions.

Table 17

Compound	*Formula*	*Free enthalpy of formation* $A + \frac{B}{100}\,.\,T$				*a °K*	*Calculated from values given by*
		300 ÷ 600° K		*600 ÷ a °K*			
		A	*B*	*A*	*B*		
ethane	C_2H_6	−21·539	4·583	−24·588	5·093	1500	39
carbon monoxide	CO	−26·582	−2·122	−26·582	−2·122	1500	39
carbon dioxide	CO_2	−94·076	−0·061	−94·234	−0·035	1500	39
methanol	CH_3OH	−49·440	3·480	−51·330	3·795	1500	63, 46, 29
phosgene	$COCl_2$	−52,01	0·94	−52·01	0·94	1000	52
cyanogen chloride	CNCl	34·151	−0·430	34·151	−0·430	1000	49
cyanogen oxide	CNI	49·268	−0·596	49·268	−0·596	800	49
cyanogen	$(CN)_2$	71·889	−1·059	71·889	−1·059	1000	53
sulphur dioxide	SO_2	−77·157	1·735	−77·157	1·735	1500	16
sulphur trioxide	SO_3	−100·203	3·943	−100·203	3·943	1200	51
nitric oxide	NO	21·543	−0·301	21·543	−0·301	1500	16
nitrogen dioxide	NO_2	7·933	1·486	7·933	1·486	1000	17
nitrogen tetroxide	N_2O_4	7·112	5·460				17
carbon oxi-sulphide	COS	39·714	−0·245	−39·569	−0·265	1500	11
carbon disulphide	CS_2	−16·000	−0·150	−16·196	−0·177	1500	11

NOTATION

C; D etc.	= Compounds
E_1; E_2	= Elements
K_f	= Equilibrium constant for formation from the elements
K_{eq}	= Equilibrium constant
A and B	= Constants
ΔG_f	= Free enthalpy of formation (American terminology: free energy of formation)
ΔG_f°	= Free enthalpy of formation in the ideal gaseous state and at a fugacity of 1 atm. (American terminology: free energy of formation)
$\Delta G_{reaction}$	= Free enthalpy change as a result of the reaction (American terminology: free energy change)
R	= Gas constant
T	= Absolute temperature
σ	= Symmetry number
Φ	= Arbitrary thermodynamic function
$\frac{G^\circ - H_0^\circ}{T}$	= Free enthalpy function in the ideal gaseous state at a fugacity of 1 atm. (American terminology: free energy function)
$H^\circ - H_0^\circ$	= Heat content in the ideal gaseous state at a fugacity of 1 atm.
C_p°	= Specific heat at constant pressure in the ideal gaseous state at a fugacity of 1 atm.
ΔH_f°	= Heat of formation in the ideal gaseous state at a fugacity of 1 atm.

REFERENCES

[1] ANDERSEN, J. W., BEYER, G. H. and WATSON, K. M.; Nat. pet. news 1944 **36** R 476. [2] ASTON, J. G.; Thermodynamic data on hydrocarbons. [3] ASTON, J. G., EIDINOF, M. L. and FORSTON, W. S.; J. Amer. Chem. Soc. 1939 **61** 1539. [4] ASTON, J. G., SAGENKAHN, M. L., SASZ, G. J., MOESSEN, G. W. and ZUHR, H. F.; J. Amer. Chem. Soc. 1944 **66** 1171. [5] ASTON, J. G., SILLER, C. W. and MESSERLEY, G.; J. Amer. Chem. Soc. 1937 **59** 1743. [6] BARROW, G. M. and PITZER, K. S.; Ind. and Engng Chem. 1949 **41** 2737. [6a] BARROW, G. M. and MCCLELLAN, A. L.; J. Amer. Chem. Soc. 1951 **73** 573. [7] BICHOWSKY, F. R. and ROSSINI, F. D.; The thermochemistry of the chemical substances. Reinhold, New York: 1936. [8] BINDER, J. L.; J. Chem. Phys. 1949 **17** 499. [9] BREMNER, J. G. M. and THOMAS, G. D.; Trans. Faraday Soc. 1948 **44** 230. [10] CROSS, P. C.; J. Chem. Phys. 1935 **3** 168. [11] CROSS, P. C.; J. Chem. Phys. 1935 **3** 825. [12] DOBRATZ, C. J.; Ind. and Engng Chem. 1941 **33** 759. [13] DRAYTON, L. G. and THOMPSON, H. W.; J. Chem. Soc. **1948** 1416. [14] EWELL, R. H. and BOURLAND, J. F.; J. Chem. Phys. 1940 **8** 635. [15] FRANKLIN, J. L.; Ind. and Engng Chem. 1949 **41** 1070. [16] GIAUQUE, F. W. and CLAYTON, J. O.; J. Amer. Chem. Soc. 1932 **54** 1731. [17] GIAUQUE, F. W. and KEMP, J. D.; J. Chem. Phys. 1938 **6** 40. [18] GIAUQUE, F. W. and OVERSTREET, R.; J. Amer. Chem. Soc. 1932 **54** 1731. [19] GODNEV, I. N. and FILETOVA, N. N.; Compt. rend. de l'académie des sciences de l'U.R.S.S. (Doklady) 1946 **52** 43. [20] GODNEV, I. N. and MOROZOV, V.; J. Phys. Chem. (U.S.S.R.) 1948 **22** 801. [21] GODNEV, I. N., PAYUKHINA, A. and SVERDLIN, A.; J. Phys. Chem. (U.S.S.R.) 1940 **14** 374. [22] GORDON, A. R.; J. Chem. Phys. 1937 **5** 30. [23] GORDON, A. R. and BARNES, C.; J. Chem. Phys. 1933 **1** 692. [24] GWINN, W. D. and PITZER, K. S.; J. Chem. Phys. 1948 **16** 303. [25] HERZBERG, G.; Infrared and Raman spectra of polyatomic molecules. Nostrand, New York: 1945. [26] HOUGEN, O. A. and WATSON, K. M.; Chemical process principles Part II: Thermodynamics. Wiley, New York: 1947. [27] HALVERSON, F., STAM, R. F. and WHALEN, J. J.; J. Chem. Phys. 1948 **16** 808. [28] International Critical Tables. [29] KASSEL, L. S.; J. Chem. Phys. 1936 **4** 493. [30] KHARASCH, M. S.; J. Res. Nat. Bur. Stand. 1929 **2** 359. [31] KLINE, C. H. and TURKEVITCH, J.; J. Chem. Phys. 1944 **12** 300. [32] MURPHY, G. M.; J. Chem. Phys. 1936 **4** 344. [33] MURPHY, G. M. and VANCE, J. E.; J. Chem. Phys. 1939 **7** 806. [34] PARKS, G. S. and HUFFMAN, H. M.; The free energies of some organic compounds. Chemical Catalog Comp., New York: 1932. [35] PITZER, K. S.; J. Chem. Phys. 1940 **8** 711. [36] PITZER, K. S. and GWINN, W. D.; J. Amer. Chem. Soc. 1941 **63** 3313. [37] PITZER, K. S. and WELTNER, W.; J. Amer. Chem. Soc. 1949 **71** 2842. [38] RICHARDS, R. E.; J. Chem. Soc. **1948** 1931. [39] ROSSINI, F. D. a. o.; Selected values of properties of hydrocarbons, Nat. Bur. Stand. Circular C 461, 1947. [40] ROSSINI, F. D. a. o.; J. Res. Nat. Bur. Stand. 1949 **42** 225. [41] ROSSINI, F. D. a. o.; J. Res. Nat. Bur. Stand. 1949 **42** 379. [42] ROSSINI, F. D. a. o.; J. Res. Nat. Bur. Stand. 1949 **43** 245. [43] SCHEFFER, F. E. C.; De toepassing van de thermodynamica op chemische processen. Waltman, Delft: 1945. [44] SCHUMAN, S. C. and ASTON, J. G.; J. Chem. Phys. 1938 **9** 485. [45] SMITH, J. M.; Chem. Engng Prog. 1948 **44** 521. [46] SOUDERS, M., MATTHEWS, C. S. and HURD, C. O.; Ind. and Engng Chem. 1949 **41** 1037. [47] STEPHENSON, C. C. and MCMAHON, H. O.; J. Amer. Chem. Soc. 1939 **61** 437. [48] STEVENSON, D. P.; J. Chem. Phys. 1939 **7** 171. [49] STEVENSON, D. P. and BEACH, J. V.; J. Chem. Phys. 1938 **6** 25, 108. [50] STOCKMAYER, W. H., KAVANAGH, G. M. and MICKLEY, H. S.; J. Chem. Phys. 1944 **12** 408. [51] THOMPSON, W. H.; Trans. Faraday Soc. 1941 **37** 251. [52] THOMPSON, W. H.; Trans. Faraday Soc. 1941 **37** 344. [53] THOMPSON, W. H. and TEMPLE, R. B.; J. Chem. Soc. **1948** 1428. [54] ULICH, H.; Chemische Thermodynamik, Dresden und Leipzig: 1930. [55] VALENTIN, F. H. H.; J. Chem. Soc. **1950** 498. [56] VVEDENSKY, A. A., IVANNIKOV, P. YA. en NEKRASOVA, V. A.; J. Gen. Chem. (U.S.S.R.) 1949 **19** 1094. [57] WADDINGTON, G. a. o.; J. Amer. Chem. Soc. 1949 **71** 797. [58] WALKER, C. A.; *Thesis:* Yale school of engineering. 1948. [59] WENNER, R. R.; Thermochemical calculations. McGraw Hill, New York: 1941. [60] YOUNG, S.; Scientific proceedings of the Royal Dublin Society 1909–1910 **12** 410. [61] ZEISE, H.; Z. Elektrochem. 1939 **45** 456. [62] ZEISE, H.; Z. Elektrochem. 1942 **48** 693. [63] ZIOMEK J. S. and CLEVELAND, F. F.; J. Chem. Phys. 1949 **17** 578.

Application de la mesure de la constante diélectrique des suspensions à l'étude de la décantation

RENÉ JOTTRAND

Ingénieur I. C. M. E., Service de Chimie Industrielle de l'Université Libre de Bruxelles

(Received 15 July 1951)

Summary—The concentration of a suspension at any point is determined by measuring the capacity of a condenser which is designed not to interfere with the effect being studied.

Experiments with silica powder of 56 μ diameter in a mixture of benzene and nitrobenzene indicate that the degree of packing of the sediment is a function of its height and not of the time it is left in the settling tank.

The method can also be employed for measurements in cyclone separators or in fluidized beds.

Resumé—La mesure de la constante diélectrique d'une suspension permet de suivre l'évolution des concentrations en chaque point.

La méthode a le grand avantage de permettre des mesures instantanées, bien localisées et suffisamment précises.

Si le condensateur de mesure est convenablement dessiné, sa présence ne trouble pas le phénomène étudié.

Nous avons étudié de cette façon la décantation d'une poudre de quartz dans un liquide, dans un appareil à fonctionnement discontinu. Nos mesures indiquent notamment que le tassement du dépôt est fonction de la hauteur de celui-ci et non du temps de séjour dans le décanteur.

La même méthode de mesure pourrait s'appliquer à l'étude du fonctionnement d'un appareil de décantation continu, d'un épaisseur cyclone ou d'une colonne de fluidisation.

ETUDE DE LA DÉCANTATION PAR LA MESURE DE LA CONSTANTE DIÉLECTRIQUE

Le but de cette note est de décrire une méthode de mesure rapide et précise de la concentration de suspensions de particules solides dans un liquide, à l'aide d'une mesure de la constante diélectrique de la suspension.

Nous nous proposions d'étudier le problème suivant: quelle est l'évolution de la concentration d'une suspension en ses différents points au cours d'une décantation. Un seul auteur, à notre connaissance, a fait des mesures dans ce sens (COMINGS [2]), il procède à l'analyse d'échantillons prélevés à l'aide d'une pipette en un point donné de la suspension en train de décanter. Cette méthode présente un inconvénient: pour que la prise d'échantillon ne trouble pas le phénomène de décantation qu'on est en train d'étudier, il faut qu'elle soit très lente. Comme il ne faut pas non plus que la concentration varie au cours de la prise d'échantillon, la méthode ne s'applique qu'à l'étude de poudres décantant très lentement.

La méthode par mesure de la constante diélectrique que nous avons utilisée donne au contraire une mesure *instantanée* et *locale*, ne troublant l'écoulement que d'une façon négligeable.

Le principe de la méthode est simple: on mesure la capacité d'un condensateur plongé dans la suspension; le rapport de cette capacité à celle du même condensateur dans l'air donne la constante diélectrique de la suspension. Celle-ci est une fonction de la concentration.

En prenant un condensateur suffisamment petit et de forme convenable on arrive à mesurer la constante diélectrique en un point, ou tout au moins dans un plan horizontal donné du milieu étudié. L'appareil de mesure que nous avons utilisé est un dielcomètre (*Haardt & Co*, Düsseldorf) qui permet une mesure très rapide et très précise à la fois de capacités de faible grandeur (20 à 110 μμF).

D'une façon générale la méthode présente de l'intérêt dans tout problème où il s'agit de suivre l'évolution dans le temps et dans l'espace d'une concentration pouvant varier assez rapidement.

RELATION ENTRE LA CONSTANTE DIÉLECTRIQUE ET LA CONCENTRATION DES SUSPENSIONS

Dans les cas de suspensions de grains solides dans un liquide les règles de mélange simples applicables au cas des solutions ne sont plus valables.

Différents auteurs ont proposé des lois dont la justification théorique est basée sur un certain nombre d'hypothèses sur la forme des grains et leur répartition dans le milieu liquide. Ces lois ont été plus ou moins bien vérifiées expérimentalement dans un certain nombre de cas particuliers.

On trouve dans l'article de BRUGGEMAN [1] (1935) une étude théorique assez complète des différentes formules proposées.

ε_2 = constante du liquide; ε_1 = constante du solide; δ = concentration de solide.

La formule de RAYLEIGH [5] s'écrit :

$$\varepsilon = \varepsilon_2 \left[1 - \delta \frac{\alpha + 1}{\frac{\alpha \varepsilon_2 + \varepsilon_1}{\varepsilon_2 - \varepsilon_1} + \delta - s \frac{\varepsilon_2 - \varepsilon_1}{r \varepsilon_2 + \varepsilon_1} \delta^r} \right]$$

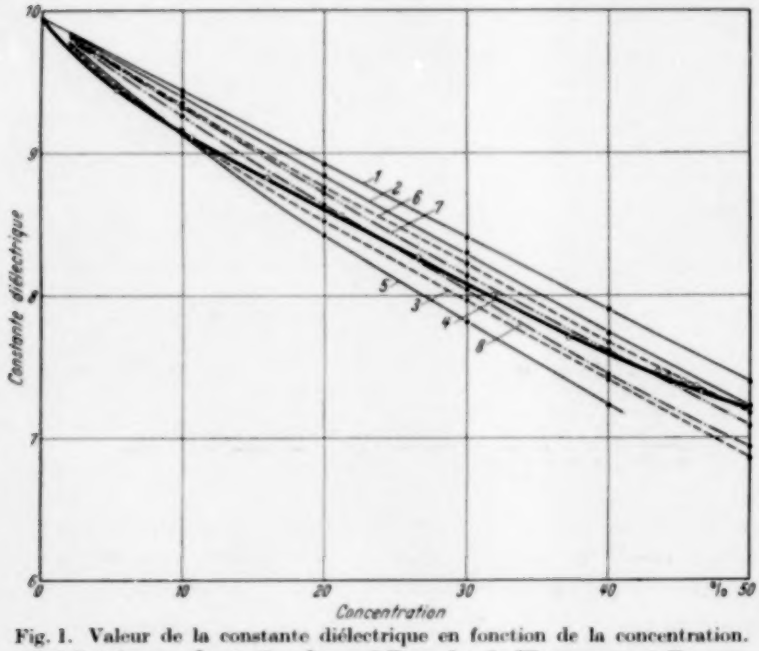

Fig. 1. Valeur de la constante diélectrique en fonction de la concentration. *1* Loi linéaire $\varepsilon = \delta\varepsilon_1 + (1-\delta)\varepsilon_2$. *2* Formules de WACHHOLTZ et FRANCESON $\varepsilon_0 = \frac{\varepsilon_2(1+\alpha-\delta^{\frac{1}{3}}\alpha)}{1+\alpha-\delta^{\frac{1}{3}}\alpha+\delta\alpha}$. *3* Formules de WACHHOLTZ et FRANCESON $\varepsilon_M = \frac{\varepsilon_2(1+\delta^{\frac{1}{3}}\alpha-\delta\alpha)}{1+\delta^{\frac{1}{3}}\alpha}$. *4* Valeurs expérimentales. *5* Loi linéaires pour les polarisations $p = \delta p_1 + (1-\delta)p_2$ $p = \frac{\varepsilon-1}{\varepsilon+2}$. *6* Formule de RAYLEIGH $\varepsilon = \varepsilon_2\left[1 - \delta \frac{3}{\frac{2\varepsilon_2+\varepsilon_1}{\varepsilon_2-\varepsilon_1} + \delta - 1{\cdot}65 \cdot \frac{\varepsilon_2-\varepsilon_1}{\frac{4}{3}\varepsilon_2+\varepsilon_1} \cdot \delta^{\frac{10}{3}}}\right]$. *7* Formule de WIENER $\frac{1}{\varepsilon+u} = \frac{\delta}{\varepsilon_1+u} + \frac{1-\delta}{\varepsilon_2+u}$ $u = 2\sqrt{\varepsilon_1\varepsilon_2}$. *8* Formule de LICHTENECKER $\varepsilon = \varepsilon_1^{\delta} \cdot \varepsilon_2^{1-\delta}$.

avec

	Grains sphériques	*Grains cylindriques*
α	2	1
r	$\frac{4}{3}$	1
s	1·65	0·306
x	$\frac{10}{3}$	4

si δ est petit elle devient :

$$\frac{\varepsilon - \varepsilon_2}{\varepsilon + \alpha\varepsilon_2} = \delta \frac{\varepsilon_1 - \varepsilon_2}{\varepsilon_1 + \alpha\varepsilon_2}.$$

La formule de WIENER [8] généralisée s'écrit :

$$\frac{1}{\varepsilon+u} = \frac{\delta}{\varepsilon_1+u} + \frac{1-\delta}{\varepsilon_2+u}$$

où u dépend de la forme des grains.

La formule de LICHTENECKER [4] est de la forme

$$\varepsilon = \varepsilon_1^{\delta_1(1+k\delta_2)} \cdot \varepsilon_2^{\delta_2(1-k\delta_1)} \quad \text{où} \begin{cases} \delta_2 = 1 - \delta_1 \\ k \text{ dépend de la forme} \end{cases}$$

on simplifie parfois en faisant $k = 0$

$$\varepsilon = \varepsilon_1^{\delta} \cdot \varepsilon_2^{1-\delta}.$$

BRUGGEMAN propose 2 nouvelles formules donnant des valeurs limites correspondant aux cas de grains sphériques

$$1 - \delta = \frac{\varepsilon_1 - \varepsilon}{\varepsilon_1 - \varepsilon_2} \sqrt[3]{\frac{\varepsilon_2}{\varepsilon}}$$

et de grains cylindriques

$$1 - \delta = \frac{\varepsilon_1 - \varepsilon}{\varepsilon_1 - \varepsilon_2} \cdot \frac{2\varepsilon_1 + \varepsilon_2}{2\varepsilon_1 + \varepsilon}.$$

GUILLIEN [3] (1941) a entrepris une vérification expérimentale assez poussée de ces diverses formules, il a trouvé la meilleure concordance avec la formule de WIENER dans laquelle on fait $u = 2\sqrt{\varepsilon_1\varepsilon_2}$ la formule de LICHTENECKER est souvent aussi bien vérifiée par les expériences pourvu que le rapport $\varepsilon_1/\varepsilon_2$ ne diffère pas trop de l'unité.

WACHOLTZ et FRANCESON [7] (1940) ont également entrepris des expériences en vue de contrôler les différentes formules proposées. Ces expériences montrent que la forme des grains joue un rôle important ; si $\varepsilon_2 < \varepsilon_1$, ε est d'autant plus faible que la forme des grains est proche de sphères ; ce résultat les conduit à rejeter les formules qui ne tiennent pas compte de ce facteur de forme ; ils proposent deux valeurs limites

$$\varepsilon_0 = \frac{\varepsilon_2(1+\alpha-\delta^{\frac{1}{3}}\alpha)}{1+\alpha-\delta^{\frac{1}{3}}\alpha+\delta\alpha} \qquad \alpha = \frac{\varepsilon_2 - \varepsilon_1}{\varepsilon_1}$$

$$\varepsilon_M = \frac{\varepsilon_2(1+\delta^{\frac{1}{3}}\alpha-\delta\alpha)}{1+\delta^{\frac{1}{3}}\alpha}$$

correspondant aux cas de particules cubiques ou parallélipipédiques. Dans la formule de WIENER ils proposent d'écrire $u = f \cdot v$ avec f facteur de forme.

Dans le même ordre d'idées il faut encore signaler l'étude D'ANDRIES VOET [6] 1947 qui montre que les écarts par rapport à la formule de BRUGGEMAN pour des sphères peuvent servir de mesure du degré de non

VOL. 1 1952

sphéricité des grains, et qui en déduit un moyen de suivre la floculation et l'agglomération des grains.

Nous avons calculé les différentes formules pour le cas particulier correspondant à nos expériences: *liquide:* solution de benzène et nitrobenzène ($\varepsilon = 9{\cdot}94$) *solide:* particules de quartz anguleuses ($\varepsilon = 4{\cdot}85$) les résultats sont inscrits sur le graphique (1) ainsi que les résultats des mesures directes.

On voit qu'aucune des courbes proposées ne rend vraiment bien compte des nos résultats, comme le but de notre travail n'est pas de vérifier ces formules, mais bien d'étudier la décantation, nous nous sommes basés dans la suite sur les valeurs données par la courbe d'étalonnage.

Réalisation Expérimentale

1) *Le Dielcometre*—Cet appareil construit par la firme *Haard & Co* Düsseldorf est décrit en détails dans l'article de WACHHOLTZ et FRANCESON. Le principe de son fonctionnement est le suivant: un circuit oscillant comporte en parallèle la capacité à mesurer et un condensateur variable étalonné, on compense les variations de la première en réglant le second, on vérifie que la somme de ces deux capacités est constante en comparant la fréquence du circuit oscillant à celle d'un autre circuit oscillant dont la fréquence est maintenue constante à l'aide d'un quartz. La comparaison des deux fréquences se fait en cherchant à annuler la fréquence du battement qu'elles produisent. La précision de la mesure dépend surtout de la précision et de l'étalonnage du condensateur variable.

2) *Le Condensateur de mesure.*—Après quelques essais nous avons adopté un condensateur qui comprend deux armatures en forme de grille situées toutes deux dans un même plan, chaque élément d'une grille se trouve situé entre deux éléments de l'autre. Le plan des grilles est orienté horizontalement, les fils, minces, ne troublent l'écoulement que d'une façon négligeable. Le peu de distance (2 mm) entre les éléments successifs des deux armatures empêche que les lignes de force du champ ne divergent d'une façon appréciable en dehors du plan de la grille. La mesure est donc bien localisée dans un plan donné.

3) *Les conducteurs d'amenée*—Le condensateur proprement dit étant relativement petit, sa capacité à vide ne dépasse pas 8 $\mu\mu$F la mesure est donc susceptible d'être fortement entachée d'erreur si on ne prend pas des précautions tout à fait spéciales pour éliminer les capacités parasites entre les conducteurs d'amenée de courant et les objets extérieurs raccordés à la terre. Nous avons obtenu les meilleurs résultats en utilisant un câble coaxial dont le conducteur extérieur est raccordé à la masse et constitue blindage. Ce câble a une capacité assez importante mais tout à fait invariable et indépendante de la position des objets extérieurs.

Etude de la Décantation d'une Suspension de Silice dans un Liquide

Le mode operatoire est le suivant—un poids donné de la poudre étudiée est mis dans le liquide (mélange opératoire de benzène et de nitrobenzène) contenu dans un cylindre gradué, le condensateur de mesure est fixé à un niveau donné et raccordé à l'appareil de mesure, la suspension est rendue homogène par une violente agitation du cylindre, puis on la laisse reposer et on commence immédiatement à faire des mesures de la capacité toutes les cinq secondes, jusqu'à ce que le tassement final soit atteint.

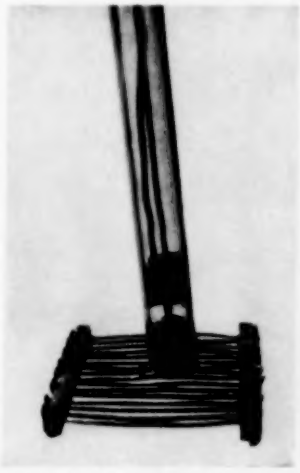

Fig. 2. Le condensateur de mesure.

On recommence le même processus pour chaque hauteur du condensateur, on relève ainsi des courbes semblables à celle de la Fig. 3 donnant la capacité en fonction du temps pour chaque hauteur, de cette famille de courbes on déduit ensuite facilement celles des Fig. 4 et 5 qui sont beaucoup plus intuitives; les courbes 4 donnent en fonction du temps les hauteurs où sont réalisées différentes concentrations, les courbes 5 donnent pour chaque valeur du temps, la concentration en fonction de la hauteur.

Ces courbes permettent de suivre d'une façon quantitative un processus de décantation: dès que quelques secondes se sont écoulées on peut reconnaître trois zones: A) une zone supérieure claire dans laquelle ne subsiste qu'un léger voile de particules très fines; B) une zone moyenne dans laquelle la concentration reste approximativement égale à la concentration initiale et C) une zone inférieure à concentration plus élevée, dans laquelle le solide est déposé.

Alors que la simple observation visuelle permet de mesurer d'une façon précise, seulement la vitesse de

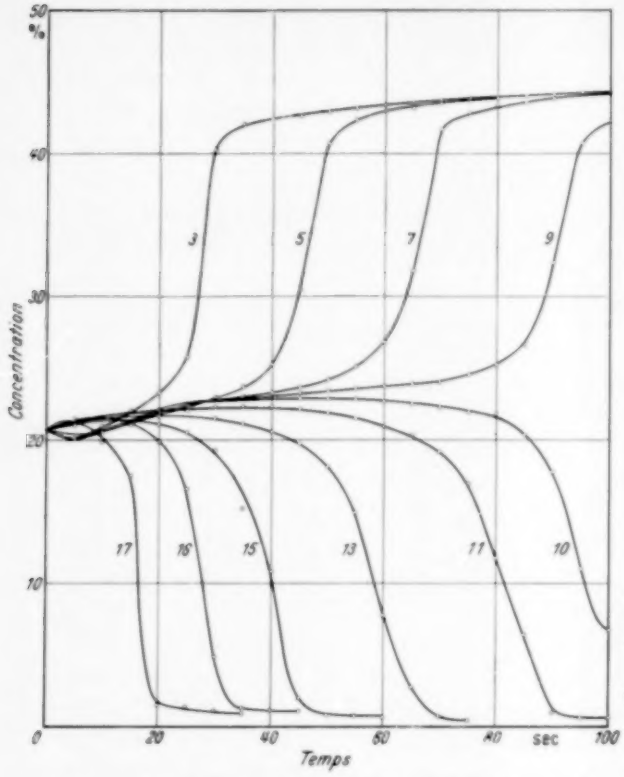

Fig. 3. Evolution de la concentration aux différents niveaux au cours de la décantation d'une poudre de quartz ($D = 58\ \mu$) dans une solution de benzène et de nitrobenzène—(Concentration initiale = 21%). H initiale = 20 cm. H finale = 9·65 cm.

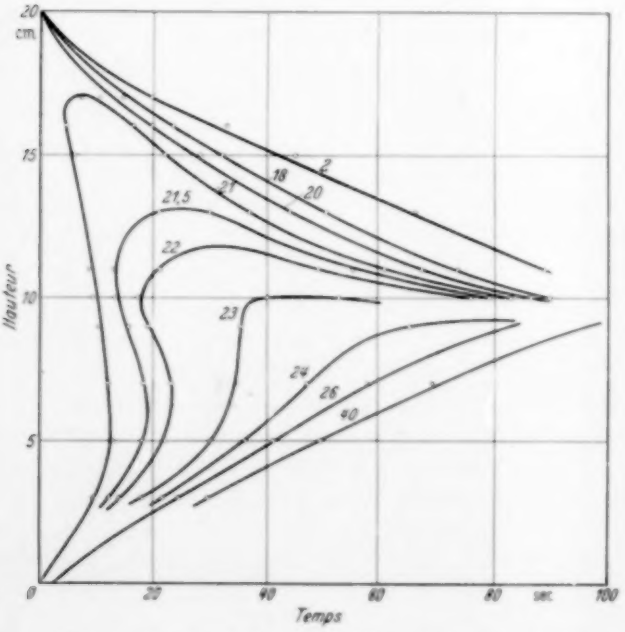

Fig. 4. Représentation des points ou une concentration donnée est réalisée en fonction du temps.

descente du niveau A–B, la mesure de la concentration en chaque point à chaque instant donne une connaissance complète du phénomène.

C'est ainsi que les courbes 4 mettent en évidence une certaine augmentation de la concentration dans la partie supérieure de la zone B dès les premières secondes. Cette augmentation n'est pas très considérable (1 ou 2%) mais elle persiste durant toute la décantation

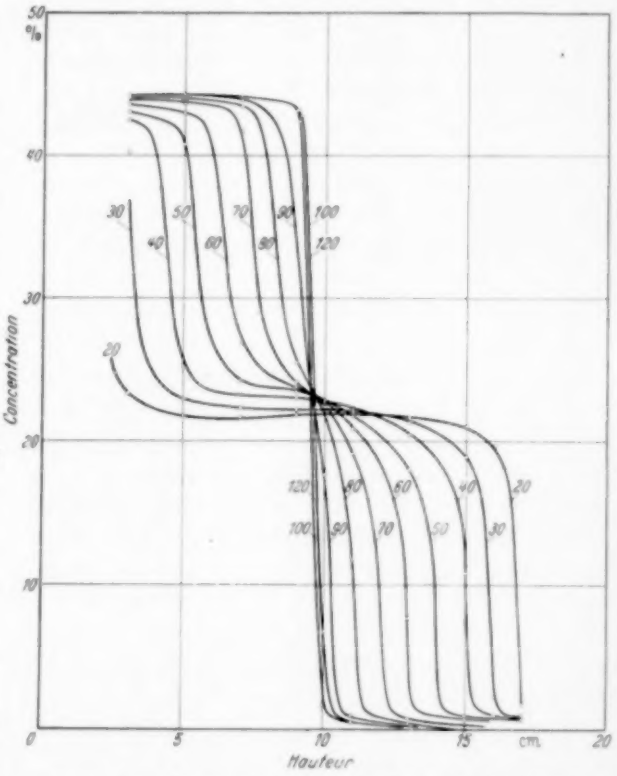

Fig. 5. Représentation de la concentration en fonction de la hauteur pour chaque valeur du temps.

et nous l'avons remarquée avec des suspensions de concentrations diverses. C'est donc un phénomène assez général.

Simultanément d'ailleurs la concentration de toute la zone B croît progressivement et lentement, cet accroissement qui atteint 2 à 3% en 100 sec pourrait probablement être plus important si la décantation était plus lente. Nos expériences ne nous permettent pas de dire dès maintenant s'il en est bien ainsi.

On peut cependant en conclure que ce n'est qu'en première approximation que cette zone B a une concentration homogène et constante.

Un autre problème est de connaître l'étendue des zones de transition qui existent certainement entre les

VOL. 1 1952

zone A, B, C. On voit, par les courbes 4 que la concentration passe de 2% à 18% sur une hauteur de 1·5 cm et de 26% à 40% sur une hauteur de 1 cm. Ceci indique donc que la séparation des zones B–C est au moins aussi brusque que celle des zones A–B. L'observation visuelle indique d'ailleurs que la zone de transition A–B n'a certainement pas 1·5 cm d'épaisseur. Les valeurs plus grandes déduites des mesures peuvent être expliquées facilement: quelles que soient les précautions prises, les lignes de force du champ sortent un peu du plan de la grille de sorte que la mesure est déjà modifiée avant que la zone de transition n'ait atteint le niveau du plan de mesure.

De toute façon la méthode permet de suivre facilement et avec une approximation très suffisante la montée du niveau de transition B–C qu'il n'est guère possible d'observer directement dans la généralité des cas.

Les mesures de constante diélectrique nous permettent encore de mieux connaître le problème assez controversé du processus de tassement de la zone C.

On constate en effet que le dépôt n'atteint pas d'emblée la concentration maximum qu'il est susceptible d'atteindre finalement. Certains auteurs sont d'avis que le tassement maximum n'est atteint qu'au bout d'un délai relativement long au cours duquel les particules glissent l'une sur l'autre, le mouvement étant entravé par les frottement entre grains. Pour ces auteurs la concentration de la boue épaisse obtenue dans un décanteur industriel dépend du temps de séjour dans le décanteur.

D'autres auteurs pensent que le tassement est dû à la compression exercée par le poids des couches de dépôt successives. A chaque pression correspond un état d'équilibre entre les grains qui est rapidement atteint. Pour ces auteurs la concentration de la boue d'un décanteur dépend de la hauteur de la couche de dépôt.

Les mesures que nous avons faites montrent que le tassement continue à augmenter en un point de la zone C tant que celle-ci augmente c'est-à-dire tant que le poids de poudre déposé augmente, mais ce tassement cesse de se modifier dès que ce poids reste constant.

Ces mesures montrent aussi que le tassement final varie d'une façon appréciable d'un niveau à l'autre de la zone C, en diminuant de bas en haut, ceci confirme que le facteur principal dont dépend le tassement est la compression due au poids des couches supérieures le temps nécessaire pour réaliser l'équilibre pour un état de force donné étant inappréciable.

Il faut remarquer ici que les expériences ont été faites avec une poudre relativement grosse (silice C: $dm = 58\mu$) ne floculant pas il est probable que le facteur temps est plus important quand il y a floculation. Cette hypothèse explique d'ailleurs le désaccord entre les différents auteurs.

Finalement il faut encore indiquer que la méthode de mesure est surtout intéressante pour suivre l'évolution des concentrations plutôt que pour en faire des mesures absolues très précises. Il est en effet toujours possible que la présence de la grille modifie légèrement les concentrations, cela est même probable lors des mesures dans la zone C plus ou moins tassée, mais il est bien certain que le sens et la durée des variations de ces concentrations n'est pas changé.

Le présent travail a été effectué au laboratoire de Chimie Industrielle de l'Université de Bruxelles sous la direction de Monsieur le Professeur DE KEYSER grâce à une subvention du Comité Tassel.

NOTATION

k, r, s, u, α, x = constantes numériques
ε = constante diélectrique de la suspension
ε_1 = constante diélectrique du solide
ε_2 = constante diélectrique du liquide
δ_1 = fraction du volume occupé par le solide
δ_2 = fraction du volume occupé par le liquide
d_m = diamètre équivalent moyen des grains
H_i = hauteur initiale de la suspension
H_f = hauteur finale du dépôt de poudre.

BIBLIOGRAPHIE

[1] BRUGGEMAN, D.A.G.; Ann. Phys. F. 5 1935 **24** 636. [2] COMINGS, E.W.; Thickening calcium carbonate slurries, Ind. Eng. Chem. 1940 **32** 663. [3] GUILLIEN, R.; Ann. Phys., Paris 1941 (11e série 16) 205. [4] LICHTENECKER, K.; Phys. Z. 1918 **19** 374. [5] RAYLEIGH, J.W.; Phil. Mag. 1892 **34** 481. [6] VOET, A.; Dielectrics and Rheology of non aqueous dispersions, J. Phys. Coll. Chem. 1947 **51** 1037. [7] WACHHOLTZ, F. et FRANCESON, A.; Dielektrische Messungen an Pigment-Leinölsuspensionen. Koll. Z. 1940 **92** 75. [8] WIENER, O.; Abh. d. Sächs. Ges. d. Wiss. Math. Phys. Kl. 1912 **32** 509.

Calculation of the efficiency of counter-current stage-wise mass transfer processes with constant distribution factor, when in the stationary state*

I. Distribution of one component only

A. KLINKENBERG

N. V. De Bataafsche Petroleum Maatschappij, Royal-Dutch/Shell Group, The Hague

(Received 19 July 1951)

Summary—A rapid and easy method is presented for the derivation of equations for counter-current stage-wise mass transfer of a single solute with a constant distribution factor, when in the stationary state. The method is valid for a group of related processes but it is specifically applied to extraction.

Equations are derived for extraction with an intermediate feed point ("complete rectification") and for extraction with introduction of the feed at an end ("extraction" or "washing"). Some of their consequences are discussed.

The use of reflux is included in the treatment.

Equations are also given for the accumulation of solute in the feed stage.

The separation of two solutes is to be discussed in a subsequent paper.

Résumé—L'auteur présente une méthode rapide et commode pour la dérivation d'équations convenant à l'état stationnaire dans les problèmes de transfert de masse étagés à contre-courant, lorsque le système présente un facteur de distribution constant. Cette méthode, valide pour tout un groupe de procédés d'échange, est particulièrement applicable à l'extraction.

Dans ce cas, les equations s'appliquent aussi bien à la rectification complète (alimentation à un niveau intermédiaire) qu'à l'extraction simple ou lavage (alimentation en tête).

L'auteur discute certaines conséquences de ces équations. Il étudie également le cas du reflux. Il donne aussi les équations correspondant à l'accumulation de corps dissous dans l'étage d'alimentation.

La séparation de deux corps dissous fera l'objet d'une publication ultérieure.

VOL. 1 1952

1. Distribution Factors such as the Extraction Factor

The following calculations apply to counter-current mass transfer processes, carried out in ideal stages under such conditions that the amounts of a certain solute leaving a stage with the two streams have a constant ratio.

In counter-current extraction the amount of the solute, whose extraction is being studied, may be small with regard to the amount of liquid originally carrying this solute and also with regard to the amount of solvent. Under these conditions we may neglect the volume effect of the extraction so that the throughputs of the two streams will not change from stage to stage.

Under these same conditions in most cases the ratio of the concentrations of the solute in the two streams will also be constant (Nernst Distribution Law). This constant ratio is called distribution coefficient or partition coefficient K. The concentration is to be expressed in any units per unit of volume.

We define

$$K = \frac{C}{c} = \frac{\text{concentration in solvent rich phase}}{\text{concentration in solvent poor phase}} \qquad (1)$$

under equilibrium conditions.

For the purpose of this paper throughputs are much more important than concentrations.

If the concentrations (C, c) are multiplied by the throughputs of the phases (volume per time):

V = throughput of solvent rich or extract phase in volumes per unit time;

v = throughput of solvent poor or residue phase in volumes per unit time;

we obtain

Q = throughput of solute by solvent rich phase (any unit per unit time);

q = throughput of solute by solvent poor phase (same unit per unit time).

Under equilibrium conditions, *i.e.* when leaving an ideal stage, Q and q will also have a constant ratio, the extraction factor E.

$$E = \frac{\text{amount of solute leaving ideal stage with extract phase}}{\text{amount of solute leaving ideal stage with residue phase}} \qquad (2)$$

so that

$$E = \frac{Q}{q} = \frac{CV}{cv} = K\frac{V}{v}. \qquad (3)$$

The same reasoning applies to the class of extraction processes sometimes called "fractional distribution," where a mixture of solutes is added to two solvents flowing in counter-current. However, the choice of the phases to be used in numerator and denominator in the above definitions becomes an arbitrary one.

* This paper was presented to the XII International Congress of Pure and Applied Chemistry, New York, September 10–13, 1951.

The concept extraction factor may be generalized to cover other unit operations. We may call it in general a distribution factor. Such distribution factors are of considerable use in the study of:

Liquid-liquid extraction.

Solid-liquid extraction (leaching).

Stripping.

Absorption (under isothermal conditions),

where they are often very nearly constant.

In distillation the distribution factors in general are variable because of the temperature gradient. FENSKE's well-known equation, however, is of the type discussed here.

It should be realized that the low concentrations required for the application of constant distribution factors should not occur in extraction with two solvents. If they do, the system has been insufficiently loaded with solutes and is, therefore, not working economically.

It is felt that calculations based on constant distribution factors will:

1. in many cases offer a good quantitative approximation;

2. very often be useful for rough estimates;

3. be extremely useful for educational purposes, because many features of the stage-wise mass transfer processes can be studied here in their simplest form.

The perhaps oldest application of distribution factors is found in absorption, where KREMSER [1] introduced the absorption factor A.

2. Definition of Processes to be studied

The processes to be considered are *continuous* in the time. We shall not consider working on a *batch* of feed, as in batch rectification, nor discuss transient phenomena occurring before the stationary state is reached.

They are operated in *stages, i.e.* the concentrations, etc. assume a number of discrete values as a function of another discrete variable, the stage number.

The stages may be operated either *intermittently*, as in separating funnels, or *non-intermittently*, as in systems of mixers and settlers. This difference does not influence the results of the calculations.

The *counter-current* principle as such does not require clarification. However, it is to be stated particularly that the feed need not be introduced at an end of the system. A treatment will be developed which is valid for two solvents flowing counter-currently with introduction of feed mixture at some intermediate point.

In continuous distillation it is obvious that the mixture to be distilled must not be introduced at the top (or the bottom) of the column, since this would not allow obtaining the more (or less) volatile component in the pure state. Hence the use of columns for complete rectification, comprising a "rectifying section" and a "stripping section."

The same object was achieved in extraction by VAN DIJCK [2] by the use of two immiscible solvents, flowing in counter-current with introduction of the feed at some intermediate point. This process is in use for the extraction of lubricating oils ("Duo Sol Process," solvents: propane and a mixture of phenol and cresylic acid) and citrus oils (VAN DIJCK and RUYS [3], VAN WIJK and VAN DIJCK [4], solvents: pentane and aqueous methanol). More recently SCHEIBEL [5] called attention to it. Here again we shall speak of complete rectification. Rectification is understood to be a process for purifying a phase by counter-current contact with another phase containing certain materials (the reflux) produced from the first phase. Obviously this definition applies on both sides of the feed stage, in distillation, extraction and several other processes.

In distillation the reflux is usually produced outside the system (in condenser and reboiler); in extraction it is usually—when both solvents are originally free of solute—produced within the system.

3. Basic Equations

The calculations will employ extraction factors and throughputs of solute.

The following convention is used for defining extraction factors with the aid of eq. (2) when a polar solvent is used in counter-current to a hydrocarbon solvent:

phase rich in polar solvent is called extract phase,

phase rich in hydrocarbon solvent is called residue phase.

The section of a complete rectification between feed and inlet of polar solvent by analogy of single-solvent extraction is called an extraction section; the section between feed and inlet of less polar solvent a washing section.

This is shown in Fig. 1.

The stages will be numbered in the direction of the flow of the non-polar solvent; the transport of solute thereby is represented by the q values.

Flow rates of solute carry a subscript to show the stage of origin.

A section of a counter-current system is represented by Fig. 2. The squares represent the stages*, the arrows the flows of solute.

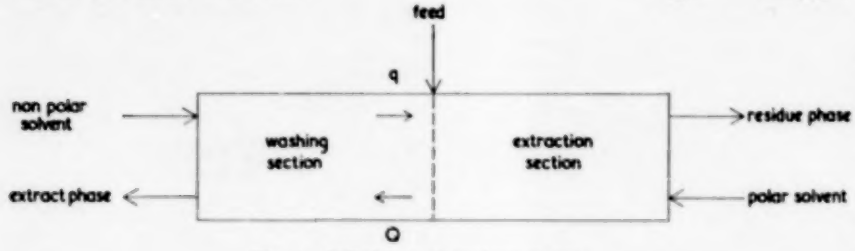

Fig. 1. Definitions of various terms.

For a system of ideal stages in stationary operation the basic equations are:

$$Q_k = E\,q_k \text{ (equilibrium condition).} \qquad (4)$$

$$q_k - Q_{k+1} = \text{constant (material balance).} \qquad (5)$$

The latter equation is a finite difference equation.

This set of equations may be solved by starting from the end(s) of the system and working towards

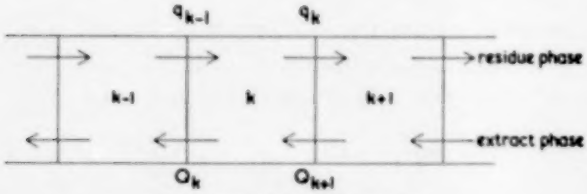

Fig. 2. Definitions of flow rates.

the feed such as was KREMSER's procedure when he derived an equation describing counter-current absorption [1]. SCHEIBEL [5] when studying the process of complete rectification in extraction proceeded numerically from both ends toward the feed.

The calculus of finite differences has been employed by TILLER and TOUR [6] and TILLER [7], who showed that the solutions assume the form of series of powers of the extraction factor.

The present paper tends to avoid the lack of elegance of the step-wise procedure on the one hand and the use of a not too familiar mathematical technique on the other.

To this end the material balance of the k'th stage

$$q_k - Q_{k+1} = q_{k-1} - Q_k \qquad (6)$$

* In a conventional drawing of a plate column the dividing lines represent stages.

with the aid of (4) is rewritten in the form

$$\frac{Q_k}{E} - Q_{k+1} = q_{k-1} - q_k\,E \qquad (7)$$

or, after multiplication by $-E^k$:

$$-Q_k\,E^{k-1} + Q_{k+1}\,E^k + q_{k-1}\,E^k - q_k\,E^{k+1} = 0. \qquad (8)$$

This equation describing the extraction in the k'th stage is found by giving the streams entering the stage a positive and those leaving a negative sign, multiplying each stream by a power of E, the exponent of which is the number of the stage into which the stream *enters*, and equating the sum to zero.

Upon adding the corresponding equation for the adjacent stage $(k+1)$ the terms for the transports between stages k and $k+1$ are seen to cancel. This procedure may be continued in the same way.

Consequently for any counter-current system with constant extraction factor the procedure for finding the equations governing the extraction is the following:

1. Number the stages in the direction of the flow of that phase whose solute flow is in the definition of E in the denominator (*i.e.* the residue phase).

2. Assign a positive sign to solute flow rates entering, and a negative sign to flows leaving the extraction system.

3. Multiply each solute flow rate by a power of E the exponent of which is the number of the stage in which such flow *enters*.

For this purpose it will be necessary to add fictitious stages for all streams leaving the system.

4. Equate the sum of the flows found under *2* to zero (= overall material balance).

5. Equate the sum of the products found under *3* to zero (= extraction equation).

6. Reduce the two equations to a single one by eliminating one of the unknowns.

4. Application to Complete Rectification

Fig. 3 represents a complete rectification, in $n+m-1$ stages, with feed F in the m'th stage.

According to the procedure described in section 3 the two equations are found to be:

$$\left.\begin{aligned} -Q_1 + q_0\,E + F\,E^m + Q_{n+m}\,E^{n+m-1} - \\ - q_{n+m-1}\,E^{n+m} = 0, \end{aligned}\right\} \qquad (9)$$

$$-Q_1 + q_0 + F + Q_{n+m} - q_{n+m-1} = 0. \qquad (10)$$

Case I.—No reflux at the ends

If the solvents are pure, so that no reflux is applied at the ends, we have:

$$q_0 = 0, \tag{11}$$

$$Q_{n+m} = 0, \tag{12}$$

so that:

$$q_{n+m-1} = F\,\frac{E^m - 1}{E^{n+m} - 1}, \tag{13}$$

$$Q_1 = F\,\frac{E^m (E^n - 1)}{E^{n+m} - 1} \tag{14}$$

and the ratio R of the amounts of solute in the two products is given by:

$$R = \frac{Q_1}{q_{n+m-1}} = \frac{E^m (E^n - 1)}{E^m - 1}. \tag{15}$$

Special cases are:

a) $E = 1$.

$$q_{n+m-1} = F\,\frac{m}{n+m}, \tag{16}$$

$$Q_1 = F\,\frac{n}{n+m}, \tag{17}$$

$$R = \frac{n}{m}. \tag{18}$$

b) $E \gg 1$.

$$R \approx E^n. \tag{19}$$

c) $E \ll 1$.

$$R \approx E^m. \tag{20}$$

d) $n = m$.

$$q_{2n-1} = F\,\frac{1}{E^n + 1}, \tag{21}$$

$$Q_1 = F\,\frac{E^n}{E^n + 1}, \tag{22}$$

$$R = E^n. \tag{23}$$

The symmetrical case discussed under *d* has been studied by ROMETSCH [8].

Equation [15] for the general case has been derived by BARTELS and KLEIMAN [9].

Related equations have also been derived by STENE [10], but his mathematical approach, through intermittent batch processes (non-stationary extractions in separating funnels), is rather complicated.

Case II.—Total reflux

Total reflux is applied when the solute leaving the system at either end is re-introduced with the other solvent at that same end, *i.e.*

$$q_0 = Q_1,$$
$$Q_{n+m} = q_{n+m-1}$$
$$F = 0.$$

Equation (9) then gives:

$$R = \frac{Q_1}{q_{n+m-1}} = E^{n+m-1}. \tag{24}$$

In a symmetrical system ($n = m$) the ratio R obtainable is:

E^{2n-1} with total reflux (eq. 24);

E^n without external reflux (eq. 23).

As ROMETSCH [8] has pointed out, this shows what maximum improvement is obtainable by the use of reflux.

Case III.—Finite reflux

Reflux ratios r_e and r_w at the ends of the extraction and the washing section are defined by:

$$\frac{q_{n+m-1}}{Q_{n+m}} = \frac{r_e + 1}{r_e},$$

$$\frac{Q_1}{q_0} = \frac{r_w + 1}{r_w}.$$

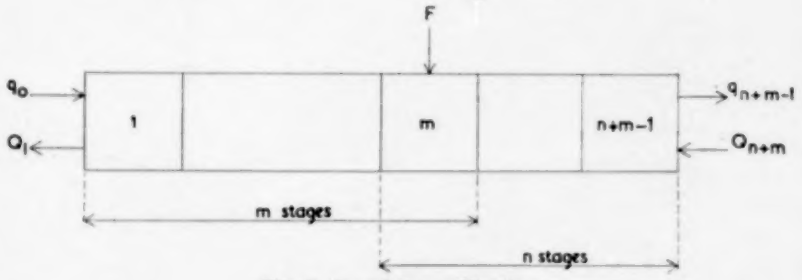

Fig. 3. Complete rectification.

Substitution in eq. (9) and (10) gives:

$$R = \frac{Q_1 - q_0}{q_{n+m-1} - Q_{n+m}} = \frac{(r_e + 1)\,E^{n+m} - r_e\,E^{n+m-1} - E^m}{(r_w + 1)\,E^m + r_w\,E - (r_w + 1)}. \tag{25}$$

Use of reflux has been discussed by ASSELIN and COMINGS [11], who have used graphical methods of computation. They stated that it may improve the separation obtainable; however, the higher solute concentrations will counteract this through a reduction of the separating effect of the single stage. The accumulation of solute which is responsible for this reduction will be discussed in Section 8. The use of reflux in the washing section has been described by TIJMSTRA [12].

Discussion of Case I, no reflux

The significance of the equations (21), (22) and (23) for symmetrical systems is easy to visualize. Eq. (23) is represented in Fig. 4.

Thus, if $E = 2$ in a system of 11 stages, $n = 6$, the ratio $R = E^n = 64$ so that 98·5% of the feed leaves the system with the extract phase and 1·5% with the residue phase.

In a plot of log R against log E a straight line is obtained with an angle of inclination α, for which $\operatorname{tg} \alpha = n$.

Such a graph is shown in Fig. 5.

Asymmetrical systems, described by eq. (15), are represented in this graph by curves having asymptotes under inclination $\operatorname{tg} \alpha = m$ [see eq. (20)] and $\operatorname{tg} \alpha = n$ [see eq. (19)].

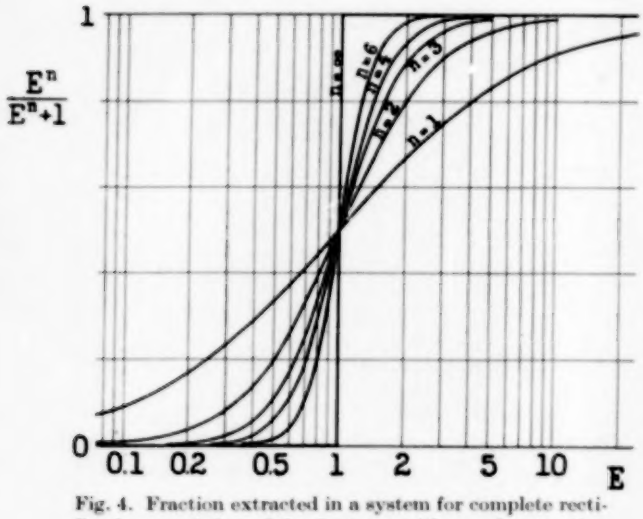

Fig. 4. Fraction extracted in a system for complete rectification consisting of $2n$-1 stages with equal extraction factors and in which the feed is introduced in the middle.

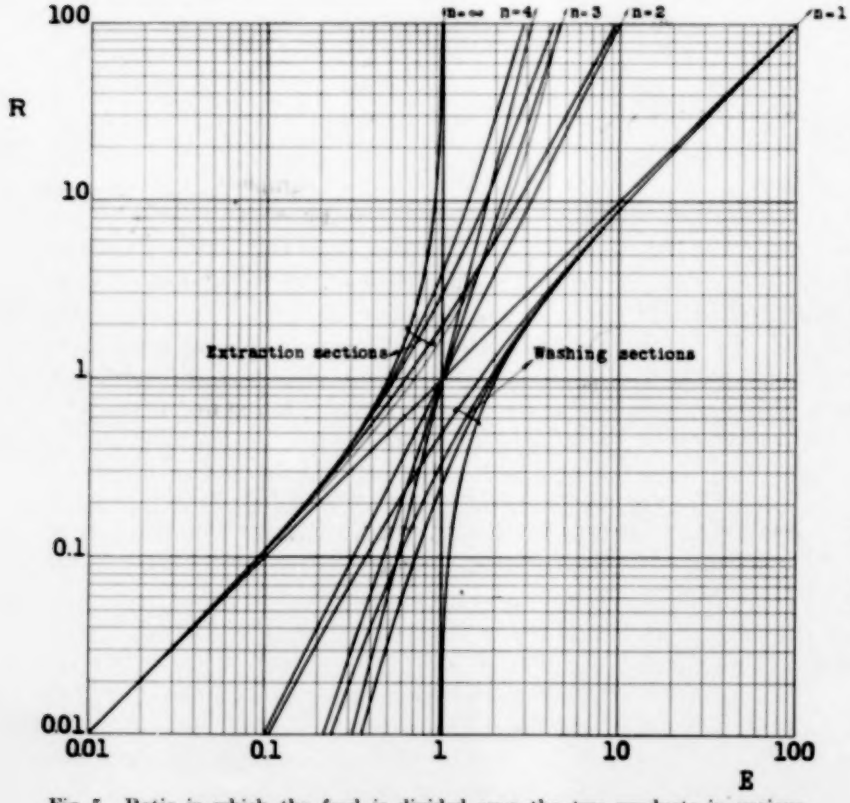

Fig. 5. Ratio in which the feed is divided over the two products in various systems with constant extraction factor.

5. Application to Ordinary Counter-Current Extraction with an Initially Pure Solvent

Equations for extraction with a pure solvent in an extraction section only (see Fig. 6) are obtained by substituting $m = 1$ in eq. (13)–(15), or by straight application of the principles of section 3.

$$q_n = F \frac{E-1}{E^{n+1}-1}, \tag{26}$$

$$Q_1 = F \frac{E(E^n-1)}{E^{n+1}-1}, \tag{27}$$

$$R = \frac{E(E^n-1)}{E-1}. \tag{28}$$

Equation (26) is known as KREMSER's equation. The consequences have been discussed by many authors and it is found in various other forms, see *e.g.* PERRY [13].

It is readily seen that the extraction can be made to approach completeness, $\lim_{n\to\infty} q_n \to 0$, only for $E \geq 1$.

For $E < 1$, $\lim_{n\to\infty} q_n = F(1-E)$. In words: If the solvent is not good enough (K too low) or not enough of it is used (V/v too low) the extraction cannot be carried to completeness.

This is also easily seen from the graph Fig. 7.

KREMSER's equation allows solving such problems as determining the minimum amount of solvent required (corresponding to $E = 1$) and determining the economic optimum for the combination of cost of solvent circulation and cost of stages.

6. Application to a Washing Process

The washing process (see Fig. 8) is obtained by putting $n = 1$, whence from eq. (13)–(15):

$$q_m = F \frac{E^m-1}{E^{m+1}-1}, \tag{29}$$

$$Q_1 = F \frac{E^m(E-1)}{E^{m+1}-1}, \tag{30}$$

$$R = \frac{E^m(E-1)}{E^m-1}. \tag{31}$$

VOL. 1 1952

7. Application to Ordinary Counter-Current Extraction with an Impure Solvent

When the solvent is impure ($Q_{n+1} \neq 0$) the two fundamental equations read:

$$-Q_1 + F + Q_{n+1} - q_n = 0,$$

$$-Q_1 + F E + Q_{n+1} E^n - q_n E^{n+1} = 0$$

whence

$$q_n = F \frac{E-1}{E^{n+1}-1} + Q_{n+1} \frac{E^n - 1}{E^{n+1}-1}. \quad (32)$$

q_n is the sum of two terms representing the result of an n stage extraction of the feed F with pure solvent [eq. (26)] and an n stage washing process carried out on the impurity Q_{n+1} [eq. (29)].

Equation (32) may be re-arranged to:

$$\left(q_n - \frac{Q_{n+1}}{E}\right) = \left(F - \frac{Q_{n+1}}{E}\right) \frac{E-1}{E^{n+1}-1}. \quad (33)$$

Hence the alternative method of describing this process consists in deducing the solute flow in the residue phase that would be in equilibrium with the solute flow Q_{n+1} in the extract phase $\left(viz.\ \frac{Q_{n+1}}{E}\right)$, subtracting this from all solute flows in the residue phase and applying KREMSER's equation to the remainder.

Both forms of the equations have been given by SOUDERS and BROWN [14].

8. Accumulation of Solute

The feed stage (m) in a system for complete rectification (Fig. 3) receives flows q_{m-1} and Q_{m+1} from adjacent stages, so that the solute load may be a multiple of that caused by the feed only.

The total load of the feed stage is also given by $q_m + Q_m = (E+1)\, q_m$.

One may calculate q_m from q_{n+m-1} and Q_{n+m} by applying equations for extraction with impure solvent.

The following is found:

$$\left.\begin{aligned} \frac{q_m + Q_m}{F} &= \frac{E+1}{E-1} \times \\ \times \frac{\{E^m + r_w E - (r_w+1)\}\{(r_e+1)E^n - r_e E^{n-1} - 1\}}{(r_e+1)E^{n+m} - r_e E^{n+m-1} + r_w E - (r_w+1)}& \end{aligned}\right\} \quad (34)$$

Conclusions worth noting are:

1. For a symmetrical system ($n = m$) in the absence of reflux ($r_e = 0$; $r_w = 0$):

$$\frac{q_n + Q_n}{F} = \frac{E+1}{E-1} \cdot \frac{E^n - 1}{E^n + 1}. \quad (35)$$

This ratio approaches unity for $E \gg 1$ or $E \ll 1$ and reaches a maximum value equal to n for $E = 1$.

Accumulation, therefore, is most pronounced for the component with $E = 1$ and in systems with many stages.

The accumulations are of practical importance because they increase the miscibility of the solvents, thereby reducing the selectivity of the separation, so that they may limit the throughput.

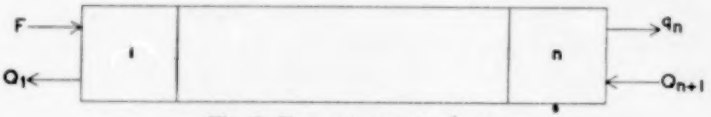

Fig. 6. Extraction section only.

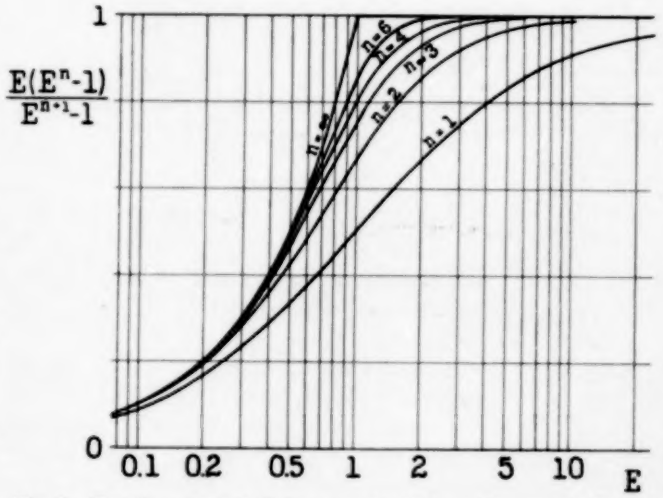

Fig. 7. Fraction extracted in an extraction section consisting of n-stages with equal extraction factors.

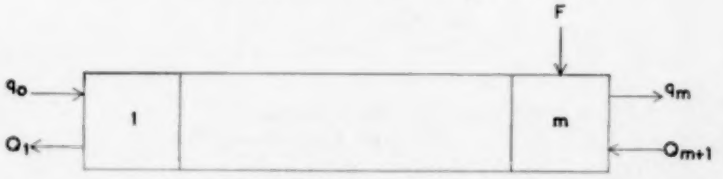

Fig. 8. Washing section only.

They also increase the time required for reaching stationary conditions.

2. If E^n and $E^m \gg 1$, when the ratio R of solute in final extract phase to solute in final residue phase according to eq. (25) is very high, eq. (34) reduces to:

$$\frac{q_m + Q_m}{F} = \frac{E+1}{E-1} \quad (35\,a)$$

i.e. the accumulation is independent of the reflux ratios. Similarly for low R, $E^n \ll 1$; $E^m \ll 1$

$$\frac{q_m + Q_m}{F} = \frac{E+1}{1-E}. \quad (35\,b)$$

Consequently if a sharp separation is obtained between components 1 and 2 with $R_1 \ll 1$ and $R_2 \gg 1$ the separation can

be improved by the use of reflux, whereas the accumulation of solute and therefore the maximum throughput are, in first approximation, not changed.

The accumulation has also been studied by STENE [10] for systems of separating funnels. Equation (35a) due to STENE, has been used by O'KEEFFE, DOLLIVER and STILLER [15] for the study of the accumulation of two streptomycins ("A" and "B") in the feed stage of a symmetrical system. In their experiment the distribution coefficients were $K_A = 2{\cdot}2$; $K_B = 0{\cdot}63$, so that $K_A/K_B = 3{\cdot}49$. The ratio V/v was adjusted so as to make $E_A = \sqrt{3{\cdot}49} = 1{\cdot}87$ and $E_B = 1/\sqrt{3{\cdot}49}$.

The ratio $\frac{q_m + Q_m}{F}$ in all 11 stage system ($m = 6$) was found to be for both components 2·15. Equation (35a) also gives 2·15. From eq. (35), the exact equation to be applied in this case, a value 2·05 is found. Obviously for $E = 1$ STENE's equation, as quoted by O'KEEFFE et al. would not be applicable at all. STENE, however, also gives the exact eq. (35).

The rate of approach to the steady state in symmetrical systems has been discussed by SCHEIBEL [6]. He showed that the approach to steady conditions is slower the higher the number of stages, and furthermore, it is slowest for the component with $E = 1$. This is understandable in view of the similar trend of the accumulation.

9. INTRODUCTION TO THE PROBLEM OF THE SEPARATION OF TWO SOLUTES

Two solutes 1 and 2 are characterized by their distribution coeficients K_1 and K_2, where $K_2/K_1 = \beta$ ($\beta > 1$).

NOTATION

Symbol	*Definition*	*Unit*
C	concentration in solvent-rich phase	any unit per unit volume
c	concentration in solvent-poor phase	any unit per unit volume
E	extraction factor [see eq. (2)]	dimensionless
F	rate of input of solute as feed	same units as Q
K	distribution coefficient [see eq. (1)]	dimensionless
m	number of stages in washing section (incl. feed stage)	dimensionless
n	number of stages in extraction section (incl. feed stage)	dimensionless
Q	rate of throughout of solute by solvent-rich phase	same unit as used in defining concentrations, per unit time
q	rate of throughput of solute by solvent-poor phase	same unit as used in defining concentrations, per unit time
R	ratio of the amounts of solute in final extract and extraction residue [see eq. (15)]	dimensionless
r_e	reflux ratio at the end of the extraction zone	dimensionless
r_w	reflux ratio at the end of the washing zone	dimensionless
V	throughput of solvent-rich phase	volume per unit time
v	throughput of solvent-poor phase	volume per unit time
α	angle of inclination in Fig. 5	dimensionless
β	ratio of distribution coefficients K_2/K_1	dimensionless

Indices indicating stages (see Fig. 1 and 2):

0	fictitious stage beyond end of washing section
1	last stage of washing section
k	any stage
m	feed stage
$n + m - 1$	last stage of extraction section
$n + m$	fictitious stage beyond end of extraction section

Indices indicating components:

1	component with lower distribution coefficient
2	component with higher distribution coefficient

VOL. 1 1952

In view of eq. (3) their extraction factors will have this same ratio:

$$\frac{E_2}{E_1} = \beta. \tag{36}$$

The factor β characterizes the difficulty of the separation. It is equivalent to the relative volatility in distillation.

We may now be faced with either of two problems.

1. Given: Feed composition, partition coefficients K_1 and K_2, conditions of extraction (number of stages, feed point, and ratio of phase volumes).

Asked: Product compositions.

Since n, m, E_1 and E_2 are known, this is easily solved with the aid of eq. (13) and (14).

2. Given: Feed composition, product compositions and ratio β of partition coefficients.

Asked: Conditions of extraction (n, m, E_1, E_2).

The three given compositions may also be replaced by two compositions and a yield.

This second problem is of considerably more practical importance and is also more difficult to handle. It will be examined in the second part of this paper.

LITERATURE

[1] KREMSER, A.; Nat. Petr. News (21. May) 1930 **22** No. 21 43. [2] DIJCK, W. J. D. VAN; U.S. Pat. 2023109, Dec. 3, 1935 (convention date June 3, 1929). [3] DIJCK, W. J. D. VAN and RUYS, A. H.; Perfumery and Essential Oil Record 1937 **28** 91. [4] WIJK, W. R. VAN and DIJCK, W. J. D. VAN; U.S. Pat. 2154713, April 18, 1939 (convention date April 17, 1936). [5] SCHEIBEL, E. G.; Chem. Eng. Progress 1948 **44** 681. [6] TILLER, F. M. and TOUR, R. S.; Trans. Am. Inst. Chem. Engrs 1944 **40** 317. [7] TILLER, F. M.; Chem. Eng. Progr. 1949 **45** 391. [8] ROMETSCH, R.; Helv. Chim. Acta 1950 **53** 184. [9] BARTELS, C. R. and KLEIMAN, G. M.; Chem. Eng. Progr. 1949 **45** 589. [10] STENE, S.; Arkiv för Kemi 1944 **18** A N:o 18. [11] ASSELIN, G. F. and COMINGS, E. W.; Ind. Eng. Chem. 1950 **42** 1198. [12] TIJMSTRA, S.; Brit. Pat. 452537, Aug. 25, 1936 (convention date Dec. 26, 1934). [13] PERRY, J. H.; Chem. Engrs. Handbook, 3rd Ed., 1950 p. 554, Fig. 29. [14] SOUDERS, M. jr. and BROWN, G. G.; Ind. Eng. Chem. 1932 **24** 519. [15] O'KEEFFE, A. E., DOLLIVER, M. A. and STILLER, E. T.; J. Amer. Chem. Soc. 1949 **71** 2452. [16] SCHEIBEL, E. G.; Ind. Eng. Chem. 1951 **43** 242.

Calculation of the efficiency of counter-current stage-wise mass transfer processes with constant distribution factor, when in the stationary state†

II. Stage requirements for the separation of two components by two solvent extraction

A. KLINKENBERG*, H. A. LAUWERIER** and G. H. REMAN**

(Received 19 July 1951)

Summary—The equations governing counter-current extraction as derived in Part I, "Distribution of one component only," are applied to the two components of a binary mixture.

Methods are described to derive the minimum number of stages required for the separation of a given feed into products of a given composition.

The results were applied to experiments reported by SCHEIBEL.

Résumé—Les équations correspondant à l'extraction à contre-courant, établies dans la Ière partie, sont appliquées aux deux constituants d'un mélange binaire. Les auteurs décrivent la méthode permettant de déterminer le nombre minimum d'étages nécessaires pour la séparation d'une alimentation donnée en deux produits de composition imposée. Les résultats sont appliqués à des résultats expérimentaux de SCHEIBEL.

I. INTRODUCTION

A problem generally encountered in practice is that of separating a given feed by two-solvent extraction into two products of specified composition while the coefficients of distribution of the two components for the solvents used are known. The question is to find the total number of stages, the feed point and the extraction factors of the two components.

In the literature special cases of this problem have been treated on several occasions.

VAN DIJCK and SCHAAFSMA [1] obtain a good separation of a mixture of equal amounts of propane-1,1-dicarbonic acid and propane-1,3-dicarbonic acid by means of extraction with ethyl acetate and water as solvents in a symmetrical extraction system under conditions that the product of the extraction factors of the two components equals 1. This result agrees with calculations made by STENE [2] for symmetrical extraction systems. In a symmetrical

† This paper was presented to the XII International Congress of Pure and Applied Chemistry, New York, September 10–13, 1951.

* N. V. De Bataafsche Petroleum Maatschappij, Roya Dutch/Shell Group, The Hague.

** Koninklijke/Shell-Laboratorium, Amsterdam.

system a mixture of equal amounts of two components is split into products of equal purity when the product of the extraction factors equals 1.

BUSH and DENSEN [3] treat the problem of the separation of a mixture of different amounts of two components according to CRAIGS procedure. They too mention that for a symmetrical system and for products of equal purity the product of the extraction factors of the two components should be equal to 1.

The treatment of ROMETSCH [4] is likewise restricted to symmetrical systems.

However, no information is found in the literature on the general problem as stated above. In the following the mathematical formulation of the problem and a numerical as well as a graphical method for solving the equations will be given.

2. Discussion of Special Solutions

For the treatment of the problem we start from the ratios R_1 and R_2 in which the two components are distributed over the two products. These quantities are readily calculated from the overall material balances for both components. In this respect it is sufficient that either the compositions of the feed and the products are known or two of these three compositions together with the yield.

As explained in the preceding paper* the following equations hold good for R_1 and R_2:

$$\frac{E_1^m (E_1^n - 1)}{E_1^m - 1} = R_1, \tag{1}$$

$$\frac{E_2^m (E_2^n - 1)}{E_2^m - 1} = R_2. \tag{2}$$

Further:

$$\frac{E_2}{E_1} = \beta. \tag{3}$$

Component 2 is to be the one with the higher distribution coefficient, so that $\beta > 1$. Then in practical cases $E_2 > 1 > E_1$; $R_2 \gg 1$ and $R_1 \ll 1$. In order to measure the E-values it is further convenient to introduce the parameter

$$x = \frac{\log E_2}{\log \beta} \tag{3a}$$

(see graphical method).

As a consequence of the above: $0 < x < 1$.

In the three equations given R_1, R_2 and β are known, it is asked to find V/v, hence the E-values, n and m. These 3 equations with 4 unknowns still allow an infinite number of solutions. It is reasonable to demand that $n + m - 1$, the total number of stages, be a minimum.

These simultaneous equations of higher, and possibly fractional, order do not allow a straightforward solution. In several special cases, however, the equations can be simplified.

These include:

Case 1 $x = 0$

$$E_1 = \beta^{-1}, \tag{4a}$$

$$E_2 = 1. \tag{4b}$$

Method of solution:

From (2) and (4b)

$$\frac{n}{m} = R_2. \tag{5}$$

From (1), (4a) and (5):

$$\frac{\beta^{-m}(\beta^{-R_2 m} - 1)}{\beta^{-m} - 1} = R_1. \tag{6}$$

Find m by trial and error, and then n from m and (5).

Case 2.

$$2m = n. \tag{7}$$

Method of solution:

From (1) and (7):

$$E_1^m = \tfrac{1}{2} + \sqrt{\tfrac{1}{4} + R_1}. \tag{8}$$

From (2) and (7):

$$E_2^m = \tfrac{1}{2} + \sqrt{\tfrac{1}{4} + R_2}. \tag{9}$$

From (3), (8) and (9):

$$\beta^m = \frac{\tfrac{1}{2} + \sqrt{\tfrac{1}{4} + R_2}}{\tfrac{1}{2} + \sqrt{\tfrac{1}{4} + R_1}}. \tag{10}$$

Solve for m and then find n from (7). Find E_1 from (8) and then E_2 from (3). Calculate x.

Case 3. $x = \tfrac{1}{2}$

$$E_1 = \beta^{-\frac{1}{2}}, \tag{11a}$$

$$E_2 = \beta^{+\frac{1}{2}}. \tag{11b}$$

Method of solution:

Divide (2) by (1) and substitute (11a) and (11b):

$$\beta^{\frac{1}{2}(m+n)} = \frac{R_2}{R_1}. \tag{12}$$

$$(m + n - 1) = 2\,\frac{\log \frac{R_2}{R_1}}{\log \beta} - 1. \tag{13}$$

* Same title, Part I, Distribution of one component only, by A. KLINKENBERG. Chem. Eng. Science 1951 **1** 86.

VOL. 1 1952

Substitute (12) in (2):

$$\beta^{1-m} = \frac{R_2}{R_1} \cdot \frac{1+R_1}{1+R_2}, \tag{14}$$

$$m = \frac{2 \log \frac{R_2}{R_1} \cdot \frac{1+R_1}{1+R_2}}{\log \beta}. \tag{15}$$

Find n from (13) and (15):

$$n = \frac{2 \log \frac{1+R_2}{1+R_1}}{\log \beta}. \tag{16}$$

Case 4.

$$m = n. \tag{17}$$

Method of solution:

From (1) and (2) after substituting $m = n$:

$$E_1^n = R_1, \tag{18}$$

$$E_2^n = R_2. \tag{19}$$

Dividing (19) by (18):

$$\beta^n = \frac{R_2}{R_1}. \tag{20}$$

$$n = \frac{\log \frac{R_2}{R_1}}{\log \beta}, \tag{21}$$

$$m + n - 1 = 2 \frac{\log \frac{R_2}{R_1}}{\log \beta} - 1. \tag{22}$$

Find E_1 and E_2 from (18), (19) and (21). Calculate x

Case 5.

$$m = 2n. \tag{23}$$

Method of solution:

From (1) and (23):

$$E_1^n = \tfrac{1}{2} R_1 + \sqrt{\tfrac{1}{4} R_1^2 + R_1}. \tag{24}$$

From (2) and (23):

$$E_2^n = \tfrac{1}{2} R_2 + \sqrt{\tfrac{1}{4} R_2^2 + R_2}. \tag{25}$$

From (3), (24) and (25):

$$\beta^n = \frac{\tfrac{1}{2} R_2 + \sqrt{\tfrac{1}{4} R_2^2 + R_2}}{\tfrac{1}{2} R_1 + \sqrt{\tfrac{1}{4} R_1^2 + R_1}}. \tag{26}$$

Solve for n and then find m from (23). Find E_1 from (24) and then E_2 from (3). Calculate x.

Case 6. $x = 1$

$$E_1 = 1, \tag{27a}$$

$$E_2 = \beta. \tag{27b}$$

Method of solution:

From (1) and (27a):

$$\frac{n}{m} = R_1. \tag{28}$$

From (2), (27b) and (28):

$$\frac{\beta^m (\beta^{R_1 m} - 1)}{\beta^m - 1} = R_2. \tag{29}$$

Find m by trial and error, and then n from m and (5).

It is to be noted that cases 3 and 4 require the same total number of stages, so that the optimum number corresponds to conditions intermediate between those of these two cases.

A plot can be made showing $(n + m - 1)$ against $x = \frac{\log E_2}{\log \beta}$.

The above theory has been applied to experimental results obtained by SCHEIBEL [5] for the separation of ortho- and parachloronitrobenzene with a heptane mixture ("Skellysolve *C*") and aqueous methanol (15% water) as solvents.

There was a slight change (of 2%) in the extraction factors at the feed inlet. This was neglected in the present treatment.

For this pair of substances in the solvents mentioned $E_2/E_1 = \beta = 1{\cdot}620$, where component 2 = ortho and component 1 = para and

$$E = \frac{\text{amount of component in methanol}}{\text{amount of component in heptane}}.$$

In expt. 5 the product quantities and compositions were: in methanol solution 3·39 lb/hr with 12% para isomer (solvent-free), in heptane solution 1·96 lb/hr with 81·7% para isomer, so that:

$$R_1 \text{ (para)} = \frac{3{\cdot}39 \times 0{\cdot}12}{1{\cdot}96 \times 0{\cdot}817} = 0{\cdot}256,$$

$$R_2 \text{ (ortho)} = \frac{3{\cdot}39 \times 0{\cdot}88}{1{\cdot}96 \times 0{\cdot}183} = 8{\cdot}28.$$

The results obtained are given in the following table, together with the E-values corresponding to SCHEIBEL's experimental conditions and the stage numbers calculated by his trial and error method. The stage numbers have been plotted against x in Fig. 1.

It is seen that the total number of stages $(n + m - 1)$ passes through a flat minimum. Consequently the total number of stages corresponding to both the symmetrical position of the feed (case 4) and the symmetrical position of the E-values (case 3) will in many cases be sufficient as an estimate of the minimum total number of ideal stages.

It is also seen, upon comparing cases 3 and 4, that a change in position of the feed under nearly optimum

Table 1

Case	m	n	$n+m-1$	x	E_1 *(para)*	E_2 *(ortho)*
1	3·4	28·0	30·4	0	0·617	1·00
2	5·1	10·1	14·2	0·357	0·735	1·19
3	6·2	8·2	13·4	0·5	0·790	1·27
4	7·2	7·2	13·4	0·605	0·828	1·34
5	11·0	5·5	15·5	0·838	0·925	1·50
6	18·0	4·5	21·5	1·0	1·00	1·62
SCHEIBEL expt. 5	7·45	7·15	13·6	0·627	0·836	1,353 (mean)

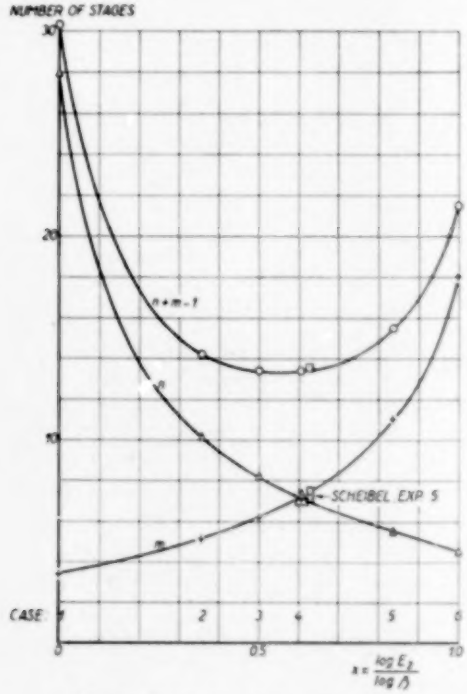

Fig. 1. Evalution of SCHEIBEL's expt. 5.

conditions can simply be corrected by a slight change in the solvent ratio.

Safe operating conditions will be in the range between cases 3 ($x = \frac{1}{2}$) and 4 ($n = m$). Outside this range the total number of stages increases rapidly.

SCHEIBEL's expt. 5 corresponded to conditions only just outside the range mentioned.

SCHEIBEL's total number of ideal stages was 13·6. Cases 3 and 4 require 13·4 ideal stages and it is seen from Fig. 1 that the minimum could not be below about 13·2.

Further it is to be noted that for cases 3 and 4 the total number of stages depends on the ratio of R_2 to R_1 only, *i.e.* only product compositions are required and feed composition and yields have no influence.

The above method does not allow of an accurate calculation of the minimum number, and the value of $m + n - 1$ obtained for cases 3 and 4 (viz. eq. 22) would have to be used as an upper estimate.

A graphical method was therefore worked out which allows finding all solutions of the original equations instead of a limited number only.

3. A General Graphical Solution

The following equations are given [see eq. (1)–(3)]:

$$\left.\begin{aligned} E_1^{m+n} - E_1^m(1+R_1) + R_1 &= 0 \\ E_2^{m+n} - E_2^m(1+R_2) + R_2 &= 0 \\ \frac{E_2}{E_1} &= \beta . \end{aligned}\right\} \tag{30}$$

They can be brought in the following symmetrical form

$$E_1^{\frac{1}{2}(m-n)}(1+R_1) = E_1^{\frac{1}{2}(m+n)} + E_1^{-\frac{1}{2}(m+n)} R_1$$
$$E_2^{\frac{1}{2}(m-n)}(1+R_2) = E_2^{\frac{1}{2}(m+n)} + E_2^{-\frac{1}{2}(m+n)} R_2 .$$

Introducing new variables by means of

$$\left.\begin{aligned} E_1 &= \beta^{-y} & E_2 &= \beta^{x} \\ v &= \tfrac{1}{2}(m-n)\log\beta & s &= \tfrac{1}{2}(m+n)\log\beta \end{aligned}\right\} \tag{31}$$

we find

$$10^{v\,x}(1+R_2) = 10^{s\,x} + 10^{-s\,x} R_2$$
$$10^{-v\,y}(1+R_1) = 10^{-s\,y} + 10^{+s\,y} R_1$$

or finally, when instead of R_1 and R_2 new parameters a and b defined by

$$a = \frac{1}{1+R_2} \qquad b = \frac{R_1}{1+R_1} \tag{32}$$

are used,

$$\left.\begin{aligned} 10^{v\,x} &= (1-a)\,10^{-s\,x} + a\,10^{s\,x} \\ 10^{-v\,y} &= (1-b)\,10^{-s\,y} + b\,10^{s\,y} \\ x + y &= 1 . \end{aligned}\right\} \tag{33}$$

From (32) it follows that a and b are in general small quantities. The physical meaning of a and b is clear; they denote the small amounts of the one component, relative to the feed, in the final stage, where a large amount of the other product is obtained.

The minimum problem determined by (33) and s = minimum can be solved graphically as described below.

Since the system (33) is independent of β the following important theorems are derived from eq. (31).

a) The total number of equilibrium stages plus one required is inversely proportional to the logarithm of the ratio β of the distribution coefficients.

b) The location of the feed as determined by the ratio $\frac{m-n}{m+n}$ is independent of β.

c) The logarithms of the extraction factors are proportional to $\log \beta$.

The graphical solution proceeds as follows (Fig. 2):

In a (w, t) diagram the following two curves are drawn

$$C_1: \; w = \log\{(1-a)\,10^{-t} + a\,10^{t}\}$$
$$C_2: \; w = -\log\{(1-b)\,10^{-t} + b\,10^{t}\}.$$

Every line l through the origin determines a solution of (33). Let l meet C_1 and C_2 in the points $P_1(t_1)$ and $P_2(t_2)$; then we obtain, if the slope of l is represented by Θ; from equations (33):

$$s = t_1 + t_2 \qquad v = \Theta s$$
$$x = \frac{t_1}{t_1 + t_2} \qquad y = \frac{t_2}{t_1 + t_2}.$$

The middle M of $P_1\,P_2$ has the abscissa $\frac{1}{2}s$. Consequently, the extreme left-hand point M_0 of the curve C_3 described by M for variable Θ determines the minimum total number of stages. When the values of s, Θ, t_1 and t_2 corresponding to the minimum are denoted by s_0, Θ_0, t_1^0 and t_2^0, we get the complete solution in the following form

$$\left.\begin{aligned} m+n &= \frac{2s_0}{\log\beta} \\ m-n &= \Theta_0\,(m+n) \\ \log E_1 &= -\frac{t_2^0}{s_0}\log\beta \\ \log E_2 &= \frac{t_1^0}{s_0}\log\beta. \end{aligned}\right\} \quad (34)$$

For a rather wide range of the values of a and b the C_3-curve is found to be very flat in the vicinity of M_0. In the case of an error in Θ_0 (*i.e.* the location of the feed point) the value of s_0 is not appreciably influenced. However, t_1^0 and t_2^0 (*i.e.* the extraction factors) are very susceptible to a slight alteration of Θ_0. Obviously, an error in Θ_0 has no effect on the purity of the end products, the purity being determined by the choice of the C_1 and C_2 curves.

These conclusions of course, are in line with those found in section 2.

To facilitate calculations, a graph (Fig. 3) has been constructed containing a set of C_1 and C_2 curves for

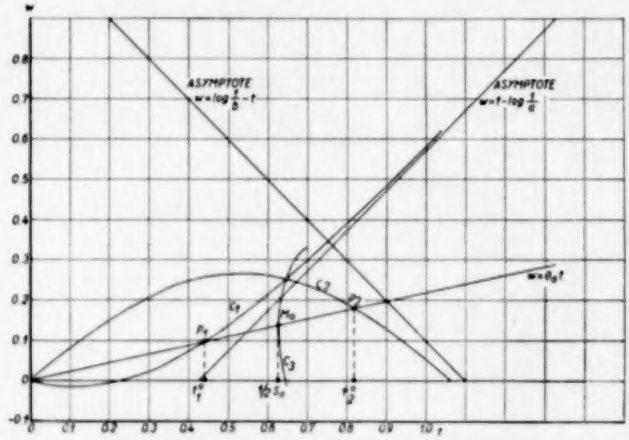

Fig. 2. The graphical determination of the total number of the stages, the feed location and the solven tratio with the aid of a w, t diagram.

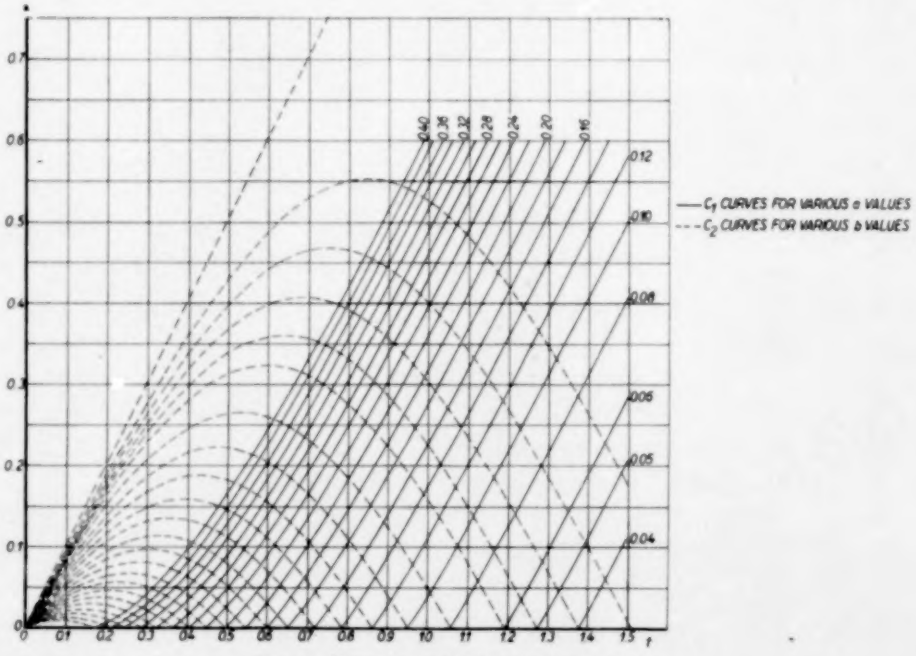

Fig. 3. Nomogram of C_1 and C_2 curves.

different a and b values. As this graph is symmetric with respect to the t axis, only the upper part is given. Hence, the dashed C_2 curves appear as the reflected continuations of the corresponding C_1 curves. For any special extraction problem the corresponding C_1 and C_2 curves have to be selected and the part of the C_3 curve in the vicinity of the minimum position has to be

constructed—it is of course unnecessary to *draw* the lines—. From the corresponding t_1^0, t_2^0, Θ_0 values all required information can be obtained.

A set of curves (Fig. 4) has been constructed giving the values of s_0 for different a en b values.

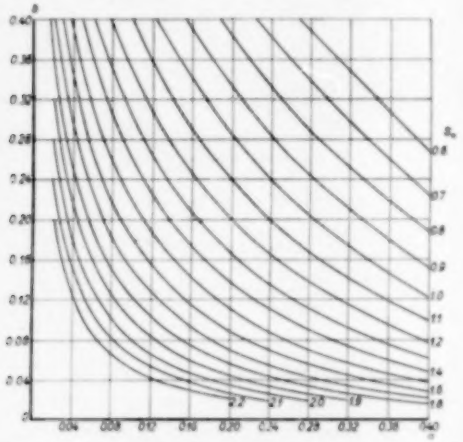

Fig. 4. Graph of $s_0 = \frac{1}{2}(m+n)\log\beta$ curves in an (a,b) diagram. Chart of relative minimum total number of stages.

Thus if 80% of component 1 leaves with the final residue phase and 90% of component 2 with the extract phase, $a = 0{\cdot}20$ and $b = 0{\cdot}10$, so that $s_0 = 1{\cdot}55$.

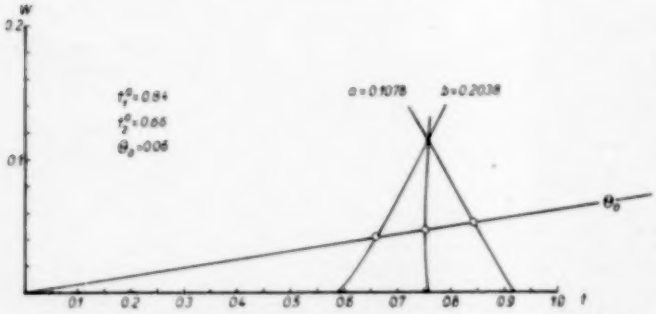

Fig. 5. Determination of minimum number of stages for product compositions and yield of SCHEIBEL's expt. 5.

The number of stages plus one is then found from

$$m + n = \frac{2\,s_0}{\log\beta}\,.$$

For small values of a and b (*i.e.* sharp separations) the total number of stages is more conveniently derived by an approx'mation which can then be shown to be very accurate. (See next section.)

It is of interest to consider the connection with the special solutions discussed in section 2.

The solution $m = n$ corresponds with $\Theta = 0$ or simply the t-axis. P_1 and P_2 become the intersections of C_1 and C_2 with the t-axis. Their abscissae can be easily found from

$$\log\{(1-a)\,10^{-t} + a\,10^{t}\} = 0$$

or simply

$$t_1 = \log\frac{1-a}{a} = \log R_2$$

and in a similar way

$$t_2 = \log\frac{1-b}{b} = -\log R_1\,.$$

Hence we find for M the abscissa $\frac{1}{2}\log R_2/R_1$, which leads to

$$m + n = \frac{2\log R_2/R_1}{\log\beta}\,.$$

The special solution $x = \frac{1}{2}$ gives $t_1 = t_2$ and corresponds with the intersection of the C_1 and C_2 curves. The abscissa can be found from

$$\{(1-a)10^{-t} + a\,10^{t}\}\{(1-b)\,10^{-t} + b\,10^{t}\} = 1\,.$$

Apart from the trivial solution $t = 0$, this has the solution

$$t_1 = t_2 = \tfrac{1}{2}\log\frac{(1-a)\,(1-b)}{ab} = \tfrac{1}{2}\log R_2/R_1$$

which leads to the same result

$$m + n = \frac{2\log R_2/R_1}{\log\beta}\,.$$

As an application of this method the example of SCHEIBEL already treated in the previous section is considered.

$$R_1 = 0{\cdot}256; \qquad R_2 = 8{\cdot}28; \qquad \beta = 1{\cdot}620\,.$$

From this we get $a = 0{\cdot}1078$ and $b = 0{\cdot}2038$.

The appropriate parts of the corresponding C_1 and C_2 curves are drawn. The results are plotted in Fig. 5. As $a < b$ we replace w by $-w$, which is allowed in view of the symmetry of Fig. 3.

A rather flat minimum is found. We obtain $t_1^0 = 0{\cdot}84$; $t_2^0 = 0{\cdot}66$ and $\Theta_0 = 0{\cdot}06$ so that

$$m + n = 14{\cdot}3\,, \qquad -m + n = 0{\cdot}86\,,$$
$$E_1 = 0{\cdot}809, \qquad E_2 = 1{\cdot}31\,.$$

It is seen that the minimum number of stages plus one $(n + m)$ is not substantially below that given for cases 3 and 4 in table 1 (viz. $n + m = 14{\cdot}4$).

The curves shown in Fig. 2 were derived from SCHEIBEL's expt. 1. Here the difference is somewhat greater.

4. An Approximate Solution

Equation (22) gives an upper estimate for the minimum number of stages. In order to judge its accuracy a lower estimate is also required.

For sharp separations eq. (1) and (2) may be simplified by putting

$$E_1^m \ll 1 \qquad E_1^m \ll 1$$

$$E_2^n \gg 1 \qquad E_2^m \gg 1 ,$$

so that:

$$\left.\begin{aligned} E_1^m &= R_1 \\ E_2^n &= R_2 \end{aligned}\right\} \tag{35}$$

whence, by using eq. (3) and (3a):

$$(m+n)\log\beta = \frac{-\log R_1}{1-x} + \frac{\log R_2}{x} . \tag{36}$$

This function is to be compared with the function used in section 3 of which 6 special solutions were derived.

They have the solutions $x = \frac{1}{2}$ and $m = n$ in common.

The minimum condition applied to eq. (36) gives

$$(m+n)\log\beta = \left(\sqrt{-\log R_1} + \sqrt{\log R_2}\right)^2 \tag{37}$$

with

$$\frac{m}{n} = \frac{\sqrt{-\log R_1}}{\sqrt{\log R_2}} .$$

This is a lower approximation for the exact minimum.

The two approximations for $(n+m)$ will differ:
by less than 2% if the ratio of $\frac{-\log R_1}{\log R_2}$ is between the limits $\frac{9}{16}$ and $\frac{16}{9}$
by less than 10% if this ratio is between $\frac{1}{4}$ and 4.

So the approximation to the exact solution is certainly better.

SCHEIBEL's expt. 5 ($R_1 = 0{\cdot}256$, $R_2 = 8{\cdot}28$) is still within the inner limits.

LITERATURE

[1] DIJCK, W. J. D. VAN and SCHAAFSMA, A.; U.S. Pat. 2 245 945, 17th June 1941 (convention date 30th March 1938). [2] STENE, S.; Arkiv för Kemi, Mineralogie och Geologi. 1944 **18 A** N:o 18, page 86. [3] BUSH, M. T. and DENSEN, P. M.; Anal. Chem. 1948 **20** 121. [4] ROMETSCH, R.; Helv. Chim. Acta 1950 **53** 184. [5] SCHEIBEL, E. G.; Chem. Eng. Progr. 1948 **44** 681.

NOTATION

Symbol	*Definition*	*Unit*
a	$\frac{1}{1+R_2}$ (eq. 32)	dimensionless
b	$\frac{R_1}{1+R_1}$ (eq. 32)	dimensionless
E	extaction factor [see part I (eq. 2)]	dimensionless
m	number of stages in washing section, incl. feed stage	dimensionless
n	number if stages in extraction section, incl. feed stage	dimensionless
R	ratio of the amounts of solute in final extract and extraction residue [see part I eq. (15)]	dimensionless
s	$\frac{1}{2}(m+n)\log\beta$ [eq. (31)]	
t	abscissa in Fig. 2	
v	$\frac{1}{2}(m-n)\log\beta$ [eq. (31)]	
w	ordinate in Fig. 2 [see eq. (33a) and (33b)]	
x	$\frac{\log E_2}{\log\beta}$ [eq. (31)]	dimensionless
y	$\frac{-\log E_1}{\log\beta} = 1-x$ [eq. (31)]	dimensionless
β	ratio of distribution coefficients $\frac{K_2}{K_1} = \frac{E_2}{E_1}$	dimensionless
Θ	v/s	

Indices:

1	component with lower distribution coefficient
2	component with higher distribution coefficient

Subscript:

0	extraction conditions for which the total number of stages is a minimum

Book review

L. Kuechler; **Polymerisationskinetik,** Springer-Verlag, Heidelberg, 1951. 44 figures, 31 tables; VIII + 287 pp., DM 36.60

This is the first up to date German book on the mechanism of polymerisation reactions. Advances in this field in the last half decade have been so rapid that the material is already scattered in the literature waiting to be collected, collated, and critically surveyed. This volume fulfils these aims and is written for physical chemists who are practising in this field and want to know how matters stand and also for the more general reader who cannot possibly keep pace with the flood of literature now being produced on this subject. Fortunately the subject can be treated in a systematic and logical manner. Furthermore recent developments have been to a very large extent quantitative which makes it much more satisfactory to write a monograph on a newly developing topic.

In writing a book on any branch of polymer chemistry it is not easy to keep strictly to the subject under review. The author has, however, carefully confined himself to the kinetics of reactions and has only made passing reference to ancillary subjects. There is a brief general introduction to say what a polymer is and to indicate what chemical kinetic analysis can do for the elucidation of mechanisms. There is too, a brief description of the various experimental methods for following polymerisation. As a necessary adjunct to these techniques molecular weight measurements are nearly always necessary if the mechanism is to be completely understood. There is therefore a short section describing the usual methods. Space is not sufficient, however, to give practical details for a newcomer to the field. The real part of the book begins with a general chapter on addition polymerisation. The theory of non-stationary state kinetics is also proposed but the new developments in this latter field are far too recent to have been incorporated in the book. The major part of the book deals with specific examples. Here every aspect of the subject is clearly discussed and appraised, including such developments as the determination of rate constants. All the developments in copolymerisation are thoroughly discussed and the more recent developments on the rates of copolymerisation are not merely added as an addendum. The controversial and less quantitative subject of ionic polymerisation is also dealt with. In such polymerisations matters are not nearly so precise kinetically and correspondingly the chapter on this topic is brief and summarises the present state of affairs. Polycondensation kinetics of linear polymers are somewhat simpler than those of addition polymerisation and the now classical treatment is given in detail not only for rates but also for molecular weight distributions. Not so much attention is given to the more difficult state of affairs in the synthesis of branched polymers. The volume is therefore an up to date survey of the whole field. It is remarkably complete and no new development has been omitted. The author has welded the material into a very readable and satisfactory account of the subject.

H. W. Melville